THE PHOTORESPONSES OF PHYCOMYCES: ANALYSIS USING MANUAL TECHNIQUES AND AN AUTOMATED MACHINE WHICH PRECISELY TRACKS AND MEASURES GROWTH DURING PROGRAMMED STIMULI

Thesis by

Kenneth W. Foster

In Partial Fulfillment of the Requirements

For the Degree of

Doctor of Philosophy

California Institute of Technology

Pasadena, California

1972

(Submitted May 22, 1972)

To Aileen

ACKNOWLEDGMENTS

I acknowledge the financial assistance of the National Research Council of Canada, the Sloan Foundation and various Caltech funds which made experiments and survival possible.

I further acknowledge the spiritual and practical assistance of all the present and former members of the Phycomyces group and all of those in the Caltech community who have helped. I would like to acknowledge the technical assistance of Richard Broderick, Cornelius Dekker, Reuben Epstein, Bertha Jones, Jeanette Navest, Ed Peterson, Murry Smigel, Grant Snellen, and Mike Walsh.

Finally I would like to thank my typist Barbara Sloan, my advisor Max Delbrück, and my wife Susan for seeing me through to the end.

Abstract

The sporangiophores of the fungus Phycomyces are sensitive to light, to gravity, to mechanical stretch, and possibly to a gas. In order to understand the processes by which these stimuli evoke response from the organism, the relationships between these input stimuli and the output responses of the fungus have been studied. The light stimulus was chosen because of its ease of quantification.

To study these responses better than in the past, automated equipment has been developed to improve the precision of observation, the control of the environment, and the collection of data. The heart of this equipment is a tracking system which stabilizes in space the sporangium, which serves as a convenient spherical marker just above the sensing and responding growing zone. Stabilization of this zone makes uniform stimulation relatively easy. Further the automatic system makes possible 6 or more hours of measurement on a single sporangiophore without requiring much operator intervention. After suppression of noise by means of a low pass filter of bandwidth 0.07 Hz, the growth velocity of typically 50 μm/min was measured to a precision of better than 5%. This compares favorably with manual techniques which optimally have a precision of about 20% for the average growth velocity over a 30 sec period.

Use of this machine as well as of conventional experimental

techniques on the newly available mutants of Phycomyces has provided a clearer understanding of the stimulus-response system. The effect of light scattering and of absorption of light inside the sporangiophore on the response to light has been investigated. These studies have resulted in appreciation of the quantitative effect of the lens focusing of the cell and in an improved action spectrum.

Evidence is presented that a major factor causing phototropism is the cell's natural twist (spiral growth) of about 6°/min in the middle of the growing zone. Each region of the cell locally adapts to the local light intensity. However with the twist of the cell, at one edge of the focused band which is produced by the lens focusing of the cell there will be a continuous entry of dark adapted area into the higher intensity band, thus giving rise to transient positive growth responses in a succession of surface elements. The response to this stimulus is expressed slowly in time and as it is expressed, it is carried around at the twist rate of the cell. This model has successfully explained both our experiments and a number from the literature.

Using the machine, latency and shape of response have been characterized as a function of temperature, stimulus size, level of adaptation and incident light wavelength. Latency is dependent on the logarithm of the absolute adaptation level and there is no wavelength dependence of the stimulus response curve. For larger stimuli the shape of the response changes markedly, with the rising

of an early peak in the growth velocity and inhibition of a later second peak.

Study of mutants defective in the chemical pathway from light stimulation to response show a great variety of mutant types implying a relatively large number of biochemical steps from stimulus to response.

Table of Contents

Page

I. GENERAL INTRODUCTION

Phycomyces sporangiophores (spphs) are sensitive to light, to an unknown gas, to gravity and to mechanical stretch. The responses are either a tropic or a time dependent growth rate change. Since Phycomyces is easy to grow and is amenable to genetic analysis, it seems to be a good microorganism to study the signal handling which is exhibited by all organisms.

Part of our laboratory's goal has been to understand the early stages of one of the transducer chains; specifically to identify the photoreceptor(s) for the case of the light response. Other parts of the transducer chain have also been studied to understand the phenomena of tropism and growth response.

The main effort of this thesis work has been to establish experimental techniques of sufficient quality and speed to make possible the study of many mutants; with respect to their tropic and growth response. The second effort has been to characterize and improve our understanding of the mechanisms underlying the tropic and light growth responses with the aid of mutants.

II. REVIEW OF SENSORY PHYSIOLOGY OF PHYCOMYCES

The sensory physiology of Phycomyces is discussed at length in the review paper, "Phycomyces" (Bergman, et al, 1969). In this section I would like to acquaint the reader briefly with the fungus and its known responses.

Development

After the fungus mycelium grows for 3-4 days, long cylindrical aerial hyphae, the sporangiophores, are sent up. A spph starts out as a single pointed tube (Stage I). Then elongation stops, the tip of the spph swells and a colored sporangium is formed. After an apparently inactive period the elongation of the spph resumes slowly and the sporangium darkens. Finally, after a moderate twist counterclockwise, the spph starts twisting clockwise and then slowly over several hours the speed of twist increases to 10-15°/min measured at the sporangium. During this time the growth rate increases to 50 μm/min. It is this final form called Stage IVb (Castle, 1942) that is used in most physiological experiments.

Only the top 2 to 3 mm of the stalk below the sporangium are growing and involved in the light, gravity, stretch and "avoidance" responses. A longitudinal cross-section is shown in Fig. II-1 with three transverse sections; the first near the top of the growing zone, the second near the bottom of the growing zone, and the third below the growing zone.

Fig. II-1.

Longitudinal and transverse cross-section of the sporangiophore of Phycomyces. The first transverse section is taken near the top of the growing zone, the second near the bottom of the growing zone, and the third below the growing zone.

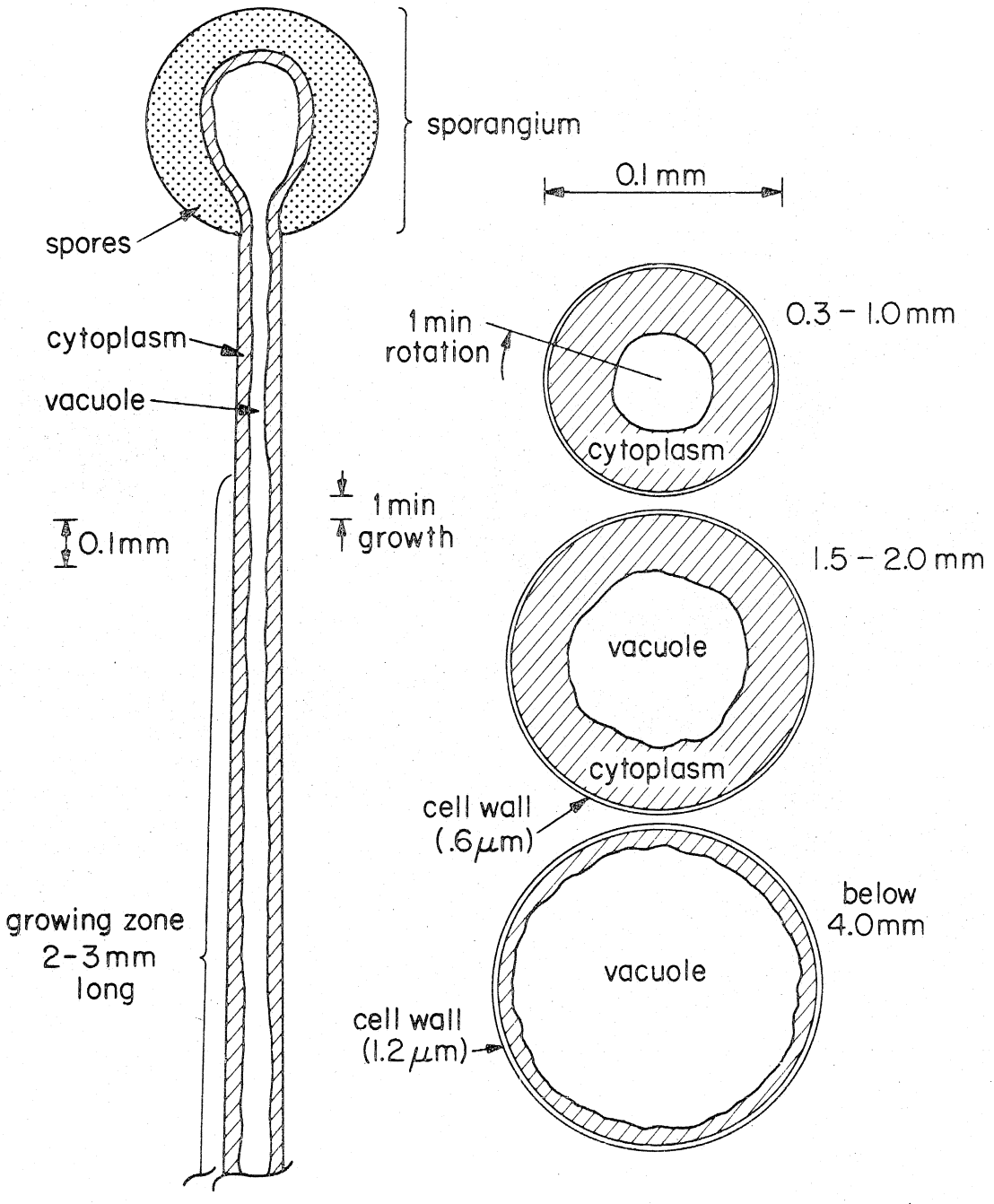
sporangium
0.1 mm
spores
cytoplasm
vacuole
1 min
rotation
0.3 – 1.0 mm
cytoplasm
1 min
growth
0.1 mm
1.5 – 2.0 mm
vacuole
cytoplasm
cell wall
(.6 μm)
below
4.0 mm
growing zone
2-3 mm
long
vacuole
cell wall
(1.2 μm)
LONGITUDINAL
SECTION
TRANSVERSE
SECTIONS
AT VARIOUS DISTANCES
BELOW SPORANGIUM

Light Responses

For convenience investigators have separated the light responses of the spph into two types. The simplest to evaluate is the light growth response in which a transient change in cell elongation rate is produced by a time-dependent light change over the whole cross section of the growing zone. The second is the phototropic response in which asymmetric elongation is produced by an asymmetric intensity distribution in the spph. Thus light causes a redistribution of growth either in time or in space. The growth rate under constant conditions from complete darkness to sunlight is typically at about 50 μm/min.

Both of these responses have the same spectral sensitivity (Delbrück and Shropshire, 1960), the same approximate intensity range of sensitivity, similar latency for response, and similar kinetics of light and dark adaptation. Both of these responses are graded. For a light pulse of duration 1 sec to 1 min the growth response is a function of only the pulse size S, which is the product of intensity (I) and duration (t). The tropic response is dependent on the dissymmetry of light intensity from one side to the other. The growth response is a transient response lasting about 40 minutes with a peak at about 5-7 minutes while the tropic response can continue indefinitely (Dennison, 1965).

Adaptation

The light responses also have a range adjustment mechanism in which the growth response depends on the intensity to which the specimen had been adapted before the stimulus. The level of adaptation, A, has been defined (Delbrück and Reichardt, 1956), either as the actual intensity to which the specimen had been adapted or as the virtual intensity to which it would have to be adapted to give a corresponding response to a standard stimulus. This effect of adaptation can be expressed by saying the responses are a function of S/A which has a dimension of time. The initial kinetics of changes in the level of adaptation approximates the equation

$$\frac{dA}{dt} = (I-A)/b \qquad \text{(II-1)}$$

where b is the time constant of adaptation and I is the light intensity. Thus if a specimen is brought to a certain level A and the adapting light is turned off, the level of adaptation will drop by a factor e during the time b. At 20°C, b equals about 5 min.

Phototropic response

The tropic response continues for as long as the geometrical relationship between the growing zone and the light source is kept constant. Also the bending rate stays constant after a short latency and initial transient phase. The steady bending rate is independent

of the light intensity over the small "normal" range (.04 μwatts/cm^2 to 10 μwatts/cm^2 blue). Over the range 10^{-7} μwatts/cm^2, to .04 μwatts/cm^2 the bending rate is a linear function of the logarithm of the intensity (Reichardt and Varjú, 1958). If a specimen is first adapted to a symmetrical high intensity and then tested for tropic response at a lower intensity, there is a delay in addition to that of the normal response latency before troping occurs. During this extra delay the general level of adaptation drops to the low level.

The explanation of the steady state of the tropic response involves a cardinal difficulty. It cannot be interpreted by saying that the specimen over the whole cross section is adapted to the locally prevailing light intensity. If it were so adapted the growth rate would be uniform all around the specimen and no differential growth would be maintained. To avoid this difficulty four different approaches have been suggested. One suggestion (Bergman et al, 1969, sec 15, Castle, 1965) is that light adaptation is uniform over the cross-section of the cell and the level of adaptation corresponds to some average of the prevailing intensity. This would imply some rapid process of communication over the whole cell in order for this spreading of adaptation to be rapid relative to other time constants of the system. Phototropism then occurs, because locally the regions of higher light intensities are always compared to a lower average level of adaptation. Jaffe (Cohen and Delbrück, 1959) suggests that much slower spreading of adaptation (too slow to

travel from one side to the other within the time constants of the system) is sufficient to cause phototropism. This also fits observations that local regions of high intensity illumination are adapted to a higher intensity than local regions of lower illumination (see section IV.C-4a). Reichardt and Varjú (1959) suggest that rotation of the cell and presumably the adapted region has an influence on phototropism. Rotation brings material adapted at relatively low intensities into the regions of higher intensity, thus resulting in local stimulation and phototropism. Castle (1966) accepts the idea of local adaptation, but suggests that prior irradiation establishes a local difference in the size of some metabolite reservoirs from which light and another unknown parallel reaction catalyzes a product that regulates the growth rate. (How phototropism works is the subject of section IV.C.). In any event, phototropism or growth dissymmetry is caused by the dissymmetry of irradiation, due to the lens properties of the cell which focus the light inside the cell. Somehow this dissymmetry leads to faster growth on the side of the cell distal to the source. The local growth rate, v, will be azimuthally asymmetric according to the equation $v(\psi) = \bar{v}(1 + \varepsilon \cos \psi)$ where ψ is the azimuth angle. Typically for wild type in unilateral blue light the bending rate is 2.9°/min with $d\alpha/dt = \varepsilon\bar{v}/r$ (r = radius of cell). This implies $\varepsilon \cong 0.05$, i.e., on the proximal side a growth rate 5% below average and on the distal side 5% above average. Such excess in growth is transiently produced by a rather slight growth response elicited

by stimuli for which S/A = 4 min. In fact S/A = 2 min gives a barely measurable response. Thus, in blue light, phototropism may be looked upon as a relatively small continuous local growth response. Below 300 nm there is sufficient absorption by the material lying between the proximal and distal photoreceptors so that we observe a negative phototropism. This phenomena is due to the greater growth of the side of the cell proximal to the light source.

The action spectrum for these responses is shown in Fig. II-2. This graph is a composite from the available data (Curry and Gruen, 1959; Delbrück and Shropshire, 1960) and the present author's work. This action spectrum is typical of that observed for a number of different organisms. Four of the most detailed action spectra are shown in Fig. II-3. In addition to the growth response of Phycomyces, they are Fusarium carotenoid synthesis (Rau, 1967), Pilobolus phototropism (Page and Curry, 1966), and Chlorella O_2 uptake (Kowallik, 1967).

Light controlled spph initiation

Bergman (1972) has shown that short periods of blue light shone on an otherwise dark-grown mycelium causes enhanced numbers of spph about 24 hrs later in the region which was the mycelial front during illumination. He showed that when light is turned off spph initiation is inhibited for a few hours.

Fig. II-2.

Action spectrum for the light response from 235-520 nm. This is a composite from the available data of Curry and Gruen (1959), Delbrück and Shropshire (1960), and the present author's work correcting for internal screening. The (relative quantum efficiency)$^{-1}$ is plotted on a logarithmic scale as a function of the wavelength.

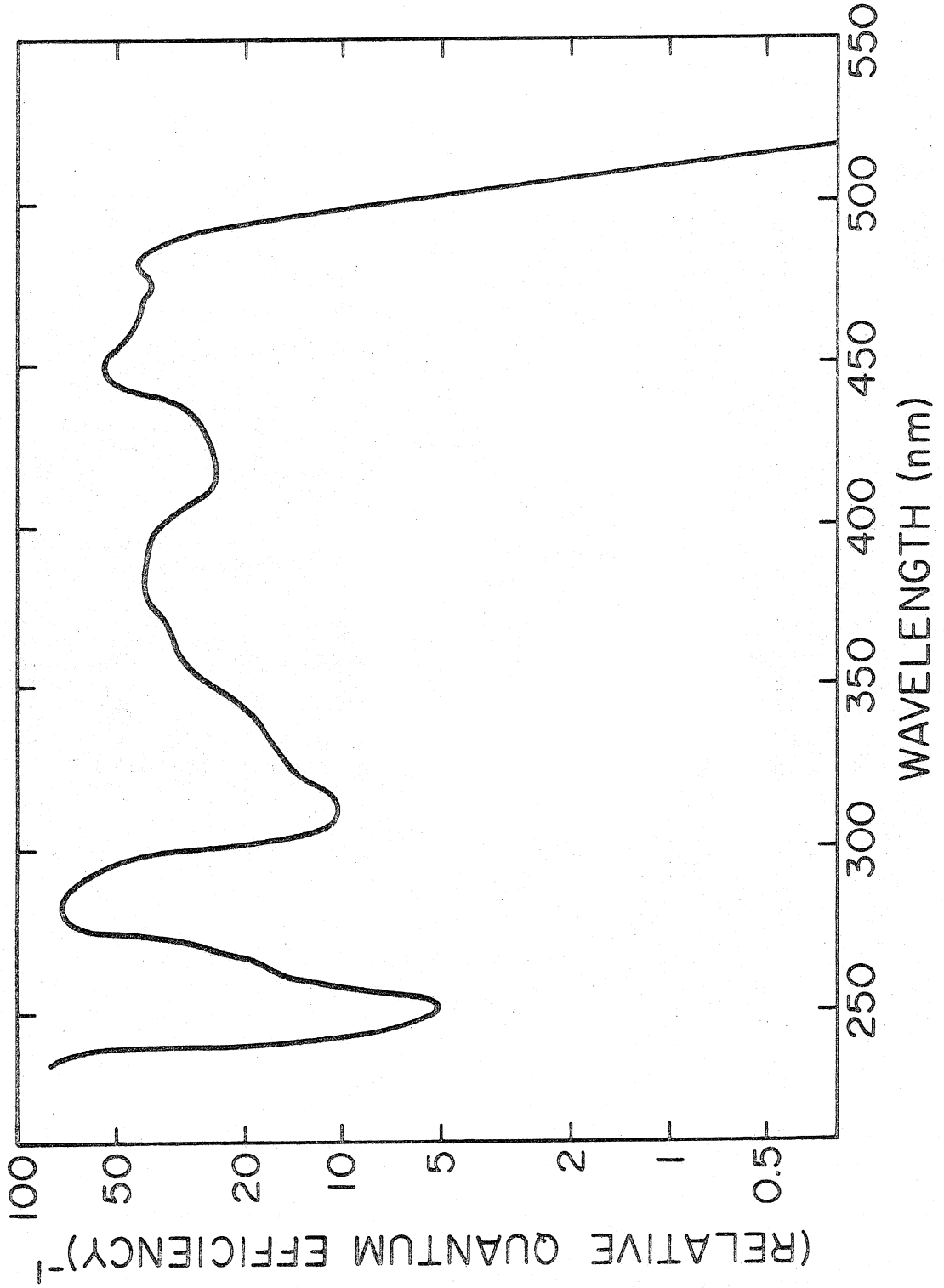
(RELATIVE QUANTUM EFFICIENCY)$^{-1}$
100
50
20
10
5
2
1
0.5
250
300
350
400
450
500
550
WAVELENGTH (nm)

Fig. II-3.

Action spectra of processes sensitive to blue light: light growth response of Phycomyces blakesleeanus (Delbrück and Shropshire, 1960); carotenoid synthesis in the ascomycete Fusarium aquaeductuum (Rau, 1967); phototropism in Stage I of the zygomycete Pilobolus kleinii (Page and Curry, 1966); and oxygen uptake in Chlorella (Kowallik, 1967).

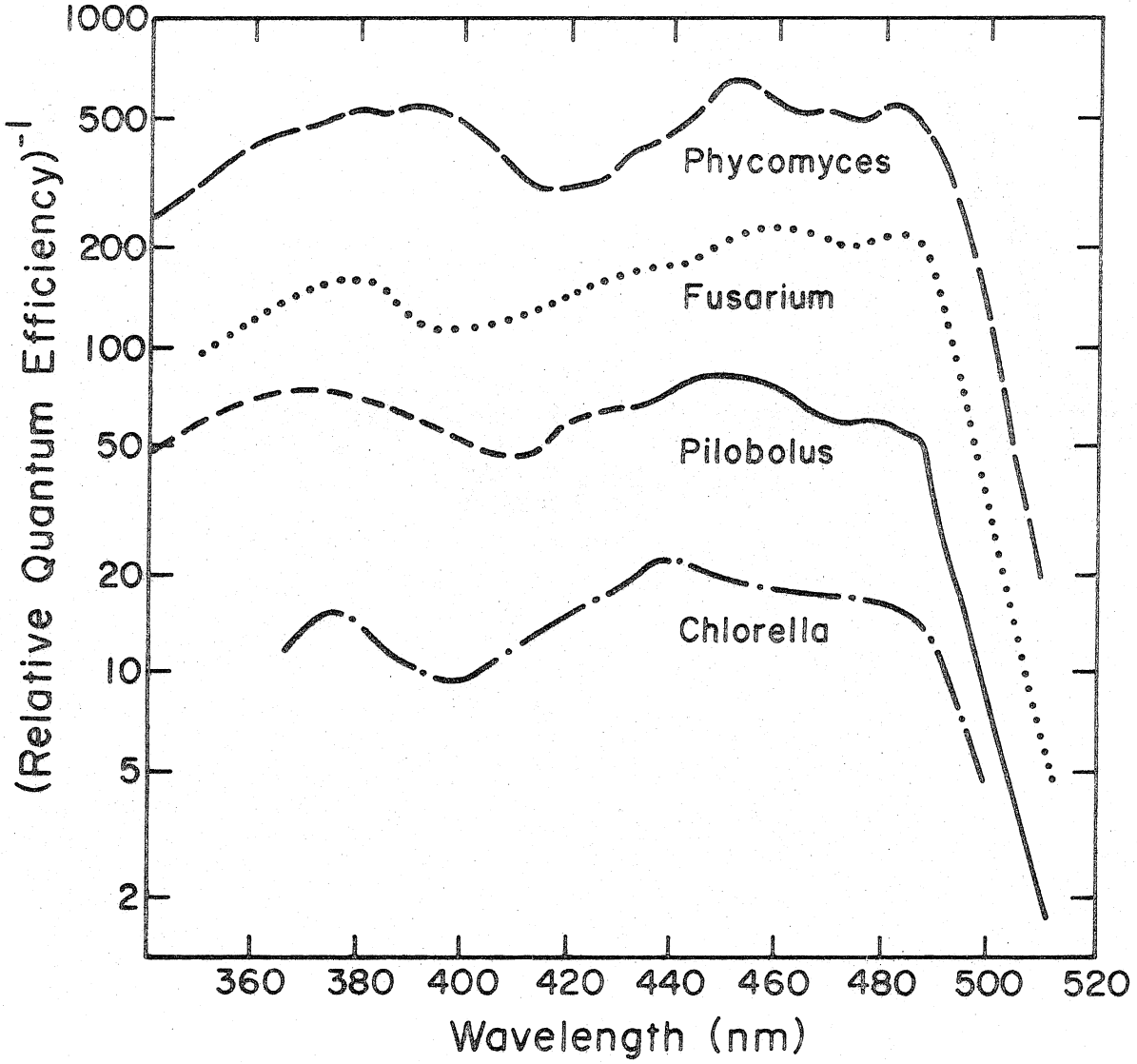
1000
500
200
100
50
20
10
5
2
(Relative Quantum Efficiency)$^{-1}$
Phycomyces
Fusarium
Pilobolus
Chlorella
360
380
400
420
440
460
480
500
520
Wavelength (nm)

Geotropism

If a spph is placed horizontally it bends upward until the direction of growth is vertical. The bending rate is proportional to the angle of its orientation relative to the vertical and is generally about 0.3°/min at 90° with a variable latency of from 30-180 min.

A phototropic-geotropic equilibrium takes place when spphs are left for sufficient time with weak light from one side. Near phototropic threshold gravity wins out and brings the spph toward the vertical.

Avoidance Response

A spph placed close to a solid barrier grows away from it. The response is quantitatively similar to that of a tropic response to light. For a barrier at about 1 mm distance tropism occurs at about 2°/min. If a symmetrical barrier or a four sided "house" encloses the specimen,a transient growth response is observed similar to a light growth response. Although the mechanism is not understood it is hypothesized that a "gas" released by the spph itself causes local inhibition or excitation of growth (R. Cohen, Y. N. Jan, private communication).

Stretch

The application of a longitudinal force of about 1 dyne stretching the cell results in a negative growth response. The growth rate drops

within 2 min after the stimulus and remains below normal for about 5 min. Response to removal of this stretching force is a positive growth response with similar latency. An applied lateral force acts locally in the same way, resulting in a rapid tropic reaction opposing the applied bend which continues at about 5°/min for about 5 min.

REFERENCES

Bergman, K., Patricia V. Burke, E. Cerdá-Olmedo, C. N. David, M. Delbrück, K. W. Foster, E. W. Goodell, M. Heisenberg, G. Meissner, M. Zalokar, D. S. Dennison, and W. Shropshire, Jr. 1969. Phycomyces. Bacteriol. Rev. 33: 99-157.

Castle, E. S. 1942. Spiral growth and the reversal of spiraling in Phycomyces, and their bearing on primary wall structure. Am. J. Botany 29: 664-672.

Castle, E. S. 1965. Differential growth and phototropic bending in Phycomyces. J. Gen. Physiol. 48: 409-423.

Castle, E. S. 1966. A kinetic model for adaptation and the light responses of Phycomyces. J. Gen. Physiol. 49: 925-935.

Cohen, R. and M. Delbrück. 1959. Photoreactions in Phycomyces. Growth and tropic responses to the stimulation of narrow test areas. J. Gen. Physiol. 42: 677-695.

Curry, G. M. and H. E. Gruen. 1959. Action spectra for the positive and negative phototropism of Phycomyces sporangiophores. Proc. Nat. Acad. Sci. 45: 797-804.

Delbrück, M. and W. Reichardt. 1956. System analysis for the light growth reactions of Phycomyces. In Dorothea Rudnick (ed.), Cellular mechanism in differentiation and growth. Princeton University Press, pp. 3-44.

Delbrück, M. and W. Shropshire, Jr. 1960. Action and transmission spectra of Phycomyces. Plant Physiol. 35: 194-204.

Dennison, D. S. 1965. Steady-state phototropism in Phycomyces. J. Gen. Physiol. 48: 393-408.

Kowallik, W. 1967. Action spectrum for an enhancement of endogenous respiration by light in chlorella. Plant Physiol. 42: 672-676.

Page, R. M. and G. M. Curry. 1966. Studies on phototropism of young sporangiophores of Pilobolus kleinii. Photochem. Photobiol. 5: 31-40.

Rau, W. 1967. Uber die lichtabhängige Carotinoidsynthetese. I. Das Wirkungsspektrum von Fusarium aquaeductuum. Planta 72: 14-28.

Reichardt, W. and D. Varjú. 1959. Der einfluss von eigen-und fremdrotation des sporangienträgers von Phycomyces auf die phototropische reaktion. Z. Naturforsch. 14b: 210-211.

III. MATERIALS AND GENERAL METHODS

A. STRAINS, MUTANTS, AND CULTURE CONDITIONS

The wild type strain of Phycomyces blakesleeanus Burgeff used in these experiments was a sexually minus strain obtained from the National Regional Research Laboratories (Peoria, Ill.) NRRL1555. Another strain used was the minus strain UBC24 obtained from R. G. Bandoni (Botany Department, University of British Columbia, Vancouver, B. C.). Mutants isolated by others were also used. The mutants used in this work are described in Table III-1 after Bergman (1972) and E. Cerdá-Olmedo (private communication).

Various mutagenesis procedures were used. In Procedure #1 the spores are mutagenized and killed directly with the chemical mutagen N-methyl-N'-nitro-N-nitrosoguanadine (Aldrich Chemical Co.). In procedure #2 the chemical mutagen is applied to growing mycelia and the surviving nuclei eventually enter spores. After the spores are harvested X-rays are used to kill to a survival rate of 10% (Bergman, 1972).

In most physiological experiments the spphs were grown in shell vials (12x35mm) containing potato dextrose agar (PDA) medium or lactate (LAC) medium (Zankel et al, 1967) filled to 10 mm from the top. In order to produce healthy spphs, a concentration of 1-2 viable spores was planted in each vial (so that in some of the vials

Table III-1

Origin of Phycomyces Strains

Strain	Genotype	Origin
NRRL1555	(-)	From Northern Regional Research Laboratories (Peoria, Ill.)
UBC24	(-)	From Botany Department, University of British Columbia (Vancouver, B. C.)
C2	car-5(-)	From NRRL1555, by procedure #1
C5	car-10(-)	From NRRL1555, by procedure #1
C9	carR21(-)	From NRRL1555, by procedure #1
C21	mad-7(-)	From NRRL1555, by procedure #1
C47	mad-35(-)	From NRRL1555, by procedure #1
C63	mad-54(-)	From NRRL1555, by procedure #1
C68	mad-59(-)	From NRRL1555, by procedure #1
C110	mad-102(-)	From NRRL1555, by procedure #1
C149	mad-120(-)	From NRRL1555, by procedure #2
S-5		From UBC24
S-14		From UBC24
S-37		From UBC24
S-18		From UBC24

mycelia did not form). The vials were first incubated enclosed in glass jars in room light at about 20 μwatts/cm^2 until the first crop of spphs had appeared. This crop was removed and the vials were then incubated with the top of the glass jar removed in a light box with a 15 watt tungsten lamp above a diffuser yielding approximately 4 μwatts/cm^2 at the spphs. The box was humidified to 60-80% and kept to temperature of about 22°C. The first crop was rarely used for experiments and always discarded during analysis of results. For most experiments only the second and third crops were used to keep variability due to age of the specimens at a minimum.

B. MANUAL TECHNIQUES

Using red backlighting from a 15 watt tungsten bulb and Schott RG610 cut off filter or equivalent, the sporangiophore was observed with a measuring microscope (Gaertner Scientific Corp.) with a M220 (32 mm focal length, 35 cm working distance) objective. For angle measurements in the plane of the stimulating light a M205 protractor eyepiece with M242 eyepiece was used. For vertical growth measurements a filar micrometer eyepiece was used and measurements were taken typically every minute.

C. AUTOMATED TECHNIQUE

1) Introduction

To improve the precision of observation and of control of the environment and to facilitate the collection of data I designed and built a machine to track the growth of Phycomyces. This electro-optical-mechanical device keeps the growing zone (about 2 mm long) in constant view and in perfect focus at all times, allowing film or videotape recording at high magnification. In addition it outputs an analog growth velocity during the experiment onto a strip chart recorder and a permanent digital record of the sporangium's trajectory in three dimensions in computer memory and magnetic tape for later analysis.

The main advantage of this new machine over previous microscope observation and manual recording of data is the accurate control of the environmental stimuli: light, gas, temperature, humidity, etc., combined with precise synchronization of stimuli with automatic handling. A second advantage, is the convenience of visual observation, since the growing and responding region is fixed in space. Concomitantly the problem of providing a uniform stimulus is greatly reduced. In fact, some experiments are possible only in this configuration. A third important advantage is a non-fatiguing

precision in measurement of the spph's growth behavior over a long period, such as 6 hours. The experimenter may analyze his data while the machine does the tedious work of making measurements. Using microphotography and a glass fibre glued on top of the sporangium Castle making use of the twist of the spph has claimed, for the relatively short period of 15 sec, uncertainties of ±2Å (Castle, 1940) for growth position. For microscope observation with a filar micrometer ±5 microns is considered good for the average experienced observer. This could be improved with relatively inexpensive electronic aids and experimental care to ±1 micron in the vertical direction. The machine's present precision is about ±0.5 μm in sporangium position determination. Using this tracking technique the probable accuracy limit is about ±0.2 μm at .1 Hz bandwidth. The machine also has the potential to measure troping angles to ±.05°, reducing the considerable error in vertical ($\Delta z/\Delta t$) velocity measurements due to sporangiophore bending and non-vertical orientation.

Estimation of the inherent biological noise is rather subjective since for any experiment it depends on the measurement criteria and how many of the environmental variables are controlled. Using Oort's criteria for response (Oort, 1932), i.e., taking the maximal positive growth deviation above what would have been the growth rate without the stimulus, data were taken for a number of responses

to a pulse of intensity 100 times the adapted level for 30 sec, run at 45 min intervals on two specimens. Specimen 1 gave a response of 76.1 ± 4.5 where 4.5 is the standard deviation of seven measurements. By comparison the second specimen gave 70.8 ± 5.3. Using as positive response the positive area of the growth velocity curve above the line that separates an equal areas of negative undershoot, results in less variability. For this size of response the machine is probably accurate to better than ±10% in the measurement of it's size, whereas the combined noise is probably a little less than ±20% on a single measurement. No account has been taken of systematic changes of spph due to changes of spph diameter, time from Stage II, or growth rate.

2. Sporangiophore growth tracking system

The heart of the machine is the tracking and servo system which maintains the sporangium of Phycomyces fixed in space. The sporangium is suited for tracking because: (1) it reaches its final constant diameter during stage II; (2) the growing and responding zone of the stalk is directly below the sporangium; and (3) the sporangium is opaque and spherical in shape.

The idea of a servo system to maintain the growing and responding zone fixed in space came from the requirement to look in detail at the growing specimen on videotape or film without loss of focus, yet with a field of view of only 3 to 4 mm at the specimen. Early attempts were made by Ed Peterson using a TV image and light sensors. Analysis of the TV signal for two dimensional tracking has been successful for tracking microorganisms (Davenport et al., 1970) and for Aplysia (Strumwasser, 1971). Both systems employ a computer to carry out the pattern recognition and calculate the movement.

However, the system I adopted was that employed by the astrophysicists to stabilize the image of the sun on their telescopes, only in reverse contrast,as suggested by Denis Matson. The shadow image of the opaque sporangium against a lighted background serves as the "negative sun". Howard Berg (1971) has built a three dimensional tracking machine for bacteria. He stabilizes the microscope image of the bacterium thereby fixing the bacterium in space.

See Fig. III-1, for the Phycomyces tracking system.

As seen at the left of this figure, the sporangiophore growing in its culture vial sits on a pillar supported by a stage. The sporangium lies in the tracking light beams which are 90° apart in the horizontal plane. Both beams come from the HeNe laser (632.8 nm) via a beam splitter and two prisms. Phycomyces is known not to be sensitive to the light of this colour. Lenses project a 50X magnified shadow at a plane at 1.5 m distant. Using mirrors both images are projected onto a common plane, one for the X-axis and the other for the Y and Z axis. Consider the X-axis. A light pipe is centered on each edge of the shadow image. The purpose of the system is to stabilize the sporangium image. The lights from the two light pipes are compared to provide an error signal of the sporangium position. If the image shifts leftward the right light pipe picks up more light than the left one. These beams are brought out to a light chopper which alternately allows the light from the right and left edge of the sporangium to fall on the X-axis photomultiplier. Information on which is incident at any time on the photomultiplier constitutes the phase information, i.e. which direction the stage should be moved. A small IR light and a silicon photodiode at the chopper plate pick up this information. With the AC coupled photomultiplier signal these signals together provide the direction and magnitude of the positioning error. This appropriately amplified and filtered signal drives a motor driven XYZ stage in order to

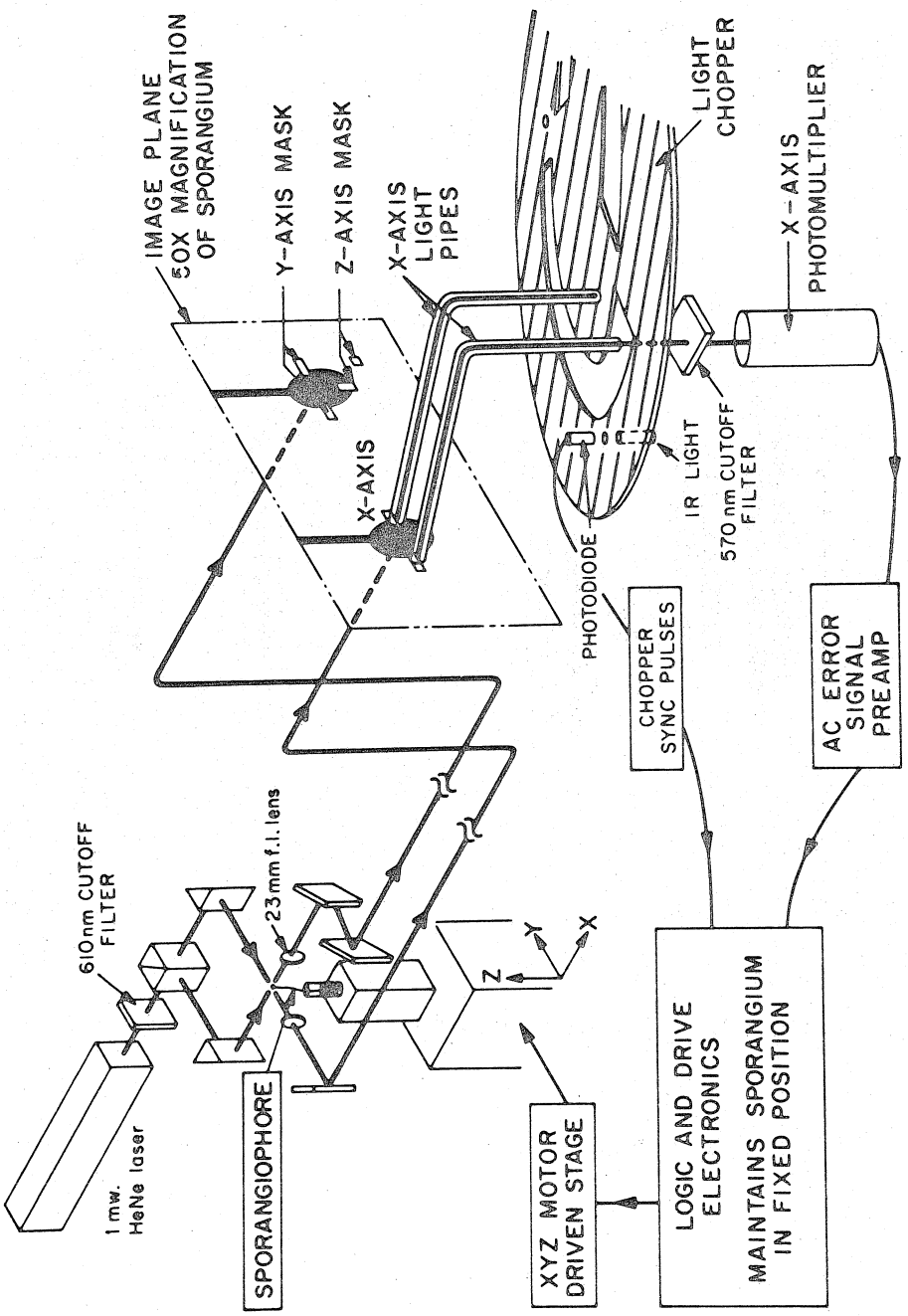
TRACKING SYSTEM
1 mw. HeNe laser
610nm CUTOFF FILTER
23mm f.l. lens
SPORANGIOPHORE
IMAGE PLANE 50X MAGNIFICATION OF SPORANGIUM
Y-AXIS MASK
Z-AXIS MASK
X-AXIS LIGHT PIPES
X-AXIS
PHOTODIODE
IR LIGHT
570 nm CUTOFF FILTER
LIGHT CHOPPER
X-AXIS PHOTOMULTIPLIER
CHOPPER SYNC PULSES
AC ERROR SIGNAL PREAMP
XYZ MOTOR DRIVEN STAGE
LOGIC AND DRIVE ELECTRONICS
MAINTAINS SPORANGIUM IN FIXED POSITION
Z
Y
X

Fig.III-1.

null the error signal and thereby keep the sporangium in one place along that axis in space. The horizontal Y-axis works similarly. Stabilization of the vertical z-axis image is not so easy to obtain because the sporangiophore stalk is attached below the sporangium. Therefore it is necessary to sacrifice the two edge comparison with its sensitivity and accuracy and place only one sensor on the top edge and one on the background light to at least eliminate light fluctuation errors. For additional detailed information including circuit diagram see Appendix A, p. 181. New technological alternatives are also briefly discussed there.

The precision of the tracking is limited (1) by the diffraction of light which limits the resolution of the error signal; (2) by mechanical response of the stage drive motors and the ball bearing stage; and (3) by vibration. In the absence of sporangium vibration using a low pass filter of bandwidth 0.1 Hz the probable limit in principle with the technique is a knowledge of the velocity to about ± 2% at normal growth rates, or ± 1 μm/min. The present system seems close to ± 8% at this bandwidth. This does not take into account that $\Delta z/\Delta t$ may not be the most accurate measure of the sporangiophore growth rate.

In the presence of high frequency movement of the sporangium, either due to mechanical vibration or to wind, which causes the sporangiophore to oscillate like a reed, the horizontal accuracy is

determined by the total amplitude of vibration and the vertical accuracy is the vertically coupled horizontal vibration. This is less than 1μm for about 40 μm peak to peak horizontal oscillation. To prevent such vibration the apparatus rests on a heavy steel table and mechanical vibration sources are mounted separately. The spph is secured by tape and grease to the top of the vial and when possible is shielded from wind by an enclosure. Removal of vibrations is discussed in Appendix A, p. 196.

Experiments are limited to about 6 hours of continuous tracking because the stage has a range of only 2.5 cm. A possible limitation is that the specimens at angles greater than 80 degrees to the vertical cannot be followed due to interference of the stalk with side edge detecting light pipes.

More seriously, one cannot stimulate at exactly the same beam directions as the tracking beam. For example, a large opaque avoidance barrier cannot be placed close to the fungus. Also the system measures the sporangium trajectory and does not measure directly the angle of troping. It is impossible to calculate accurately the troping angle from the trajectory because the troping bend cannot be assumed to be at a constant distance from the top. Even if this bend distance is assumed constant, the calculation is numerically unstable. Finally, there is sag of the specimen with growth so that the angle of trajectory does not correspond to the

relevant troping angle. This limitation may be overcome by building a separate angle-measuring servo (see Appendix H, p.239).

3. Data Collection

The sporangium is kept continuously fixed in space by the tracking system. Elongation of the stalk is determined by how much the stage has been moved to keep the sporangium fixed (see Fig.III-2, "Data Output"). As can be seen in the upper left box of the figure, the sporangium is centered in the tracking light beams. The sporangiophore vial sits on a pillar supported by the motor driven xyz stage. The position of each axis is measured with a linear variable differential transformer (LVDT). The core of the transformer is rigidly fixed to the moving element of that axis. The stage is of piggyback design so that coils of the z axis are connected to the machine table and stage support and the core of transformer moves with the z axis slide. The other axis cores and transformers are similarly mounted. The cores exert negligible friction on the transformer coil casing so that the transducer does not interfere with the stage performance or cause sticking. The transformer consists of a primary coil excited by a voltage-stabilized 10 Kz oscillator. There are two secondary coils connected in opposition. The amount of signal induced in these coils is controlled by the moving core. This arrangement provides an AC signal proportional to the position of the core with "infinite" resolution (practically about .25 μm corresponding to 10 ppm) of the 2.5 cm range. The signal goes through an amplifier

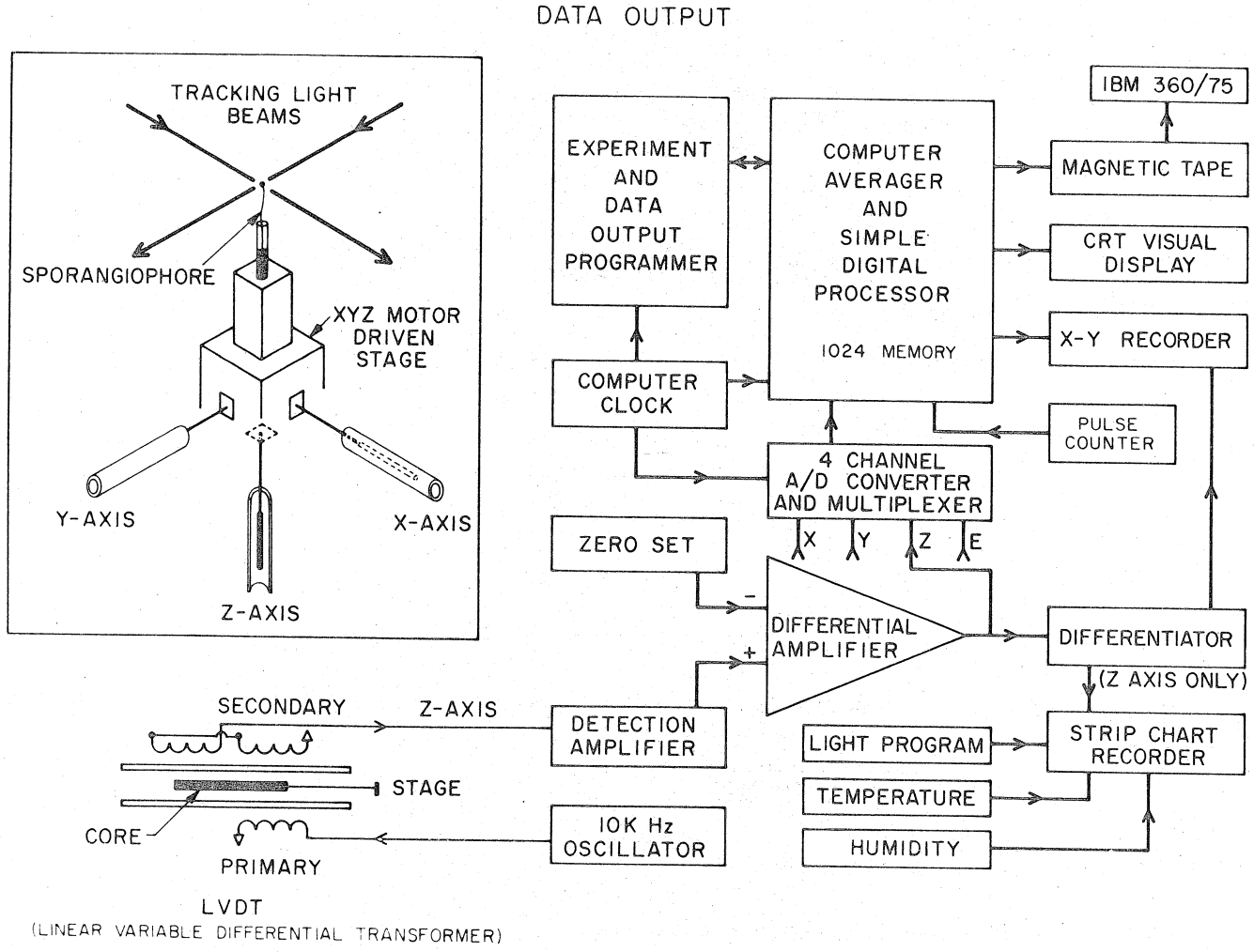
DATA OUTPUT
TRACKING LIGHT BEAMS
SPORANGIOPHORE
XYZ MOTOR DRIVEN STAGE
Y-AXIS
X-AXIS
Z-AXIS
EXPERIMENT AND DATA OUTPUT PROGRAMMER
COMPUTER AVERAGER AND SIMPLE DIGITAL PROCESSOR
1024 MEMORY
IBM 360/75
MAGNETIC TAPE
CRT VISUAL DISPLAY
X-Y RECORDER
PULSE COUNTER
COMPUTER CLOCK
4 CHANNEL A/D CONVERTER AND MULTIPLEXER
X
Y
Z
E
ZERO SET
DIFFERENTIAL AMPLIFIER
DIFFERENTIATOR
(Z AXIS ONLY)
SECONDARY
Z-AXIS
DETECTION AMPLIFIER
LIGHT PROGRAM
STRIP CHART RECORDER
STAGE
TEMPERATURE
CORE
IOK Hz OSCILLATOR
HUMIDITY
PRIMARY
LVDT
(LINEAR VARIABLE DIFFERENTIAL TRANSFORMER)

Fig. III-2.

and detector circuit which changes the signal to a DC level proportional to position of the transformer core and thereby to the displacement of the sporangium relative to the stage. This signal is fed to a differential amplifier which provides DC balance control and some further amplification and filtering. Given the limitations of accuracy and time response capability of the machine the signal bandwidth of .1 Hz has been chosen. First there is a third order low pass filter with about 3 sec time constant. This filtered signal is sent to analog-to-digital (A/D) convertors and for the vertical z-axis to an analog differentiator. The .1 Hz filtered differentiator output which corresponds to the velocity of sporangiophore growth is fed to a graphical recorder for immediate observation.

The A/D convertor digital output is stored in the memory of a instrument computer (Fabri-Tek model 1060) and can be also stored on magnetic tape for later computer analysis or displayed on the oscilloscope. The computer can be controlled automatically from the "experiment programmer" which will be discussed later in section II.C-6d.

For details of the data collection system see Appendix B, p. and for details of the data analysis using the computer see Appendix C, p. 214.

4. Visual Observation

At 45° to the x and y tracking beams is a visual observation light beam. This light backlights the sporangium to provide a 5 mm field of view. Either a movie camera or TV camera may be used to record the view. Although only wavelengths of light above Phycomyces visual sensitivity may be used there is no difficulty in providing enough light for an inexpensive vidicon tube, since such a tube has considerable sensitivity from 600 to 800 nm. A videotimelapse recorder can be used if a long record is required. A TV monitor in the adjacent electronics room enables one to see whether the specimen is properly tracking. The technique will become especially valuable if cell rotation experiments are being done since markers on the specimen may easily be seen to move around the sporangiophore.

For further details see Appendix D, p. 219.

5. Environmental Control

Since it has not been clear what the effects of avoidance, wind, temperature and humidity are on the growth of Phycomyces, the best procedure is to minimize changes in these variables when investigating effects of light stimuli. Some indication of these effects are included in avoidance (see Section IV.G) and temperature sections (IV.D-1).

Avoidance experiments with the machine suggest that in the absence of wind and thermal gradients the removal and insertion of walls near Phycomyces of a 2.5 cm square house has only a small effect on the growth of Phycomyces. A 1.5 cm square house however produces a significant response. The design of the spph house actually used provides ~ 2.5 cm in all directions to walls and the servo system fixes the reactive growing zone in one place relative to these barriers. These precautions should reduce "avoidance" influence.

The effect of wind is reduced by limiting air flow by almost completely enclosing the spph in its house. Thermal stabilization of the house and the keeping of heat sources out of the chamber prevent internal thermal gradients from causing winds.

The spph house is an approximately 15 x 7.5x 10 cm milled out aluminum block, with windows and a door. The heat conducting block minimizes temperature gradients. Three thermistors (Fenwal Electronics), a GB31J3, 1.5K at 25°C, mounted against the aluminum block in series

with two GB41L1 (10K) thermistors connected in parallel hanging in free air near the sporangium, detect the chamber temperature. These form one leg of a wheatstone bridge (circuit diagram Fig.III-3). Another leg is a temperature controlling potentiometer allowing adjustment from 15° to 30°C. Output drives electrically in series two thermoelectric devices (Borg-Warner type 930, 19 watts of cooling each) mounted on the outside of the aluminum block one on each side. If necessary, two additional elements type 492 (2.6 watts each) could be added near the position of the spph.

The thermistor on the block anticipates the change of the air temperature and so reduces overshoot during changes in heat load or temperature setting. Gain changes can be effected by the bridge amplifier gain.

The chamber is dull black anodized to reduce reflections and to be non-toxic to the spph. The black paint originally used reduced the growth rate.

Humidity can be controlled by feeding into the chamber appropriately humidified air at a slow flow rate. The procedure is to finely bubble filtered tap air through a water container at room temperature. This almost saturated air is passed through a multi-trayed aluminum chamber ~ 3 x 3 x 4". The input air is forced to pass over successive water filtered aluminum trays and out the top. The chamber is kept at a constant temperature from 0°-30°C using two thermoelectric devices (Borg-Warner model 950, 30 watts

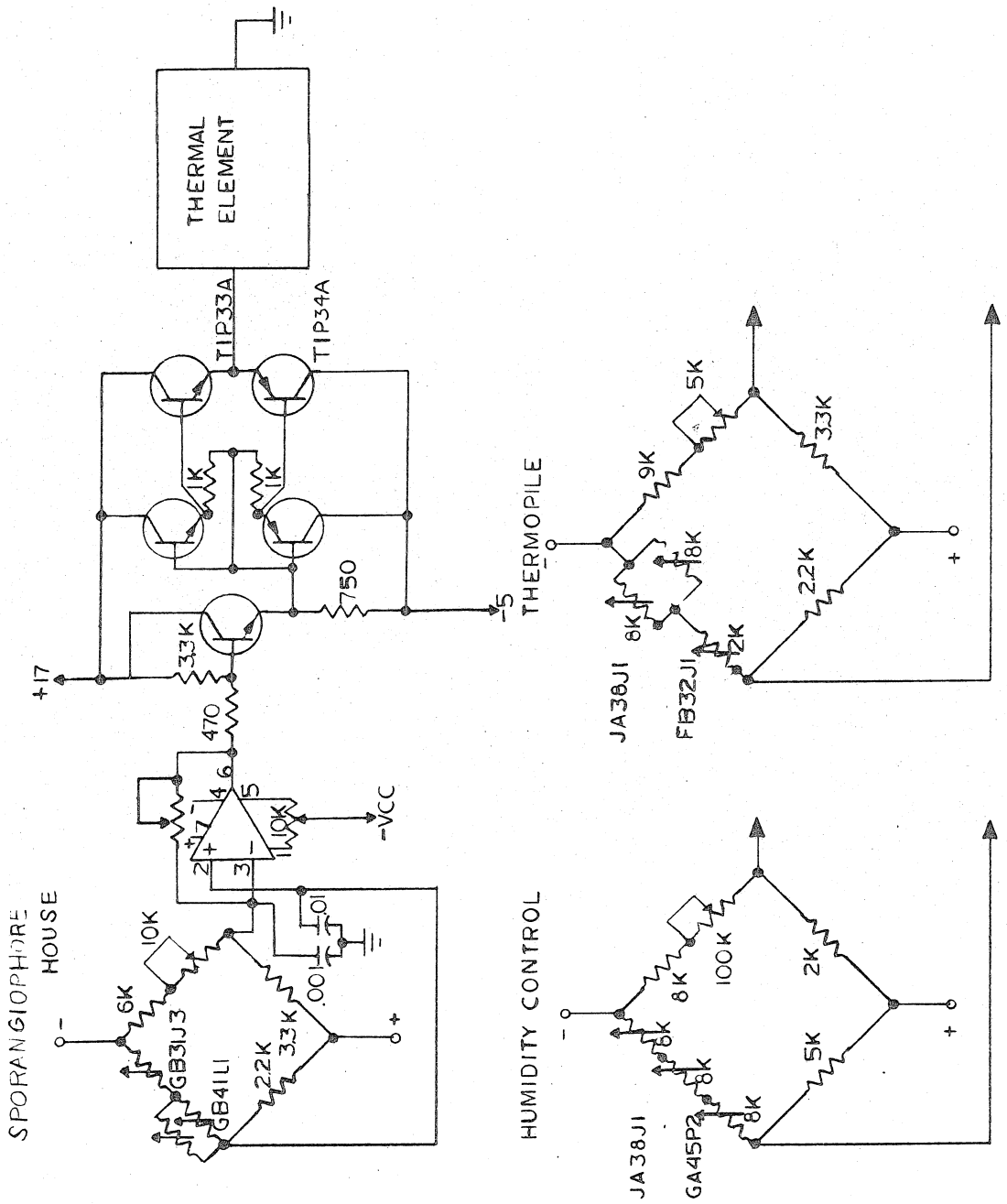

Fig. III-3. Temperature and humidity control using thermoelectric elements.

each) with essentially the same circuit explained for the spph house. Two JA3851 (8K) thermistors are used in contact with the metal case and GA45P2 (50K) in the air outlet.

The air is then passed to the spph chamber, heat exchanged with it and then bled in.

The warm saturated air loses water at the lower temperature of the humidity control chamber, i.e., it takes the saturated vapor pressure at the lower temperatures and then is warmed to the spph house temperature. The final relative humidity is the ratio of the two saturated vapor pressures.

The humidity is measured with a Yellow Springs Instrument dew point hygrometer model 91 using the 9101 probe and a 731 temperature probe in the spph house. Temperature of the humidity control chamber is checked at the air outlet with a 708 probe. This instrument provides the ambient and dewpoint as an electrical recorder output and can be recorded during the experiments.

6. Experiment Control

a. Light Sources

Various light sources have been used in the physiological experiments and here their technical specifications are summarized.

1. Argon ion laser RCA LD2108 with 28x expansion Spectra Physics collimator covers ~ 1 cm^2 of area and gives 6 mwatts of 488 nm monochromatic light.

2. Bausch and Lomb High Intensity monochromator was used with a Bausch and Lomb 5 element quartz-fluorite achromatic focusable condenser lens. Two types of sources and gratings were used; one, a quartz iodide tungsten source, 6.6 A/T2 $\frac{1}{2}$ Q/CL 45 watt, with a 500 nm blazed grating with 32 nm/mm dispersion and second a Bausch and Lomb 30 watt deuterium source with a 250 nm blazed grating, 64 nm/mm dispersion. The monochromator has an f/3.5 optical system and has variable bandwidth controlling slit which was used with a bandwidth of 2 to 10 nm.

3. Double Jerral Ash .25 meter Ebert monochromator model 82-410 was used with two gratings for each part. One for the visible region 380-800 nm blazed at 600 nm and with 3.2 nm/mm dispersion and one for ultraviolet blazed at 300 nm with 1.6 nm/mm dispersion. This monochromator

with the visible grating was used with a 3.3 nm bandwidth.

i) Ultraviolet light came from a deuterium lamp with suprasil windows (Schoffel Instrument Corp 30/60 watt lamp L201) and their LPS201 power supply (.01%, ripple, .01% line, < .01% current). The light was focused on the monochromator slit with two lenses symmetrically placed at one focal length separation. These lenses were 50 mm f.l. 1" diameter quartz (Oriel Optics A11-641-20).

ii) Visible light comes from a Q 6.6 A/T4/CL 200 watt quartz iodide tungsten lamp with a 50 mm diameter 20 mm f.l. spherical mirror (Rolyn Optics L-48-02) behind the lamp to increase the useable amount of light. This light is focussed on the slit with two symmetrically placed lenses at approximately focal length separation (Rolyn 58.8 mm f.l. achromatic lenses) and reflected by a 50 mm cold mirror (410-650 nm at 45° incidence) from Rolyn (C50-83PSP2).

The power was regulated via a 500 watt solar transformer (1% load and line) feeding a 1% Cal-Power Corp 24-32 V, DC power supply. (Unfortunately, rather a bulky item and should be replaced with light feedback control or constant current control,

e.g. Kepco JQE 36-8M, which takes 1/10 the space and gives superior performance.)

iii) High intensity arc lamp with a xenon light source, 500 watt Pek 500-A was used with a 1000 watt Hanovia Model 27801 power supply. A mercury-xenon lamp Hanovia 941B-1 is available but never was used. A better supply would be one with a photoelectric feedback, e.g. Christie Electric SCX1200-12S, as one of arc lamps main problems is variable output even at constant current.

The lamp housing was from Electropower Corp, their Universal Short Arc Lamp Housing Model 371 with front surface spherical mirror, 62 mm diameter 42 mm f.l. quartz convex lens to focus onto monochromatic slit and external controls to allow precise alignment of the optical center of the lens with the lamp arc and spherical mirror. Light is reflected onto slit with UV "cold" mirror (Rolyn C45) or the visible cold mirror.

iv) Line source calibration was done with a Oriel C-13-63 Hg lamp with C73-12 power supply and a homemade He lamp.

v) The "standard" lamp was a 150 watt GE 1958 quartz iodide tungsten lamp run at a controlled 24 V. The identical power control was used as for the visible monochromator source. Voltage was checked with a Fluke differential voltmeter across lamp terminals. This light was collimated with a Bell and Howell gunner sight lens.

b. Light Source Selector

Certain types of experimental control are required frequently in the routine handling of Phycomyces.

One is the programming of the wavelength of the source and direction of its incidence. For example, to determine the action spectrum of wild type or a mutant of Phycomyces one standard technique is the growth response null method. One alternates the illumination between a standard wavelength and a test wavelength and then on successive alternating cycles varies the test intensity and obtains by interpolation the intensity resulting in no growth response. To get straight growth, both sides of the sporangiophore have to be illuminated. A system of two movable mirror selectors is used. One mirror selects the light source and the other the side of the sporangiophore to be illuminated. Both are controlled electronically. See Fig. III-4 "Source selector and beam alternator". The side selector is alternated rapidly to provide illumination on both sides.

Another action spectrum that can be measured by a null method is that of the phototropic response. One light source is shone on one side while the standard light source is shone on the other side. After a period of time the sides are reversed producing a bending synchronized to this period. This is easily

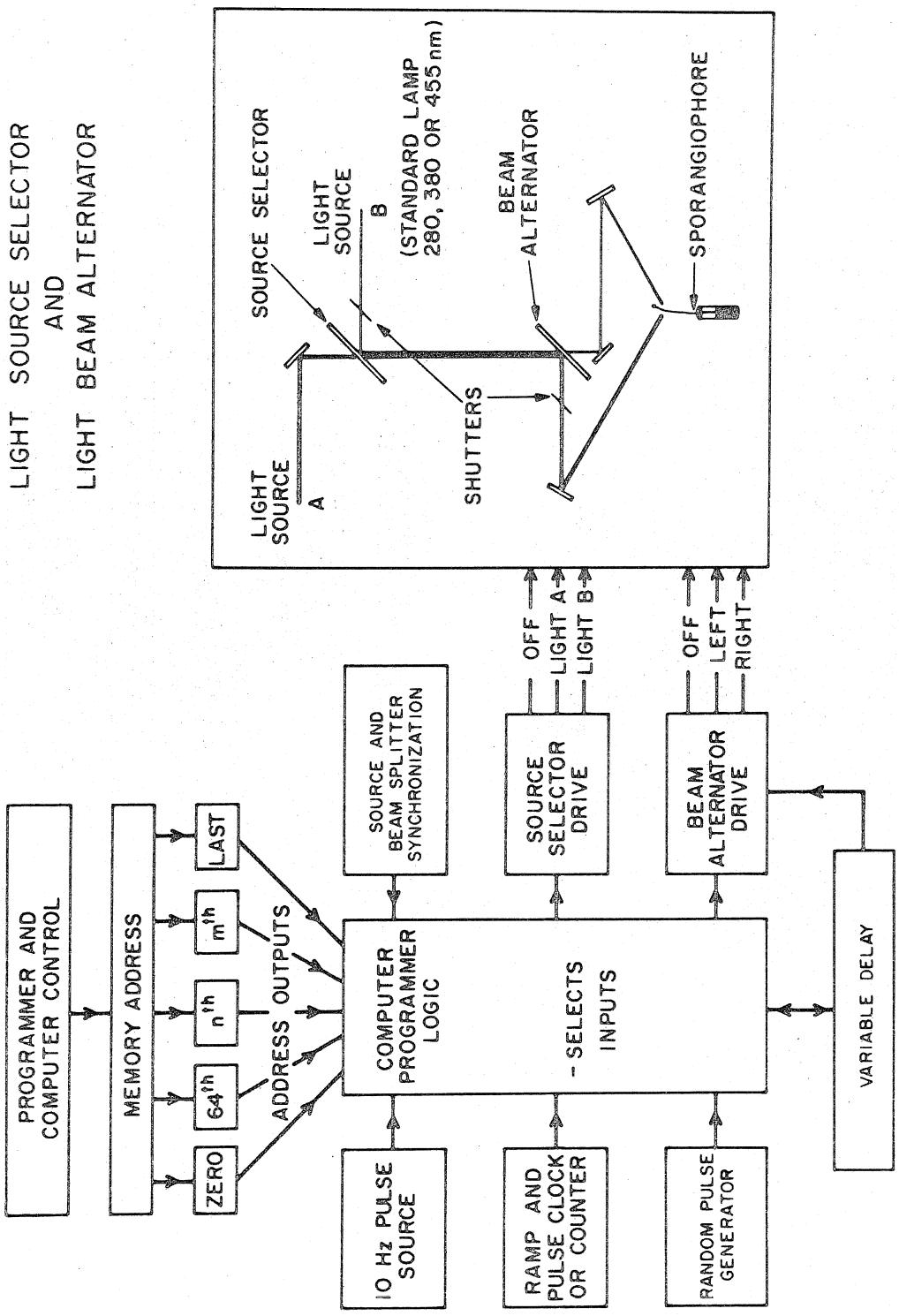
LIGHT SOURCE SELECTOR
AND
LIGHT BEAM ALTERNATOR
PROGRAMMER AND COMPUTER CONTROL
MEMORY ADDRESS
ZERO
64th
nth
mth
LAST
ADDRESS OUTPUTS
10 Hz PULSE SOURCE
COMPUTER PROGRAMMER LOGIC
SELECTS INPUTS
SOURCE AND BEAM SPLITTER SYNCHRONIZATION
SOURCE SELECTOR DRIVE
BEAM ALTERNATOR DRIVE
RAMP AND PULSE CLOCK OR COUNTER
RANDOM PULSE GENERATOR
VARIABLE DELAY
OFF
LIGHT A
LIGHT B
OFF
LEFT
RIGHT
LIGHT SOURCE A
SOURCE SELECTOR
LIGHT SOURCE B
(STANDARD LAMP 280, 380 OR 455 nm)
SHUTTERS
BEAM ALTERNATOR
SPORANGIOPHORE

Fig. III-4.

accomplished with the same system described and can be immediately programmed so that one can compare tropic and growth balances on the same specimen for an estimate of focusing advantage and screening.

Of course other systems may be used. A source consisting of a circular array of light pipes converging on the spph has been considered. For visible light this would provide several capabilities, one is as a non-directional source as uniform as possible around the specimen for stimulus response measurements (Appendix H-3). A rotating light source may also be provided this way.

Since light pipes do not transmit UV an alternate system is necessary. Such a system could be built using a rotating mirror (see Appendix H-3).

See Appendix E, p.220 for details on the light source selector.

c. Light Source Intensity Control

The intensity is controlled by a 6 inch diameter circular, optical flat, 220 to 700 nm neutral density wedge which may be rotated quickly from one density to another by a stepping motor providing an essentially continuously variable intensity and easy programming. The wedge is a Kodak inconel A 6040 on GE-105 quartz which is operated to provide about 750 positions between 0.15 and 4.0 O.D.

Ramp and pulse experiments as well as step changes of intensity are easily accomplished. Versatile programming of intensity can be set up. See Fig. III-5 "Programmed intensity control." Of course additional filters may be added in the light path to provide a wider range of intensities.

The control program illustrated in the figure shows how the light intensity is changed from one level to another level always through intermediate intensities. A number corresponding to the actual position of the wedge, is kept in a counter. When a new position corresponding to another number is requested the wedge is rotated in the appropriate direction until the correct position is reached.

See Appendix F p. 225, for details.

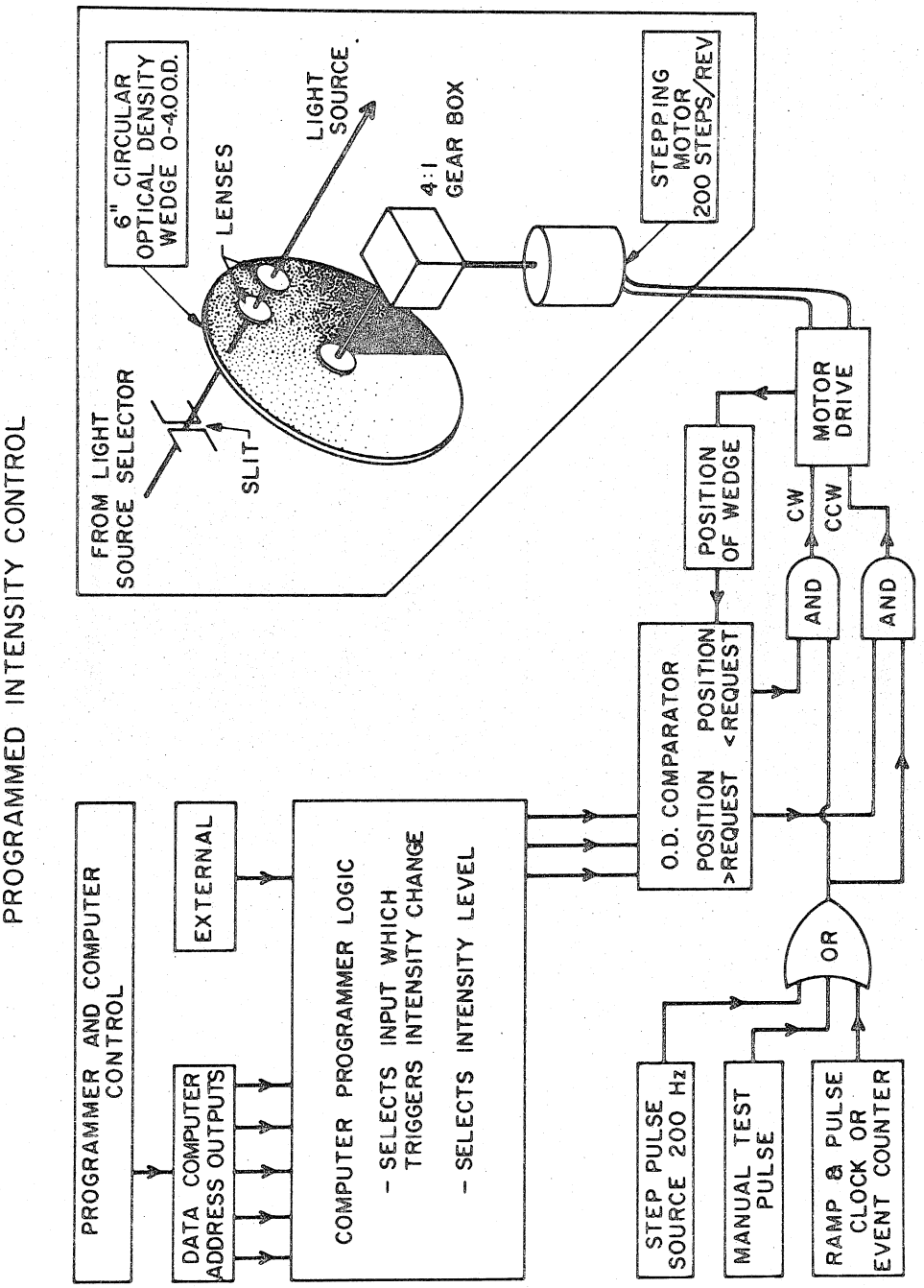
PROGRAMMED INTENSITY CONTROL
PROGRAMMER AND COMPUTER CONTROL
DATA COMPUTER ADDRESS OUTPUTS
EXTERNAL
COMPUTER PROGRAMMER LOGIC
- SELECTS INPUT WHICH TRIGGERS INTENSITY CHANGE
- SELECTS INTENSITY LEVEL
O.D. COMPARATOR
POSITION >REQUEST
POSITION <REQUEST
POSITION OF WEDGE
FROM LIGHT SOURCE SELECTOR
SLIT
6" CIRCULAR OPTICAL DENSITY WEDGE 0-4.0 O.D.
LENSES
LIGHT SOURCE
4:1 GEAR BOX
STEPPING MOTOR 200 STEPS/REV
MOTOR DRIVE
CW
CCW
AND
AND
OR
STEP PULSE SOURCE 200 Hz
MANUAL TEST PULSE
RAMP & PULSE CLOCK OR EVENT COUNTER

Fig. III-5.

d. Experiment and Data Handling Programmer

Control of a variety of experiment program functions have been put together into an experiment programmer. Two of these functions, the light source selector and light beam alternator and the programmed intensity control have already been briefly discussed.

There are several other functions included in the programmer, a ramp or light pulse clock, an address control and a digital display of the O.D. wedge position and present computer memory address.

The clock divides down a 1 KHz signal from the main computer and allows flexibility in setting the rate of a "sunrise" experiment, i.e. the rate the O.D. wedge is stepped providing an exponentially increasing light level. This clock can also be used to set the length of a pulse stimulus.

The address control is a counter which keeps track of the instrument computer's address. Address corresponds to time in the signal averager's cycle.

Means have been provided to initiate an experimental change by setting digit switches at any two variable addresses or their corresponding times. A third digit switch sets the number of addresses in any cycle and coupled with the instrument clock's time interval between each address, this digit switch

sets the length of the cycle.

The digital display tells the O.D. wedge position and present address to ease the anxious experimenter.

All the various functions are linked together with a patch board (Fig. G-4) allowing the experimenter to program the various functions together to do action spectra, stimulus response curves, "sunrise" experiments or whatever.

See Appendix G, p.231 for details.

e. Light Intensity Measurement

Light measurements are given in units of watt/cm^2 with designated wavelength, λ. These values can be converted to picoeinsteins/cm^2 sec or quanta/cm^2 sec through the following formulas:

1 μwatt/cm^2 = 5.03 x 10^{12} (λ μm) quanta/cm^2 sec

1 picoeinstein/cm^2 sec = 6.02 x 10^{11} quanta/cm^2 sec

1 μwatt/cm^2 = 8.35 (λ μm) picoeinsteins/cm^2 sec

Delbrück and Reichardt (1956) introduced a logarithmic intensity scale with a unit intensity ($\log_2$ I = 0) equal to 10 μwatts/cm^2 of an incandescent source with a Corning 5-61, 5 mm thick filter. The logarithms are taken to the base 2 so that each unit on this scale corresponds to a doubling of the intensity.

Comparison to this scale which was designed for broad blue light (see curve, Bergman et al., 1969, section 38) can be made approximately through use of the action spectra (Fig. IV-3 and Fig. IV-4). According to Delbrück and Shropshire (1960) 22 nwatts/cm^2 at 440 nm corresponds to an intensity of I = - 8 in the Delbrück and Reichardt scale. Table III-2 gives a comparison of the different units for the important intensity levels of Phycomyces data.

Table III-2. Comparison of Different Intensity Scales

	Energy at 440 nm	Delbrück and Reichardt scale (1956) (correct for broad blue) $\log_2 I$ =	Intensity (440 nm) picoeinsteins/cm^2 sec	quanta (440 nm) incident on growth zone (.002 cm^2) quantum/sec
High Intensity Threshold	360 μwatts/cm^2	+8	1320.	1.6×10^{12}
"normal range" top	5.6 μwatts/cm^2	0	20.4	2.5×10^{10}
"normal range" bottom	22 nwatts/cm^2	-8	8.1×10^{-2}	9.7×10^{7}
A_D^*	9 pwatts/cm^2	-19.2	3.3×10^{-5}	4×10^{4}
I_T (geophototropic threshold)	.15 pwatts/cm^2	-25.2	5.5×10^{-7}	700

Notes:

*A_D: adapting below A_D will give no further increase in size of response to a pulse of some absolute intensity.

Light has been measured with several different pieces of equipment and these are summarized below:

1. To check intensity as a function of wavelength

   a) Hewlett Packard Radiant Flux Meter 8335A with a Model 8334A Radiant Flux Detector option 013 with T19 Supersil 1 optical window. This has a flat response ±3% or less from 180 to 1300 nm but is poor below one μwatts/cm^2 incident energy.

   b) Charles M. Reeder RBL-500 thermopile with #7049 Corning Quartz window measured with a Keithley 150B microvoltmeter.

2. A more sensitive broad range detector was also used. United Detector Technology Schottky Barrier ultraviolet enhanced photodiode (PIN 10 UV). The current was measured with a Princeton Applied Research PAR 134 electrometer.

3. Also available to measure the lowest intensities is a EMI 6256B photomultiplier tube with 1 cm cathode, spectrosil window and type S-13 sensitivity.

4. Often Ealing calibrated quartz inconel neutral density filters were used additively and the light intensity was determined to sufficient accuracy by measuring the light without the filters and then adding the calibrated values.

REFERENCES

Berg, H. C. 1971. How to track bacteria. Rev. Scient. Instrum. 42: 868-871.

Bergman, K. 1972. Sensory responses of Phycomyces: I. Blue-light control of sporangiophore initiation. II. Classification of mad mutants. Ph.D. Diss. Califor. Instit. Tech. Pasadena, Calif., pp. 101.

Castle, E. S. 1940. Discontinuous growth of single plant cells measured at short intervals, and the theory of intussusception. J. Cellular Comp. Physiol. 15: 285-298.

Davenport, D., G. J. Culler, J. O. B. Greaves, R. B. Forward, and W. G. Hand. 1970. IEEE Bio-Med Eng. BME-17: 230-237.

Delbrück, M. and W. Shropshire, Jr. 1960. Action and transmission spectra of Phycomyces. Plant Physiol. 35: 194-204.

Oort, A. J. P. 1932. Die Wiederherstellung der empfindlichkeit nach einem lichtreiz. Verhandel. Konikl. Ned. Akad. Wetenschap. 29: 5-47.

Strumwasser, Felix. 1971. The cellular basis of behavior in Aplysia. In J. V. Brady (ed.). Problems, Practices and Positions in Neuropsychiatric Research. J. Psychiat. Res. 8: 237-257.

IV. EXPERIMENTS, RESULTS AND DISCUSSION

Mutants of the carotenoid pathway were among the first to be isolated from Phycomyces. They were selected for their color, either albino or red due respectively to the absence of colored carotenoids or to the presence of lycopene. One particularly transparent mutant has provided us with an excellent opportunity to obtain an undistorted action spectrum in the visible region. These mutants which differ in the extent of absorption by screening pigments and scattering by particulates have allowed us to study the effect of these two causes of attenuation on the tropic and growth responses. The relative effect of these pigments and scattering interspersed or interposed between the receptors can be assessed by experiment. These studies also permit an estimate of the focusing effect of the cell on the tropic response.

A. CAROTENOID MUTANT ABSORPTION SPECTRA

Essential to this discussion are the absorption spectra of wild type (NRRL1555) and of several carotenoid mutants. The transmission of light through the small photosensitive regions of individual spphs (Fig. IV-1) has been measured using a Cary model 15 spectrophotometer with a microscope attachment (Zankel et al, 1967). A narrow 5 μm slit of light 100 μm long aligned with the cell axis was focused in the center of the spph with a 20X, 0.5 N.A. (numerical aperture) microscope

Fig. IV-1. Absorption Spectra

Strain	NRRL1555	C5	C9	C2	C2
Genotype	Wild type (-)	car-10	carR21	car-5	car-5
media	PDA	PDA	PDA	PDA	LAC
mean diameter (μm)	100	81	68	103	104
cytoplasmic thickness (μm)	27	21	17	26	30
number of specimens	7	3	1	4	1

A 5 μm by 100 μm slit of light from the Cary 15 spectrophotometer was aligned with the cell and centered 1.3 mm down from the base of sporangium. The amount of transmitted light was measured.

PDA = potato dextrose agar

LAC = Lactate (Zankel et al, 1967)

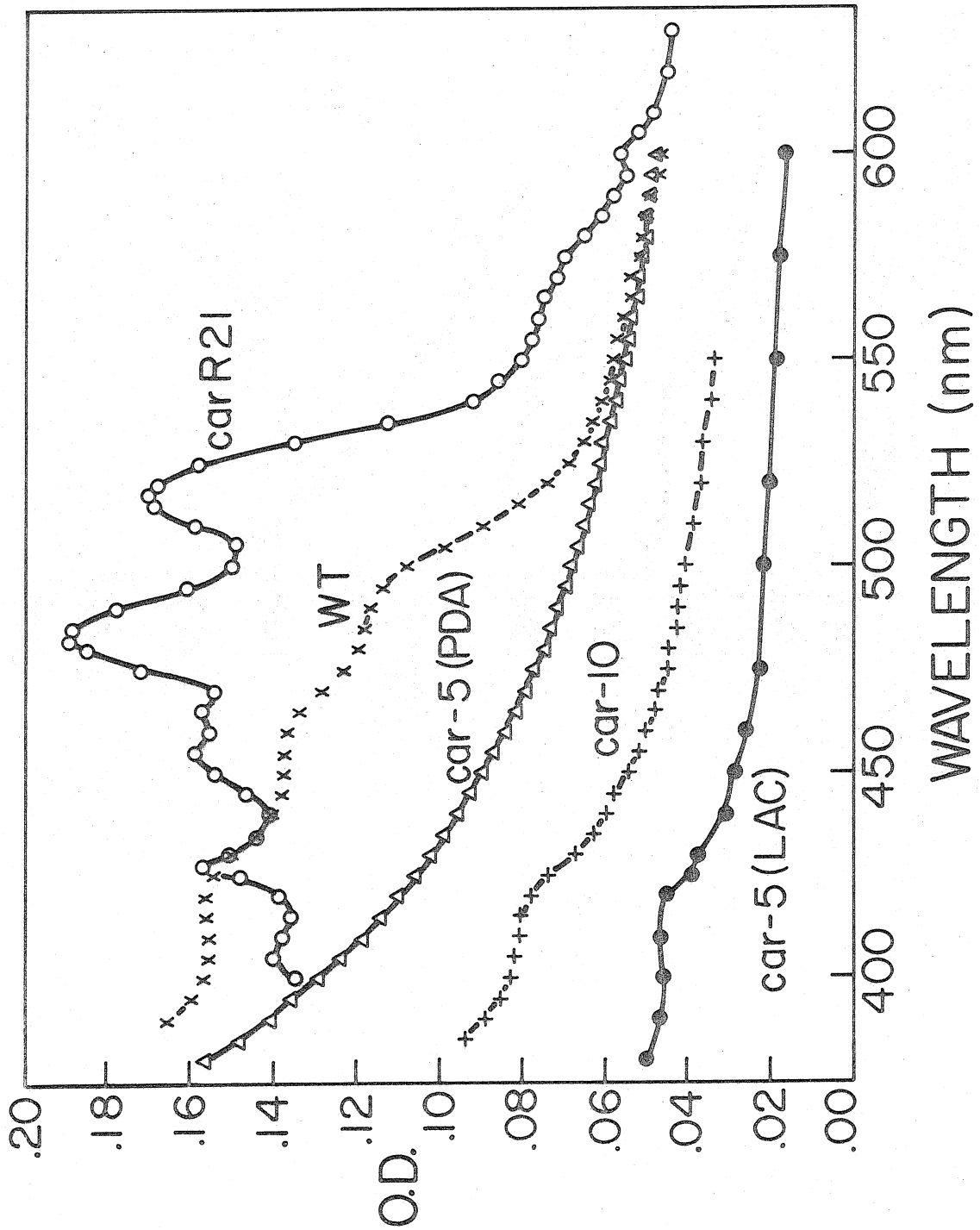
carR21
WT
car-5(PDA)
car-10
car-5(LAC)
O.D.
.20
.18
.16
.14
.12
.10
.08
.06
.04
.02
.00
400
450
500
550
600
WAVELENGTH (nm)

objective. The transmitted light was collected by a 90X 1.30 N. A., oil immersion objective. This high numerical aperture objective was found satisfactory for collecting much of the scattered light. The narrow slit was focused on the center of the spph to minimize scattering off the cell wall and off the somewhat irregularly shaped vacuole.

Absorption spectra of wild type (NRRL1555) were measured by P. V. Burke (Zankel et al, 1967). CarR21 shows lycopene absorption peaks at 517, 583, 455, and 425 nm. With extra thick specimens of wild type or tips of Stage I spphs the absorption spectra show clear peaks at 490 and 462 nm attributable to β-carotene, although normal stage IVb specimens (Fig. IV-1) show this absorption only as shoulders. Car-5 and car-10 show mostly scattering with the exception of a 0.01 O.D. (optical density) cytochrome peak at about 410 nm (Wolken, private communication, isolated cytochrome, c_{552}). This peak is particularly evident on car-5 grown on lactate (LAC) medium (Fig. IV-2). A pigment with an absorption spectrum similar to the action spectrum is not observed.

Fig. IV-2.

Absorption spectrum of C2 grown on "LAC" medium on expanded scale with another curve from the same data, but corrected for scattering assumed proportional to λ^{-4} showing more clearly what is probably a cytochrome peak.

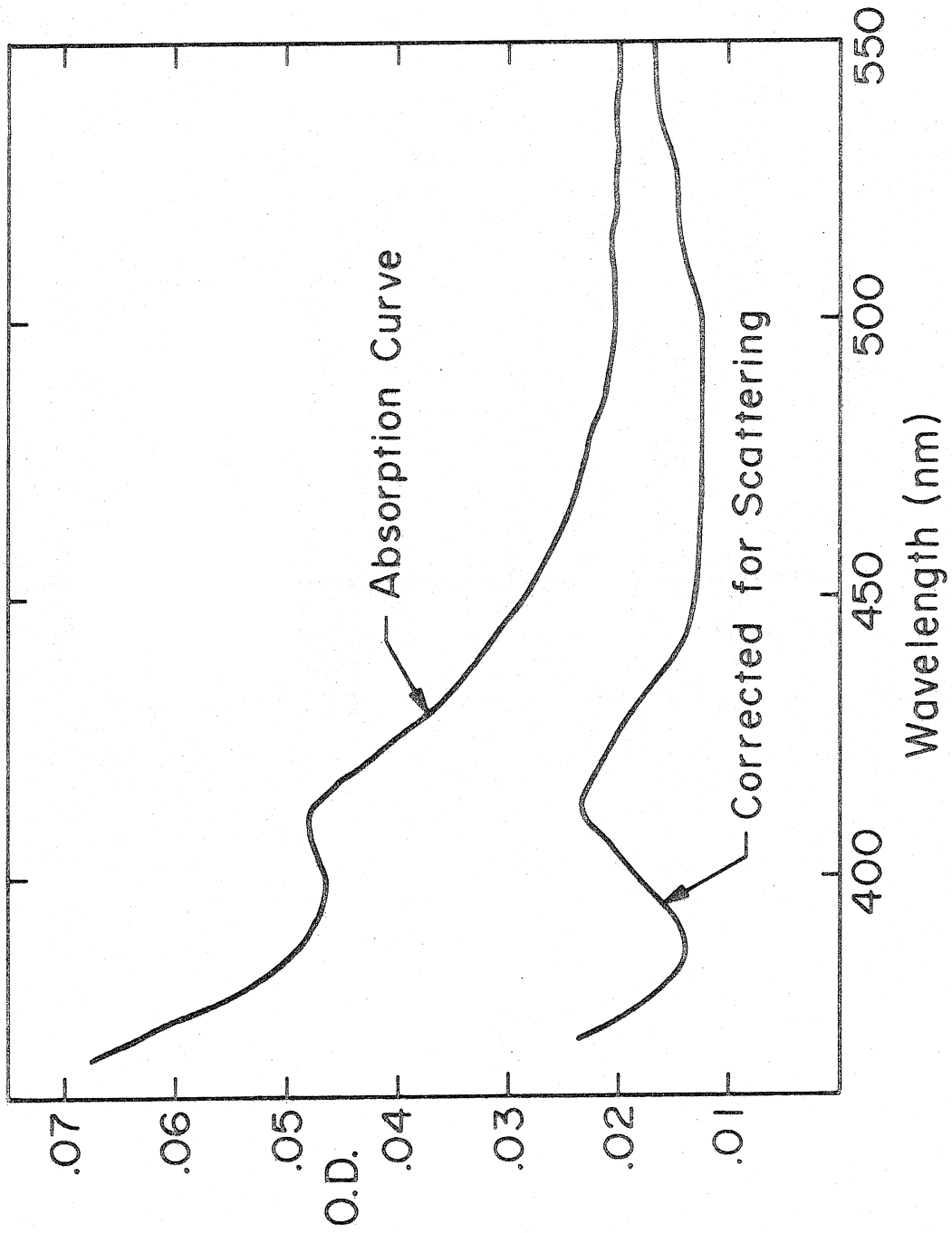
.07
.06
.05
.04
.03
.02
.01
O.D.
400
450
500
550
Wavelength (nm)
Absorption Curve
Corrected for Scattering

B. ACTION SPECTRUM OF TRANSPARENT MUTANT

A phototropic action spectrum was measured for the phototropic response of the albino mutant C2 (genotype car-5) between 445 and 560 nm. This mutant was chosen because it has only 1 to 2% of the β-carotene in wild type and has no other carotenoids, thus minimizing the influence of pigments on the shape of the action spectra (Meissner and Delbrück, 1968). This mutant was also chosen because it is a healthy grower and has a low light intensity threshold of .13 pwatts/cm^2 (blue) (Bergman, 1972). (See Section III.C-6e, Light Intensity Measurement,for discussion of intensity units.) This value is within 15% of wild type, i.e. identical within measurement error.

C2 was grown on lactate medium (Zankel et al, 1967) which apparently inhibits phenol polymerization and limits glycogen production (Meissner and Delbrück, 1968). This mutant and medium were chosen in order to minimize internal absorption and scattering. The absorption spectrum through a single specimen is shown in Fig. IV-2. The cytochrome peak is the most dominant feature.

The action spectrum of the phototropic response was measured using a null method. One light source of an adjustable wavelength is shone on one side while a standard source of a fixed wavelength is shone on the opposite side. After a period of 4 to 6 hours the orientation of the spphs is measured. The null or equal effect of

both light sources is interpolated from several measurements at different relative intensities of the source.

480-560 nm region

The region from 480-560 nm was studied near the low intensity threshold of the growth response. The standard intensity used was about 40 pwatts/cm^2 at 440 nm. This corresponds to approximately $\log_2 I = -18$ on Delbrück and Reichardt scale (Delbrück and Shropshire, 1960, also Section III. C-6e). Both C2 and wild type were studied and no significant difference was observed. Therefore a detailed curve for this spectral region of only C2 was made as shown in Fig. IV-3.

The experimental setup consisted of two opposed light sources. From one side the specimen was illuminated with a tungsten source (GE 1958-150 watt quartz iodide) with a 440 nm interference filter. This light was collimated to provide a large beam approximately 3 cm in diameter incident at 60° to the vertical. Shining on the other side of the specimen, also incident at 60° to the vertical, was the Bausch and Lomb high intensity monochromator source collimated with the Bausch and Lomb quartz-fluorite achromatic condenser lens. The monochromator was used at a 2 nm bandwidth and with cut-off filters, either two Schott OG 495 or two OG 520 (the numbers correspond to the 50% peak transmission wavelength in nm for a 3 mm thick filter). The Bausch and Lomb monochromator has about .05% scattered light from

outside the set bandwidth. A heat filter, Schott 6143, was also included in the light path. Specific neutral O. D. filters and cut off filters were added to the monochromator light beam and the wavelength adjusted until on the average the group of 5 or 6 specimens grew close to vertical. This was tested on both sides of the null point and the null wavelength was chosen by interpolation.

In Fig. IV-3 the action spectrum for the region 480-560 nm is plotted as the log of the (relative quantum efficiency)$^{-1}$ as a function of the wave number, ν. For ν_{max} = 450 nm, a plot of the logarithm of (relative quantum efficiency)$^{-1}$ as a function of $(\nu_{max} - \nu)^2$ yields, a straight line fit for the low frequency tail. A straight line fit is also obtained in the vicinity of the 480 nm peak for ν_{max} = 483 nm. In fact, the action spectrum above 445 nm can be fitted well with two Gaussian shaped bands peaked at 483 and 450 nm.

i.e.
$$\varepsilon = \varepsilon_1 \, e^{-65\ \mu m^2 (\nu_{450} - \nu)^2} + \varepsilon_2 \, e^{-250\ \mu m^2\ (\nu_{483} - \nu)^2} \qquad \text{(B-1)}$$

where $\varepsilon_2/\varepsilon_1 \cong 0.50$ (See Fig. IV-3 and IV-4.)

The motivation for studying this long wavelength tail was the possibility that the photoreceptor pigment might be a metalloflavoprotein which

Fig. IV-3.

Phototropic null action spectrum for C2. The logarithm of the (relative quantum efficiency)$^{-1}$ is plotted from 480 to 560 nm. The standard was about 40 pwatts/cm^2 of 440 nm. The solid curve is the fit of equation (B-1).

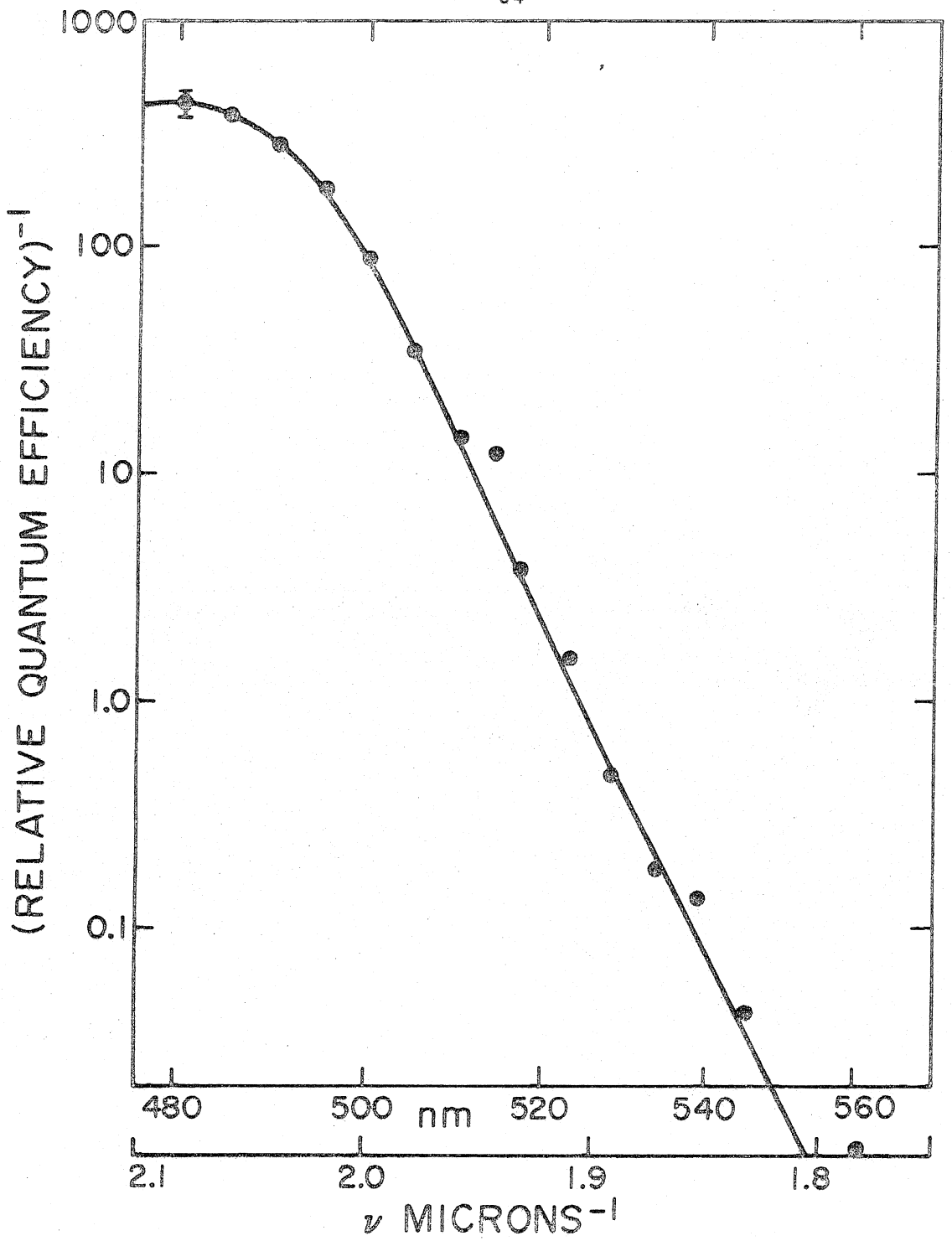
1000
100
10
1.0
0.1
(RELATIVE QUANTUM EFFICIENCY)$^{-1}$
480
500
nm
520
540
560
2.1
2.0
1.9
1.8
ν MICRONS^{-1}

should exhibit a shoulder around 550 nm. However, no such shoulder is indicated.

445-500 nm Region

The blue 445-500 nm region was studied in a somewhat different manner. The results are shown in Fig. IV-4. The standard light source was approximately 40 nwatts/cm^2 at 440 nm,effectively in the "normal" intensity range and 1000 times as bright as was used for the lower energy tail. The physical setup was identical. Small O. D. filters, 0.1, 0.2, 0.3, or 0.4 were inserted in either the test or standard beam in order to get points on both sides of the null condition of vertical growth. The angle of 5 or 6 specimens was measured after 4-6 hours with a Gaertner angle measuring protractor. Approximately every hour the specimens were lowered to compensate for their growth and thereby insure that they had even illumination throughout the period. At least two separate groups of spphs were tested at each intensity and wavelength. The angle of the spphs changes about 10° per 0.10 O.D. difference.

This 445 to 500 nm phototropic action spectrum of C2(car-5) is shown in Fig. IV-4 with the growth action spectrum of wild type, (Delbrück and Shropshire, 1960) and phototropic action spectrum of wild type (Curry and Gruen, 1959). The main peak of all three spectra is at 450 nm with a subsidiary peak at 480 nm. The only difference between them is the relative height of the 450 and 480 nm

Fig. IV-4.

crosses x — Phototropic null action spectrum of C2 (*car-5*) grown on LAC media with the standard 40 nwatts/cm^2 of 440 nm. The solid curve is the fit of equation B-1.

open circles o — Growth action spectrum of wild type (Delbrück and Shropshire, 1960) with the standard broad blue source equivalent to about 22 nwatts/cm^2 of 440 nm.

open squares □ — Phototropic action spectrum of wild type (Curry and Gruen, 1959). The solid curve is the fit of equation B-1.

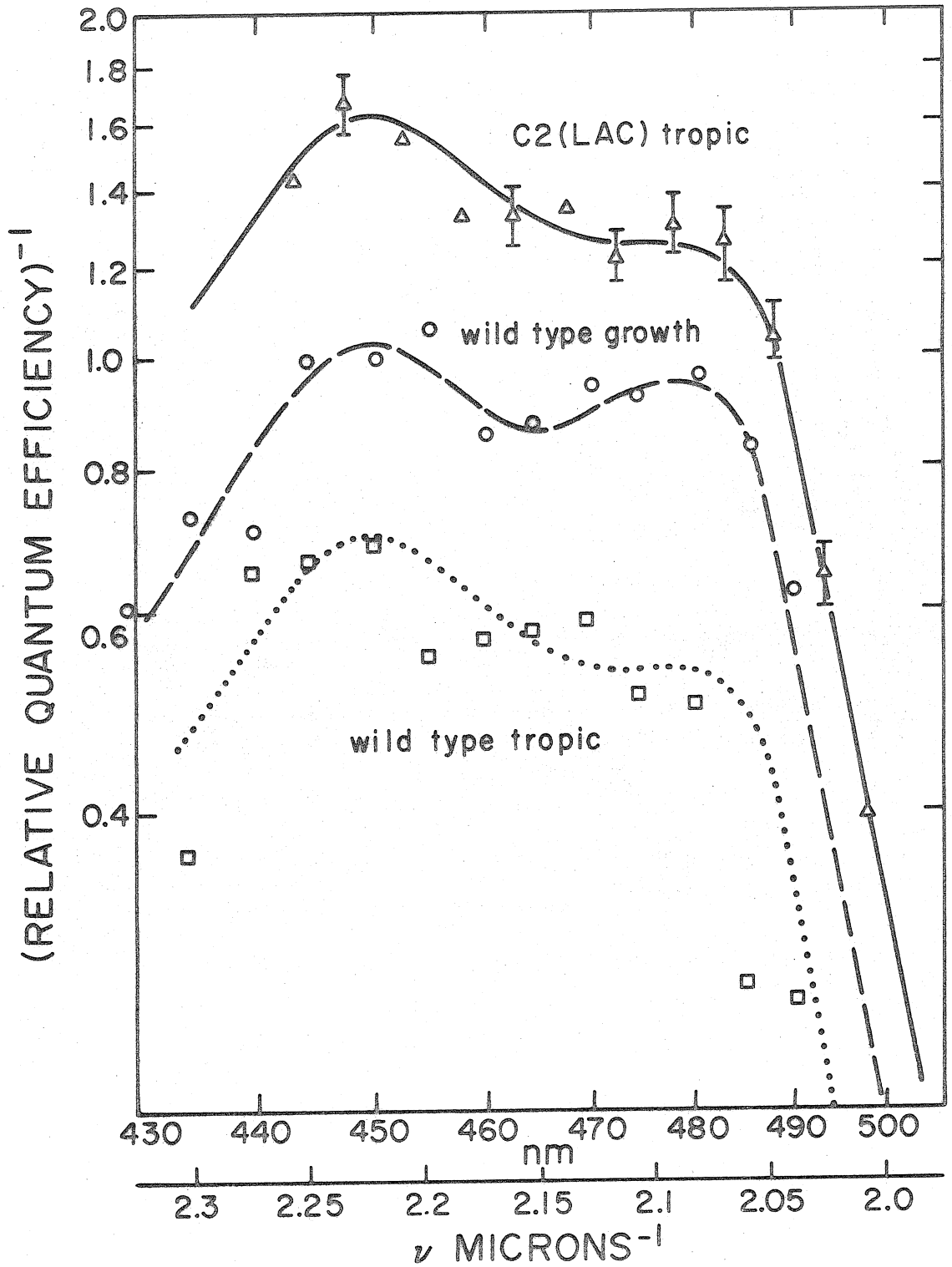
(RELATIVE QUANTUM EFFICIENCY)$^{-1}$
2.0
1.8
1.6
1.4
1.2
1.0
0.8
0.6
0.4
C2(LAC) tropic
wild type growth
wild type tropic
430
440
450
460
470
480
490
500
nm
2.3
2.25
2.2
2.15
2.1
2.05
2.0
ν MICRONS^{-1}

maxima and possibly the depth of the 460 minima. Because of the absence of β-carotene and the reduced scattering of the car 5 mutant grown on LAC media the new action spectrum may be more accurate. As mentioned by Delbrück and Shropshire (1960) peripheral or external screening by β-carotene or scattering may account for part of the 460 nm dip in the wild type.

Two major sources of error for these determinations of the action spectra are the effects of polarization of the light source which matters because of the preferred absorption of orientated photoreceptors and errors in calibration of the light source. A. Jesaitis (private communication) has shown that for the blue light growth response with the light incident perpendicular to the stalk of the spph, the vertically polarized light is more effective than the horizontally polarized light. Jesaitis calibrated this effect with unpolarized light and found the difference in effective intensity to be about 20%.

Light from a grating monochromator is partially polarized and the degree of polarization varies with the wavelength setting. Typically the ratio of horizontally to vertically polarized light may vary from one-half to two. Consequently, the effect of polarization could realistically result in a 10% error in the measured relative quantum efficiency at any wavelength. However, this would be a slow function of wavelength.

Finally, the relative calibration of the light source over a range of wavelengths is certainly not better than 3%. The absolute calibration, although not vital here, is probably not better than 50%.

C. STUDY OF PHOTOTROPISM

1) Introduction

That focusing is essential for phototropism in Phycomyces was conjectured by Blaauw (1914) and proven by Buder (1920) more than 50 years ago. Exactly how focusing brings about the differential growth on the proximal and distal sides has remained an unsolved puzzle. Blaauw tried to relate this effect to the light growth response, which he had discovered. This response consists of a transient increase in growth rate in response to a step-up in light intensity. A transient growth response might explain a transient tropic response, when the unilateral light is first turned on. This initial transient does occur and can be seen especially clearly with 280 nm light. However, typically, the tropic response is a sustained response, sustained indefinitely if the geometrical relations between light source and specimen are maintained constant.

Blaauw (1914) argued that focusing causes a higher light flux in the central band on the distal side, higher than anywhere else on the proximal side and that this higher intensity, in turn, causes faster growth. This explanation is clearly insufficient since the total flux through the distal side is certainly less than that through the proximal side, due to losses of light in transit, by scattering from particulates and by absorption by β-carotene.

Buder (1946) argued that light absorbed on the distal side is more effective because on the distal side the average distance of the stimulated receptors from the midline is greater. Calculations including this lever action weighting factor do give a net advantage to the distal side, but it is small even if one assumes that all the receptors are close to the cell wall. Further, this advantage is completely lost with only a small amount of absorption or scattering of light in the cytoplasm.

Castle (1933) argued that in a focused beam the mean length of the light path traversed in the distal half is larger than on the proximal half, if one assumes that the receptor pigments are not at the cell wall but uniformly distributed. Calculation of this path length model gives just as small a value for the net advantage of the distal side as does the lever arm model. In fact in the simplest case (ignoring the vacuole) the mathematical expressions are identical (Bergman et al., 1969). If attenuation terms are included in this model then this model, too, is very sensitive to small amounts of absorption.

The main trouble with both these calculations is that they might explain a transient differential growth response, but not a sustained one. We know that the growth response to a step-up is transient because the sporangiophore adapts to the stepped-up intensity, with

a time delay of a few minutes. Why does the sporangiophore not adapt to the differential intensities created by focusing? Two suggestions have been made in answer to this dilemma.

(a) If two regions of the sporangiophore are illuminated with different intensities local adaptation may not mirror these intensities precisely, but a certain degree of "smearing out" or spreading of adaptation may occur. An extreme assumption would be that adaptation is completely averaged around the circumference. In that case the intensity in the focused band would remain in excess over the averaged level of adaptation, thus justifying a sustained differential, i.e. tropic response.

(b) The other suggestion assumes that local adaptation does mirror closely the local intensities, but takes into account that the sporangiophore twists at an appreciable rate (typically about 6°/min in the middle of the growing zone). Therefore, at one edge of the focused band there will be a continuous entry of dark adapted surface area in the band. This gives rise to a transient positive growth response in a succession of surface elements and to a sustained positive phototropic response exhibiting an aiming error. We will call this edge the leading edge, since it is leading in the motion of the focused band relative to the twisting cell wall.

We now have ample evidence that suggestion (b) is relevant. Some new experiments on aiming errors (section IV.C-4) give proof

that the twist of the cell is important. It should be noted that the twist of the cell would have no effect if spreading of adaptation were rapid. At present we have no evidence that spreading of adaptation occurs to an extent that is relevant to our discussion of the phototropic effects.

With respect to this model we should note two points before proceeding to a discussion of experiments.

(a) While we will assume rather sharp intensity contrasts at the edges of the focusing band and correspondingly sharply contoured local adaptation, we must assume that the response is smoothly distributed around the circumference, since otherwise the cell would be torn to pieces. In other words the transfer function from stimulus to response must involve spreading.

This spreading of the response comes about in part because the response is expressed slowly in time, and as it is expressed, it is rotated around the cell. The positive phase of the response to a step stimulus is about 8 min long. Since the rate of twist is 6°/min, this corresponds to a 48° turn of the cell. For growth rates about 5% above normal rates, corresponding to the locally increased growth rates of phototropism, the response may reasonably be fit by a cosine of one-half the period of revolution. Thus there would not be much stress even if no other spreading of response occurred.

(b) The step-up in intensity occurring at the leading edge of the focused band is matched by an inverse step-down at the trailing edge of the band. The response to this step-down will not neutralize the response to the step-up since step-down light stimuli give growth responses that are much smaller than responses to step-ups and are spread out over 20 minutes or longer, about half a twist period (Fig. IV- 22).

Let us now discuss in some detail several basic experiments. The results of all these experiments were formerly difficult to account for. In the next section the influence of light scattering and absorption by screening pigments under equilibrium conditions is discussed. The data will be first presented on a simple basis to facilitate the understanding of what happens. The model will then be introduced.

C-2) The influence of light scattering and of screening pigments on phototropism

a) Phototropic equilibria of specimens illuminated from two sides with light of different wavelengths

The availability of mutants with varied amounts of screening pigments and scattering particles allows us to study the effects of absorption and scattering on the tropic response. Specimens were illuminated from the left side at 60° angle to the vertical specimen with I_L (λ_L = 485 nm) and from the right side also at 60° with I_R (λ_R = 385 nm), and the intensity ratio for a phototropic null, $R = (I_L/I_R)_{null}$, was determined.

Table IV-1 shows R for wild type and for the series of mutants discussed in section IV-A. It also lists the optical densities of the specimens at λ_L and λ_R. At λ_R = 385 nm almost all of the O. D. is due to scattering. At λ_L = 485 nm all of it is due to scattering in the albino strains. In the other strains the contributions of scattering and of absorption have been estimated from inspection of the transmission curves.

In Fig. IV-5, R is plotted versus $\Delta a^{scat} = a_R^{scat} - a_L^{scat}$ for the albino strains. We see a strong linear correlation between R and Δa^{scat} over the entire range of Δa^{scat} available (+0.025 to +0.098). The data can thus be extrapolated to zero scattering difference, giving R_o = 0.95. This value is in agreement with the corresponding ratio of the growth response action spectrum of Delbrück and

Table IV-1. Phototropic Equilibrium Results

Strain	Diameter (μm)	Age (days)	$R = I_{485}/I_{385}$	Measured OD 385 nm a_R^{scat}	485 nm a_L^{scat}	485 nm a_L^{abs}
Wild type	100	3-5	.51	.15	.07	.05
	100	6-8	.62			
C9(carR21)	110	4-6	.82	.18	.10	.17
C2(car-5) on PDA	100	4-6	.60	.14	.07	-
	110	4-6	.51	.156	.078	-
	120	4-6	.45	.168	.084	-
	130	4-6	.43	.182	.091	-
	140	4-6	.41	.196	.098	-
C2(car-5) on LAC	80	4-6	.81	.050	.025	-
C5(car-10)	85	4-6	.66	.090	.045	-

Fig. IV-5.

Specimens were illuminated from one side with 485 nm light, I_{485} and from the opposite side with 385 nm light, I_{385}. The intensity ratio for phototropic null I_{485}/I_{385} is plotted for the albino mutants in Table IV-1 as a function of the difference in measured scattering between 385 nm and 485 nm in O. D. units.

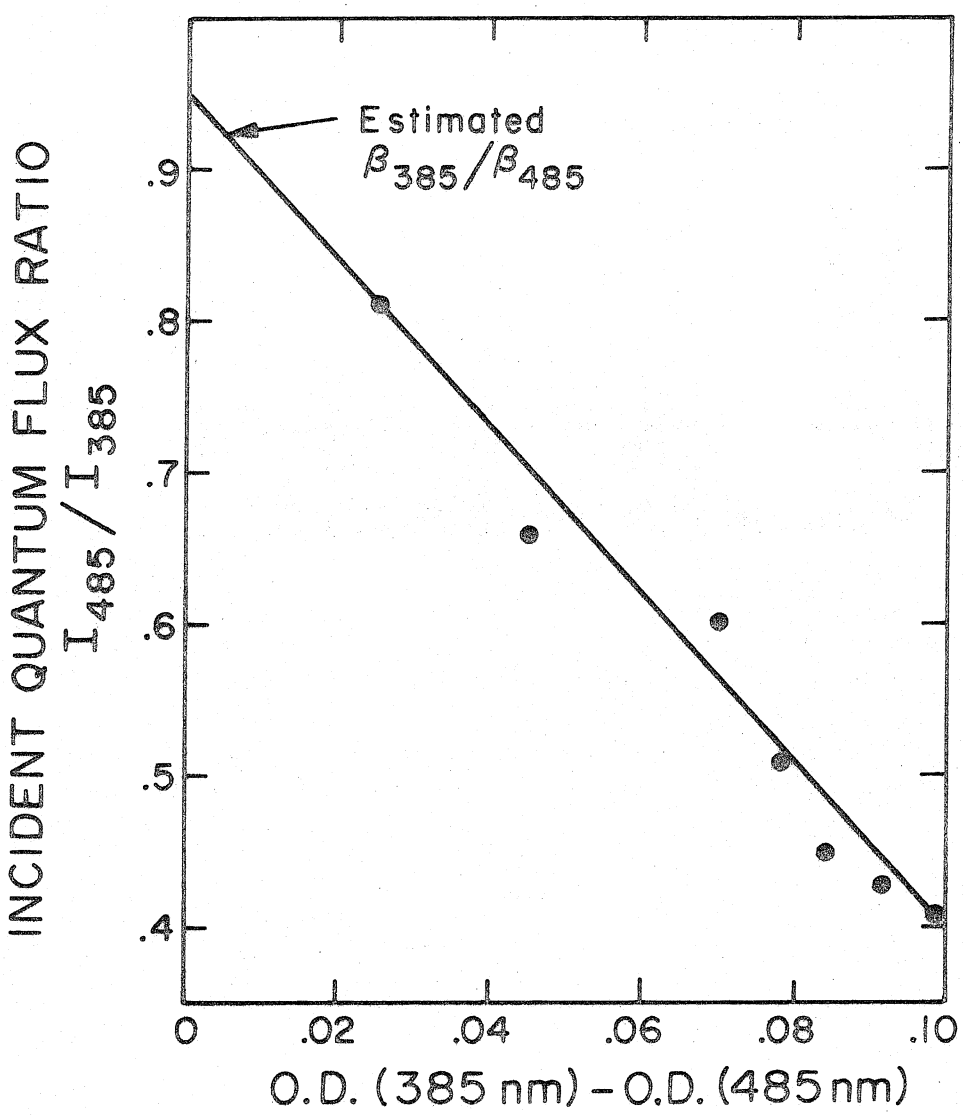
INCIDENT QUANTUM FLUX RATIO
I_{485}/I_{385}
Estimated
β_{385}/β_{485}
.9
.8
.7
.6
.5
.4
0
.02
.04
.06
.08
.10
O.D. (385 nm) – O.D. (485 nm)

Shropshire (1960). This result is reasonable since with albino mutants there are no absorbing pigments or scattered light (after extrapolation to $\Delta a^{scat} = 0$) to distort the phototropic action spectrum.

It should be noted here that screening of light which occurs peripheral to the photopigment will have the same effect on the determination of R_o for both the growth response action spectra and the extrapolated phototropic action spectra. Therefore, the fact that R_o is the same for both determinations says nothing about the peripheral screening. R_o is a measure of the relative efficienty, β, of the receptor pigment, for light of two wavelengths, i.e. $R_o = \beta_{385}/\beta_{485}$ (see Bergman et al, 1969). Furthermore, the slope of this regression line between R and Δa^{scat} gives us the relation:

$$R = R_o - 5.5\ \Delta a^{scat} \qquad (C\text{-}1)$$

We can now use this relation to estimate the effect of absorption on R_o, assuming that absorption contributes an analogous term, as follows:

$$R = R_o - 5.5\ \Delta a^{scat} - k\Delta a^{abs} \qquad (C\text{-}2)$$

$$\text{where } \Delta a^{abs} = a_R^{abs} - a_L^{abs}$$

and k is a proportionality constant. The red mutant C9 is the most useful one for estimating the effect of absorption. Substituting

Δa^{scat} = 0.08 ± .01 and Δa^{abs} = .17 ± .01 from the C9 (carR21) values into equation (C-2) gives k ≃ 1.8 ± .4. In this case the contribution from absorption (highest at 485) almost cancels that due to scattering (highest at 385). For wild type the contribution due to absorption is negligible and R lies close to the plotted regression line of the albinos. Scattering and absorption both diminish the phototropic effectiveness. This can be understood qualitatively by noting that phototropism occurs primarily because focusing gives an advantage to the distal side. This advantage is diminished by anything that tends to put the distal side at a disadvantage, and both absorption and scattering will diminish the contrast on the distal side.

These data which compare the intensity ratio for phototropic null at 485 nm and 385 nm for various situations, showing the influence of absorption and scattering, confirm these general conclusions. Without either of these modifiers, R should almost be unity as shown by the growth response action spectrum. For the albinos C2(car-5) and C5(car-10) absorption may be neglected. The intensity needed for a given amount of phototropic effect should be increased at both wavelengths, but more at I_R(385 nm) than at (I_L(485 nm), because

scattering is higher by about a factor of two at the shorter wavelength. $R = I_L/I_R$ should therefore be less than R_o as observed. On the other hand, absorption, for the lycopene mutant C9(carR21), is much larger at 485 than at 385 nm, and thus correspondingly drives the value of R back towards R_o.

The relative effectiveness of the measured scattering on phototropism is larger by a factor of three than that of the measured absorption. This high effectiveness of scattering is most likely due to the fact that scattering diminishes intensity in the focused band and increases it outside the band and is therefore more effective in reducing the focusing advantage. Also as discussed in section IV.A, a narrow beam through the center of the spph was used to measure absorption and scattering, thus minimizing light scatter off the vacuole. Scattering by the vacuole is known to have a large effect as shown by the laser line experiments of Meistrich et al. (1970, and private communication) in which a large counterclockwise deviation in bending direction is observed when a narrow line is focused near the edge of the vacuole. Therefore it is not surprising that the measured scattering has a much larger effect than the measured absorption. The effective attenuation then can be written

$$a^{att} = 3a^{scat} + a^{abs} ,$$

where a^{scat} and a^{abs} are the measured values in O. D. units.

These qualitative observations can now be quantified using our model. At each wavelength the receptor pigment has some relative efficiency (cross section), $\beta(\lambda)$. Each light source of intensity, I, then has an effective intensity of $I\beta$ which we will call i. The distribution of light at the cell wall on the proximal and distal sides of a spph in air for light perpendicularly incident from one side is shown in the top curve of Fig. IV-6. In the case of equal bilateral illumination, the light distribution will be the sum of the proximal and distal curves, with some smoothing due to scattered light. This distribution is notable for the extremely large focused peak between 15° and 20° from the beam axis. These experiments were done at 60° incidence. There the light is focused within a band of 30° (Dennison, 1965) rather than 40° so that the focused intensity is even larger. (Note that these curves are plotted on a logarithmic intensity scale).

In a bilateral phototropic equilibrium experiment the responses on the two sides must be equal ($R_L = R_R$). Since the optics of the cell is not appreciably different at the two wavelengths, 485 nm from the left and 385 nm from the right, the distribution of light on the two sides of the cell, in the absence of any absorption or scattering would be identical ($i_L = i_R$). In this experiment we can assess the effect of absorption and scattering on the response produced by the two focused beams. For all strains the scattering

at 385 nm is about twice that at 485 nm and only C9 has significant 485 nm absorption. According to our model the response is produced on each side by the contrast, C, between the neighboring region and the focused band (R = f(C)). The lower adapted region twists into the focused band resulting in a response similar to that produced by a step change in light intensity. At equilibrium, $C_L = C_R$. Since the real distribution of scattered light is not known the limiting case of exactly uniform scattering will be assumed in our model. The intensity in the focused band on the left side will be that due to the focused right light source, $i_R F$, where i_R is the effective light intensity incident onto the spph. This is attenuated by absorption and scattering, $1 - s_-^R - a^R$ where s_-^R and a^R are respectively the amount of light scattered from the direct beam by the cytoplasm and the amount absorbed. In addition there is the direct light from the left side i_L and that scattered from both sources; $i_S = i_R s_+^R + i_L s_+^L$ where s_+^R , s_+^L are the scattered intensities, $s_+ = s_-/\pi$ under the uniform scattering assumption.

The effective intensity in the neighboring lower adapted region is that due to the left source, i_L, and that scattered, i_S.

Therefore

$$C_L = \frac{i_R F(1 - s_-^R - a^R) + i_L + i_S}{i_L + i_S}$$

and analogously for C_R.

Since $C_L = C_R$, we obtain,

$$\left(\frac{i_L}{i_R}\right)^2 = \frac{(1 + i_S/i_R)\ (1 - s_-^R - a^R)}{(1 + i_S/i_L)\ (1 - s_-^L - a^L)}$$

Neglecting second order terms

$$\left(\frac{i_L}{i_R}\right)^2 = 1 - i_S\left(\frac{i}{i_L} - \frac{1}{i_R}\right) - \Delta s_- - \Delta a$$

where $\Delta s = s_-^R - s_-^L$ and

$$\Delta a = a^R - a^L \ .$$

Taking the square root of both sides

$$\frac{i_L}{i_R} = \frac{I_L\beta_L}{I_R\beta_R} = 1 - \frac{i_S}{2}\left(\frac{1}{i_L} - \frac{1}{i_R}\right) - \frac{\Delta s_-}{2} - \frac{\Delta a}{2}$$

This can be compared with our experimental equation (C-2). We set $R = I_L/I_R$, $R_o = \beta_R(385)/\beta_L(485)$ and recall that $s_-^R \cong 2s_-^L$, therefore $\Delta s_- = s_-^L$.

Then the uniform scattering term may be written,

$$-\frac{s_-^L}{2\pi}\left(\frac{i_L}{i_R} - 1\right)\left(1 + 2\,\frac{i_R}{i_L}\right) \ .$$

If we let K_s be the fraction of measured scattering effective then we may write for the albinos ($\Delta a = 0$):

$$R = R_o - \frac{R_o \Delta s_-}{2} \left\{ K_s + \frac{1}{\pi} \left(\frac{i_L}{i_R} - 1 \right) \left(1 + \frac{2 i_R}{i_L} \right) \right\}$$

The uniform scattering term may be neglected here, thus yielding the observed linear relation between R and Δs_-. However, with greater scattering this term could introduce some non-linearity.

To compare to the experiment one has to know how Δs_- corresponds to the measured Δa^{scat}. If scattering were completely uniform then we would have measured, with the optics used, two-thirds of the scattering. However, scattering will undoubtedly be peaked forward so that we will certainly have underestimated with the uniform distribution approximation. Making the 3/2 correction, K_s can be estimated from this data to be between about 1.5 and 2. In view of the underestimation of scattering and the critical role that it plays in determining the size of the stimulus it is not surprising that the measured absorption is only one-third as effective as the measured scattering.

The importance of scattering had not previously been appreciated. It therefore came as a somewhat unexpected result that for wild type the effect of scattering swamps that of absorption for the particular wavelengths chosen in this experiment.

b) Phototropic neutrality of immersed specimens, illuminated from one side only

Now let us look at the effect of focusing under different circumstances. In the preceding section, focusing was considered constant (ignoring its small dependence on wavelength). It was shown that a stimulus advantage accrued to the distal focused region such that this focusing advantage F has a larger positive effect on the distal side stimulus than can be reduced by scattered light or absorption.

However, F can be deliberately varied by immersing the specimen in media with refractive indices much closer than that of air to the refractive index of the cell contents. If the refractive index is higher than a critical value, $n_{neutral}$, phototropism to a unilateral light from one side reverses sign (Buder, 1920). By interpolation the value of $n_{neutral}$ can be determined with high accuracy. Table IV-2 gives the results for the same strains as in Fig. IV-1 at various wavelengths.

In the preceding section we showed that scattering and absorption modify the focusing advantage in proportion to the measured attenuations, a^{scat} and a^{abs}, respectively, and that a^{scat} should be given three times the weight of a^{abs}.

Table IV-2. Comparative $n_{neutral}$ Values for Wild Type and Mutant Strains

Strain	Wavelength	$n_{neutral}$	reference	Δn	a^{att}	$a^{att}/\Delta n$
C9(*carR21*)	515 nm	1.274	1	.077	.44	5.7
wild type	440 nm	1.295	2	.056	.332	5.9
wild type	495 nm	1.306	3	.045	.261	5.8
wild type	510 nm	1.312	3	.039	.217	5.6
C2(*car-5*)	495 nm	1.314	1	.037	.210	5.7
C5(*car-10*)	495 nm	1.334	1	.017	.126	7.4

1. Bergman *et al.*(1969) section 17
2. Shropshire (1962)
3 Zankel *et al.* (1967)

To aid our understanding of this case the distribution of light has been calculated for a spph illuminated at perpendicular incidence in media of different refractive indices. Calculations were made with media refractive indexes ranging from that of the cell to that of air. Three examples are shown in Fig. IV-6 for n = 1.0 (air), $\Delta n = 0.020$ and $\Delta n = 0.055$, where Δn is the difference between the refractive index of the medium and that of the cell. The distal curve has been corrected in the Δn cases for attenuation equal to that of the strain showing phototropic neutrality at the respective Δn.

These phototropically neutral refractive index examples are conspicuous for their relative lack of gradients except for the dark band 18° wide for $\Delta n = 0.020$ and 28° wide for $\Delta n = 0.055$ and some structure near the incident beam axis (due to the Δn between vacuole and cytoplasm). In the experimental region relevant to this experiment with Δn above 0.015 the dark band's width is given by:

$$\text{Dark band (degrees)} = 11.7° + 310° \, \Delta n$$

The reduced width of the focused band results in its increase in intensity by a small factor, $\left(\frac{1}{.87-3.5 \, \Delta n} \right)$.

Under these circumstances it is difficult to predict, except qualitatively, what the dependence of a^{scat} on n will be. The dominant feature may still be the leading contrast edge on the distal side. This contrast will be determined primarily by the adaptation

Fig. IV-6.

Intensities at the distal and proximal cell wall calculated for light at perpendicular incidence to the spph. The model cell consisted of a 40 μm diameter vacuole of refractive index 1.335, surrounded by a 30 μm thick cytoplasm of refractive index 1.350 and a thin cell wall. Reflection by the cell wall of 1.5 refractive index was taken into account. Each curve is plotted on a $\log_{10}$ (relative intensity) scale as a function of the angle from the center of the axis in degrees. The dashed curves correspond to light intensity at the proximal wall and the solid curves to the light intensity corrected for the measured absorption at the distal wall. The upper curves correspond to the spph in air (n = 1.0). The lower sets of curves correspond to the spph being in a refractive index respectively 0.055 and 0.020 less than that of the cytoplasm. The amount of absorption was taken equal to that of the strains showing phototropic neutrality at their respective n.

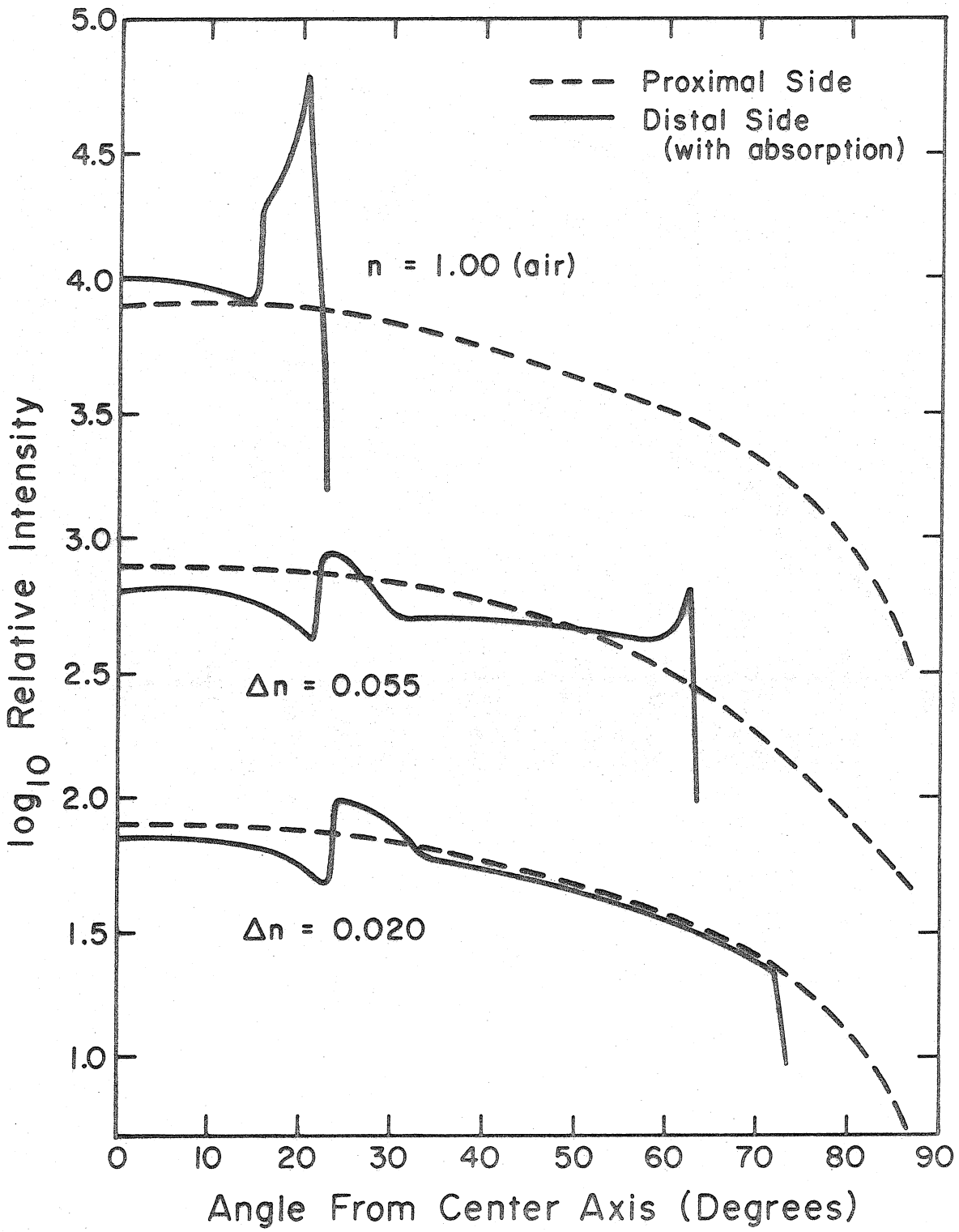
5.0
4.5
4.0
3.5
3.0
2.5
2.0
1.5
1.0
log10 Relative Intensity
Proximal Side
Distal Side
(with absorption)
n = 1.00 (air)
Δn = 0.055
Δn = 0.020
0
10
20
30
40
50
60
70
80
90
Angle From Center Axis (Degrees)

reached during passage through the dark band in the presence of scattered light. In the slower rotating (less than 3°/min) lower part of the growing zone there will be sufficient time to adapt to the scattered light intensity, and therefore the contrast will be inversely proportional to the amount of scattered light.

In Fig. IV-7 $n_{neutral}$ is plotted as a function of the measured $a^{att} = 3a^{scat} + a^{abs}$. As seen in this figure, for these small Δn, $n_{neutral}$ is linearly correlated with a^{att} with a slope of $a^{att}/\Delta n = 5.8$. This correlation also permits the extrapolation to a value of $n^{o}_{neutral} \cong 1.35$ for a $a^{att} = 0$. This refractive index nicely matches that of the cell contents, as explained in Bergman et al. (1969), section 17.

Zankel et al., (1967) measured Δn at two wavelengths which show a measured absorption change of about 0.05 O.D. and wondered how a small change of Δn (0.006) could offset the rather large change of screening between the receptors at the proximal and distal sides. In fact, however, such a change in absorption would tend to reduce both the adapted level and the intensity in the focused region about equally. Therefore the response should be very insensitive to absorption changes.

Fig. IV-7.

Neutral refractive index versus attenuation. The neutral refractive index is plotted for wild type at different wavelengths and for several mutants strains (Table IV-2) as a function of their weighted attenuation, i.e., $a^{att} = 3a^{scat} + a^{abs}$ in O.D. units.

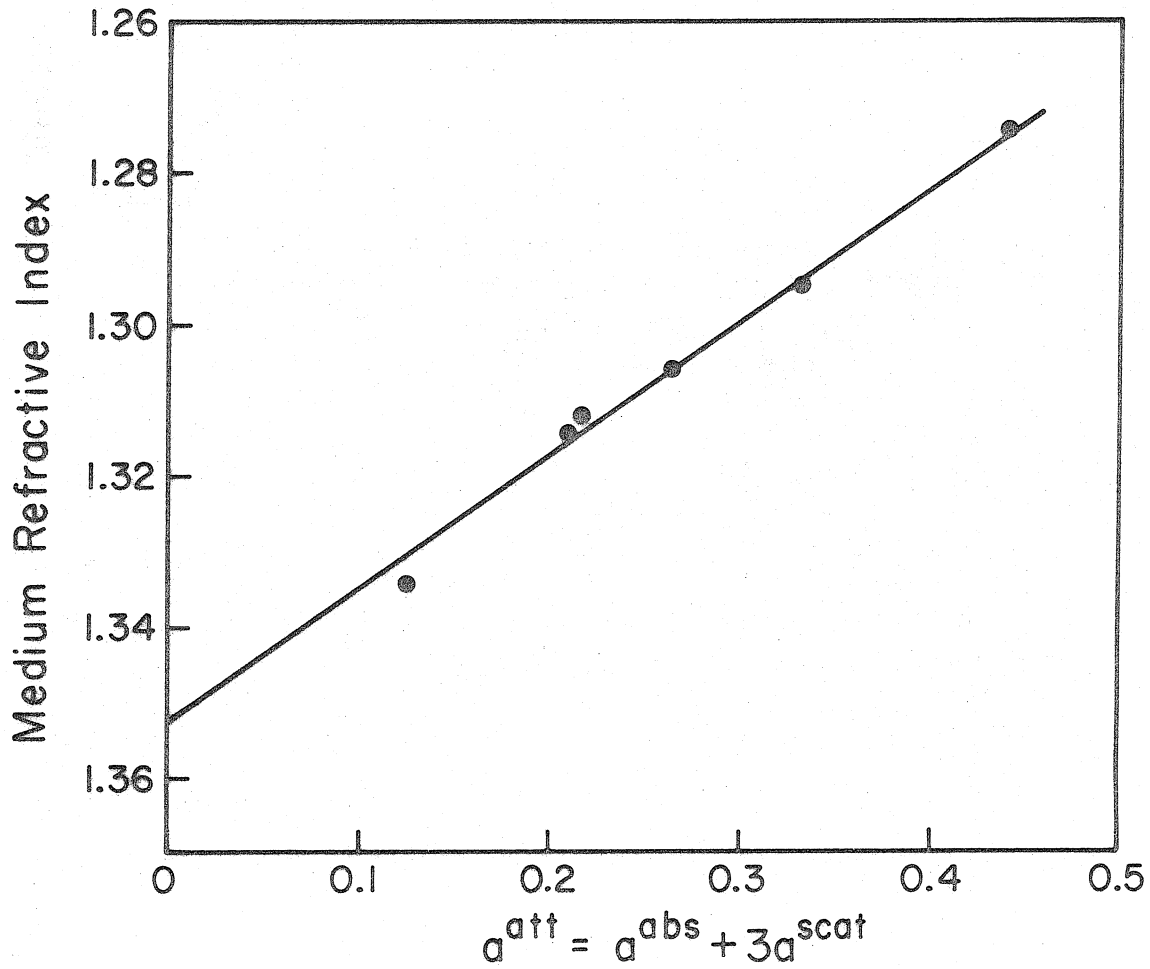
1.26
1.28
1.30
1.32
1.34
1.36
Medium Refractive Index
0
0.1
0.2
0.3
0.4
0.5
$a^{att} = a^{abs} + 3a^{scat}$

3. Review of several published experiments from our new perspective.

a) Null tropic and growth responses as a result of balancing intensities of 460 nm and 280 nm light.

Shropshire and Delbrück (1960) measured the intensity ratio for phototropic null and growth response null between $I_b(\lambda_b = 460$ nm) and $I_u(\lambda_u = 280$ nm). The relative effectiveness of the photopigment at the two wavelengths should be the same for the two responses.

In the tropic experiment both the 280 nm and 460 nm light are incident on the left side. However the 280 nm light is so strongly absorbed in the cytoplasm and vacuole that it has no effect on the distal side. The stimulus on the distal side is then due to the focused 460 nm light relative to the neighboring dark regions lit by scattered 460 nm light. The stimulus on the proximal side is due to the cosine distributed 460 nm light, and augmented with the 280 nm light relative to the dark region lit only by scattered 460 nm light. At null the two responses are equal. Since the stimulus on the proximal side occurs over a larger part of the circumference than on the distal side the local stimulus on each segment of the proximal side need not be as great.

Let us first compare the effectivenesses of these two wavelengths under the simple conditions of the null growth response. The spph

is rapidly rotated to insure uniform distribution of adaptation and light. The relative intensities are adjusted until there is no response when the two lights are alternated every 5 minutes. After correcting for the fact that the 460 nm light excites both sides of the cell while the 280 nm light excites only the proximal side, we obtain a photochemical effectiveness ratio for 280 nm and 460 nm. Shropshire and Delbrück (1960) found that the tropic null effectiveness ratio is 3.5 times greater than the photochemical effectiveness ratio for 280 nm versus 460 nm. This means that an augmentation of only 1/3.5 or 25-30% of the effective intensity of the 460 nm light was required on the proximal side to balance the distal focused 460 nm band. Considered in this way the high effectiveness of the 280 nm light for the balanced tropic response is related to the fact that in blue light alone tropism is due to a slight excess of growth response on the distal versus the proximal side. It takes little added response on the proximal side to tip the balance in the opposite direction. 280 nm light gives this added response because it is limited to the proximal side.

b) Tropic rates as a result of unilateral blue (460 nm) or 280 nm light.

Phototropism in blue light results from competition between the narrow focused distal band of large contrast and the wide low contrast proximal band. In the steady-state it is observed that after the transient response has disappeared most of the response occurs in the lower region of the growing zone (Castle, 1962). It is likely that in this slowly rotating region there is nearly complete adaptation and very little stimulus on the proximal side and as a result the distal focused line wins out. In the faster rotating upper portion of the growing zone the two responses approximately balance with steady-state conditions resulting in no bending in this part. This should not be too surprising since as discussed in the last section only a 25-30% augmentation of the intensity over the whole growing zone on the proximal side is sufficient to balance.

The direction of troping in the steady state is determined, in part, by the azimuthal location of maximum stimulus, presumably near the leading edge of the focused band. This effect by itself would produce a counterclockwise aiming error of 10-20°. With the delay of 6-7 min to maximum response and an average rotation rate of 3-4°/min for the lower part of the growing zone a clockwise compensation of 20-30° occurs. The net measured aiming error is 9.1° clockwise

(Dennison, 1965). Previously it has been considered puzzling why this aiming error is so small.

Phototropism at 280 nm results from the cosine distributed light on the proximal side only, with perhaps some dark (negative going) response in the second quarter and on the distal side. As a result the tropic rate at 280 nm is about 3-4 times as rapid as with blue light. Also unlike with blue light it occurs all along the length of the growing zone, and gives the impression of the sharpest bend occurring near the top. The greatest stimulus (but not the only one) will occur near the leading edge of the cosine light distribution so a larger counterclockwise aiming error might be expected under equilibrium conditions. However, this is compensated in large part by the delay time to maximum response of 6 to 7 min and the average rotation of the cell of $\sim 6°$/min.

c) Phototropic equilibrium at constant incident angle

Dennison (1965) studied phototropism under steady state conditions with light incident at a constant angle relative to the spph in the plane of phototropic bending. He also constructed a simple optical model. As the angle of incidence is decreased between the light beam and the longitudinal axis of the spph the focused band progressively narrows until at less than 30° the focus goes within the cell. Dennison observed positive phototropism down to 14° incident angle in spite of the increased absorption between the two sides. In fact, he observed maximum troping rate at an incident angle of about 50°. In view of what has been said these results are not surprising. The sharpening of the focused band compensates for increased intracellular attenuation.

With the old model,which assumes that the response is proportional to the intensity at each point, a response proportional to the intensity squared is required before the data can be approximately fitted. With the new model no such wild assumption regarding the intensity dependence is needed.

d) Tropic stimulus at constant net light flux

Castle (1961) adapted a specimen bilaterally and then simultaneously turned off one light and doubled the intensity of the remaining beam. He found that the average growth rate did not change, i.e. the speed-up of the growth rate on the distal side is matched by a slow-down on the proximal side. On the side distal to the remaining unilateral light the focused band contrast will be approximately doubled, significantly increasing the size of the response, and accounting for the observed speed-up in growth. On the proximal side the focused band will have been removed and there will be a negative response to its removal. In addition, since the focused band has been replaced by a cosine distribution the size of the stimulus on this side will be reduced, i.e. there will no longer be a large stimulus and this removal of stimulus will result in a slow-down locally.

4). Evidence for suggested phototropism model

Both the "lever arm" and path length models as mentioned in the last sections make the assumption that the response is proportional to some function of the absolute intensity at each point where there are receptors. We have illustrated with several experiments that a different assumption provides a more reasonable explanation. We propose that the response is proportional to the local intensity relative to the local level of adaptation in the manner observed for the growth response as a whole. In order for phototropism to occur under this assumption, it must be additionally true that this local level of adaptation of the receptors must move relative to the stimulating light for otherwise the stimulus would adapt out. That this movement occurs will also be shown in the following sections.

As discussed, movement of adaptation could occur as a slow spreading across the cell due to diffusion or streaming or as a result of the physical rotation and bending of the cell. At present we do not know if there is any contribution of spreading of adaptation. We know only that in stage I, before a sporangium is formed, the tip tropes toward light although the cell does not rotate. The tip of the cell does nutate (describing a conical path) clockwise (Castle, 1958), however, which would cause movement of the focused light within the cell. What causes the nutation and what is the

geometry of the optics relative to the photoreceptor, and whether there is movement of the local adaptation are not known. Unfortunately, there are no mutants, with normal growth responses that do not twist in stage IV. The most suitable preparation to study the relative effect of rotation versus spreading would seem to be a narrow 280 nm transverse line stimulation near the bottom of the growing zone where there is relatively little cell wall rotation. Troping rates without much intrinsic rotation could then be compared to those rates when the cell is externally rotated at different speeds.

a) Evidence of local adaptation

The amount of spreading of local adaptation longitudinally has been shown limited to the extent that in 10 min, adaptation does not spread further than a distance of 100 μm (Delbrück and Varjú, 1961). The growing zone is about 300 μm around at the cell wall.

Azimuthal local adaptation has been demonstrated by R. Bozof (private communication, Dennison) who did a series of experiments in which he followed a one min 280 nm pulse perpendicularly incident on the spph by 14 min of lower intensity 280 nm light at some angle rotated around the cell relative to the first pulse. The bending direction due to the second stimulus was always influenced by the location of the first pulse. If the second pulse was clockwise with respect to the first then the bending direction to the second

pulse was clockwise with respect to that which would have been observed if the first pulse had not occurred. Castle (1961) demonstrated that during a steady-state tropic response a big step up in light intensity from any direction causes reversal of bending always in the plane of the original bend. Both of these experiments suggest local adaptation. Whether there is rotation of this local adaptation has not been clearly demonstrated with these experiments.

b) Postulated movement of local stimulation due to cell rotation and bending

Stage IVb Phycomyces normally twists 8 to 15°/min clockwise (as seen from above) as measured at the sporangium. The cell wall rotation rate increases as you progress up the 2 mm growing zone until 0.5 mm from the sporangium. This cell rotation can directly cause two effects on phototropism. The first is twisting below an already bending region. This effect is probably small since normally only a small amount of spiraling is observed. The second is possible rotation of the adapted zone of the receptors and/or of the reacting zone. I will come to the observed effects of this rotation shortly.

One other type of rotation with respect to the sporangiophore's coordinate system which we will call dislocation should be understood

before proceeding. Consider the special case of a spph at first vertical, bending with an aiming error α relative to the light source until it lies in the horizontal plane. Take a fixed point on the cell lying in the bending plane and assume no twist. At the vertical the radius to the fixed point makes an angle α with the direction to the source. During the bend α increases. When the spph is in the horizontal this angle is 90°. It is observed that in phototropism the spph bending direction shows a clockwise aiming error. Therefore the focus is dislocated. It is rotated counterclockwise in the growing zone. The focal point also moves progressively in toward the cell axis resulting in movement of the focused bands (Dennison, 1965). These movements of the regions of intense light relative to the cell probably increase the phototropic rate. In fact, Dennison (1965) measured steady-state tropic rates under conditions in which focus dislocation is eliminated and found average tropic rates of 3 to 3.4°/min compared to values of 5 to 7°/min for normal phototropism to a unilateral blue light source.

c) Observed effects of rotation

There are several ways in which cell rotation is seen to affect phototropism. The most obvious effect is the clockwise aiming error. At low intensities eventually the direction of spph growth reaches an equilibrium with geotropism, and it grows at a fixed angle to the horizontal in a plane rotated clockwise to the direction of the

light source. The aiming error has also been studied in the steady state under conditions of external rotation of the spph.

The aiming error has been carefully measured by Dennison (1965) for blue light incident on the whole growing zone. Dennison studied phototropic equilibrium at constant configuration of the spph relation to the light source. In this experiment no focus dislocation occurs and the observed aiming error is 9.1° clockwise. With 280 nm light from one side the aiming error is clockwise about 20° after starting at about 40-50°. That the amount of aiming error is tied to the twisting rate is indicated by the finding that early stage IVb spphs which twist more slowly initially bend more directly away from a 280 nm source than do faster twisting specimens. With 280 nm the aiming errors appear to persist much more than they do with blue light. The differences of the aiming errors are presumably due to the differences between the light distributions. For blue light the focused lines near the axis on the distal side dominate. For 280 nm light we have a cosine distribution on the proximal side.

At light intensities near the threshold, the greatly increased latency (see section IV-D2) results in a large clockwise aiming error of the phototropic-geotropic equilibrium bending direction. The magnitude of this aiming error increases progressively the

lower the intensity. This striking effect was noted over 50 years ago (Buder, 1920) and the aiming error has been called the "Buder angle."

In fact, a mutant, C21, whose twisting rate is normal but whose growth rate maximum for a moderate response appears later relative to wild type, has a Buder angle near its threshold with 280 nm light (1000 times above C2 threshold) sufficient to turn the spph a full 180° clockwise when the spph is bent 30° from the vertical.

Another instance in which the effect of the aiming error is observed is with long period hunting. If two opposed light beams of equal intensity, 120° or less apart (both in the vertical plane including the spph), are incident on a spph, it grows in a direction bisecting this angle but oscillating around this direction executing a counterclockwise ellipse. The latency in response and the aiming error probably account adequately for this oscillation.

The mutant C5 has an abnormally high steady-state phototropic rate, 1.35 times as fast as wild type, and also a similar abnormally large growth response. The result is hunting oscillations which have abnormally large amplitudes. Mutant C21 which appears to possess a large lateral component to its troping, resulting in a large Buder angle, is also unusual with respect to hunting, executing smaller amplitude but shorter wavelength hunting oscillations (.7 mm relative to 2.3 mm for wildtype wavelengths). All these findings suggest that the

aiming error results from the interplay between the delay before the maximum response and the twist of the cell.

To further clarify this point, tropic responses have been measured for spphs which were externally rotated at different rates under unilateral illumination.

The size of the aiming error is strongly dependent on the measured twisting rate of the cell. Using a 280 nm unilateral light, a continuous stimulus centered about 1 mm below the sporangium (a region in which the cell wall rotates at about three-quarters the sporangium rate). We rotated spphs at speeds from clockwise 36°/min to -36°/min.* We measured the troping rate, direction of troping and angular rotation of the sporangium. At moderately rapid external rotation rates the level of adaptation should be sufficiently uniform throughout the cell so that the maximum stimulus should occur near the axis of the incident beam without being so uniform that no local response occurs. At 36°/min in either direction we found that the faster the spph twists the greater is the aiming error. The aiming error increased by about 6-7 degrees per 1°/min sporangium rotation rate. This effect on the aiming error corresponds to about 6-7 min of cell twist. Let us define the quantity

---

*In collaboration with D. Dennison.

$\theta = \frac{d(\text{aiming error})}{d\omega}$ (ω = twist rate) for this parameter. We will call this quantity, which has the dimension of time, the "effective twist time." As we will see later θ is a function of the external rotation rates. Another result is that the mean aiming error varies with the external rotation rate (at high rates in either direction) by about 5-6° of aiming error per degree per min of external rotation rate. In addition, there is a constant clockwise aiming error of about 50°. Considering that the cell rotation rate in this zone is 7-8°/min all these data imply that 5-7 min of rotation occurs prior to maximum expression of phototropic response. This is about the time required to reach maximum positive response to a growth response stimulus.

Thus we have established that there is local adaptation, and that movement of the cell's responding apparatus corresponds to the rotation rate of the cell wall. Now one would also wish to know whether adaptation or receptor zone rotates, since it is their rotation which would fulfill our proposed condition for phototropism.

There is evidence that the cell wall, the reactive, and the receptor-adaptive structures are separate. Therefore it is important to know whether these structures rotate relative to each other.

d) Evidence for separation between receptor-adaptive and reactive structures

i. Review of evidence concerning longitudinal separation

By stimulating narrow longitudinal sections of the growing zone, Delbrück and Varjú (1961) were able to show that the light adaptive zone does not move significantly longitudinally relative to the sporangium. They further showed the reactive zone extends only from 0.5 mm down, therefore not coinciding with the receptor zone which they showed extends from 0.1 mm down. They had the impression that during a sustained tropic stimulus at a constant height from the ground all growth occurred above the bend; further, that in the upper region the response was stored in a structure that did not move relative to the ground. They thus postulated three moving systems: the adaptive-receptor zone, the cell wall and the reactive zone. Although the reactive zone and cell wall rotate as already discussed in the last section no experiment has yet determined for certain whether the cytoplasm and vacuole rotate or not.

ii. Evidence for azimuthal rotation of adaptation

Reichardt and Varjú (1959) rotated the cell with or against the spph twist. They found for a 4 min unilateral positive stimulus the tropic response was larger if the cell was rotated against the

intrinsic direction of rotation of the sporangium. Thus for a short stimulus a larger response occurs if the photoreceptors (and/or cell wall) are held fixed to the transient light stimulus, thus implying rotation of the receptor zone similar to that of the cell wall.

Delbrück and Varjú (1961) found that with stimuli in the region 0.1 to 0.5 mm down from the the sporangium the response is delayed in time as if there were a response storage structure which did not move relative to the ground and which had to be below 0.5 mm before the response could be expressed. This separation of receptor zone and reactive zone with the longer delays would provide an excellent opportunity to study the rotational dependence of this region, but so far no experiments have been reported. There is a delay to maximum response of about 12 min for a continuous stimulus at 0.2 mm down from the sporangium. If during this delay the response were rotated at the sporangium speed, say 75° more than for a stimulus at 0.6 mm, then the authors would have noticed and reported it.

This approach has been used by us in a 0.5 mm region centered 1.0 mm down from the sporangium.* We carried out a series of 280 nm constant stimulation experiments in which we rotated the spph at speeds from -36° to +36°/min. What we hoped to find was an external rotation speed, compensating the intrinsic one, which would result

*In collaboration with D. Dennison.

in a minimum bending rate under the expectation that the specimen would partially adapt and there would be a decreased response. A residual bending rate must be expected because the narrow band of light could not be kept exactly in the same region and because of possible averaging of adaptation by spreading. Also we hoped to see whether, as a result of this external rotation, the center of response, producing the aiming error, moved as the compensating rotation speed was taken from slower than the adaptation zone rotation rate to faster. It might be expected that the minimum troping rate would coincide with a rapid switch in the direction of the aiming error when the trailing edge and the leading edge of the focused band reverse positions.

One main result is that a continuous rotation of unilateral band of light does cause increased phototropism. Counter-rotation of the spph at speeds greater than 9°/min results in larger troping rates than at slower speeds, until 36°/min are reached. At 36°/min the troping rate is less but still double that at no rotation. Reduction from the maximum troping rates is probably due to the length of the adaptation time constant reducing the size of the effective stimulus.

There is no narrow region of rotation speeds with minimum bending rate (Fig. IV-8). The data show a broad minimum from 0 to-9°/min clockwise external rotation with two absolute minima at -9°/min and 0 to -2°/min. These minima also show up in the

Fig. IV-8.

Effects of external rotation on tropic rates to 280 nm stimulus. The spph was stimulated continuously with a 280 nm light beam, 0.5 mm vertical width centered about 1 mm down from the base of the sporangium. The steady-state phototropic bending rate (deg/min) was measured at different external rotation rates of the spph from -36°/min to +36°/min clockwise.

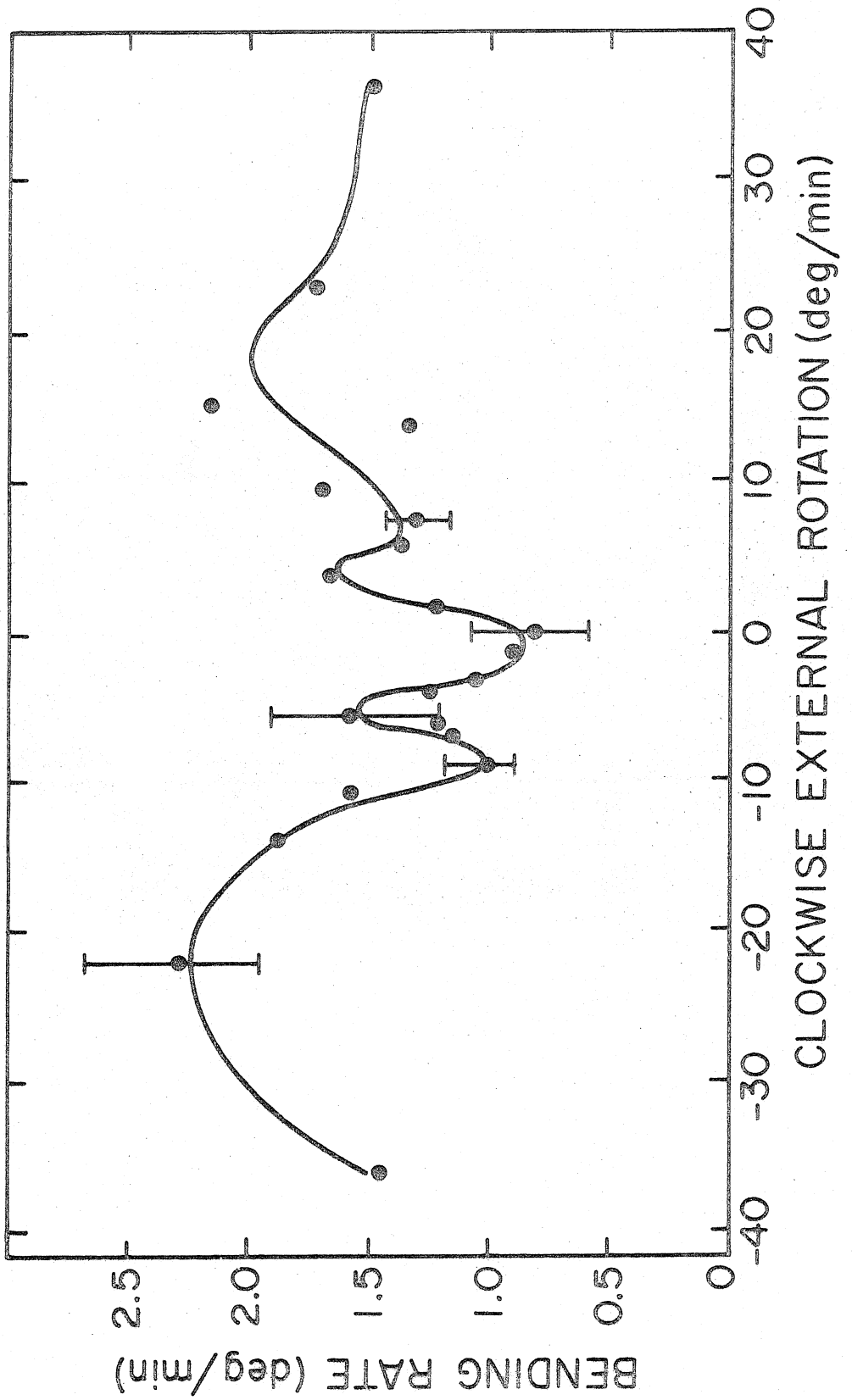
BENDING RATE (deg/min)
2.5
2.0
1.5
1.0
0.5
0
-40
-30
-20
-10
0
10
20
30
40
CLOCKWISE EXTERNAL ROTATION (deg/min)

effective twist time, θ, as a function of the external rotation rate (Fig. IV-9). At each external rotation rate the change in the bending direction as a function of the rate of sporangium rotation was calculated. In looking at the results we must keep in mind that the center of the response moves depending on whether the adaptation zone rotates faster or slower than the counter external rotation rate. Further if there are several adaptation zones which are rotating at different rates then the phototropic contribution from the zone whose rotation is exactly compensated for by the counter external rotation rate will be minimized. Fig. IV-9 shows maximum negative θ's at external rotation rates of -4 to -5.5°/min and 0 to +2.5°/min. These negative θ's occur at more clockwise external rotation rates than do the minimum troping rates. The maximum positive θ's appear to occur at -11.4°/min and -3.6°/min. These rates are both counterclockwise to the external rotation where minimum troping occurs. At moderate external compensating rotation rates (-11.4 and -22.3°/min) larger than the twist rate, θ is 10 to 15 min. At these over-compensating rotation rates with a faster twisting spph the actual rotation rate of the adapted zone relative to the stimulus is slower than with a slower twisting spph. This results in a larger clockwise aiming error for the faster twisting spphs because the maximum stimulus occurs further clockwise for a slower counterclockwise rotating adaptative zone. As a result there is a larger measured value of θ.

In this stimulus region the cell wall is considered to rotate at three-quarters of the speed of the sporangium which was measured on the average to be 9.9°/min. Therefore there appear to be two

Fig. IV-9.

Relation between aiming error and twist rate. Same experiment as in Fig. IV-8. The effective twist time, θ, in minutes is plotted as a function of the clockwise external rotation rate in degrees/min.

Closed circles: calculated from data at each external rotation rate.

Open circles: Calculated from pooled data of adjacent external rotation rates.

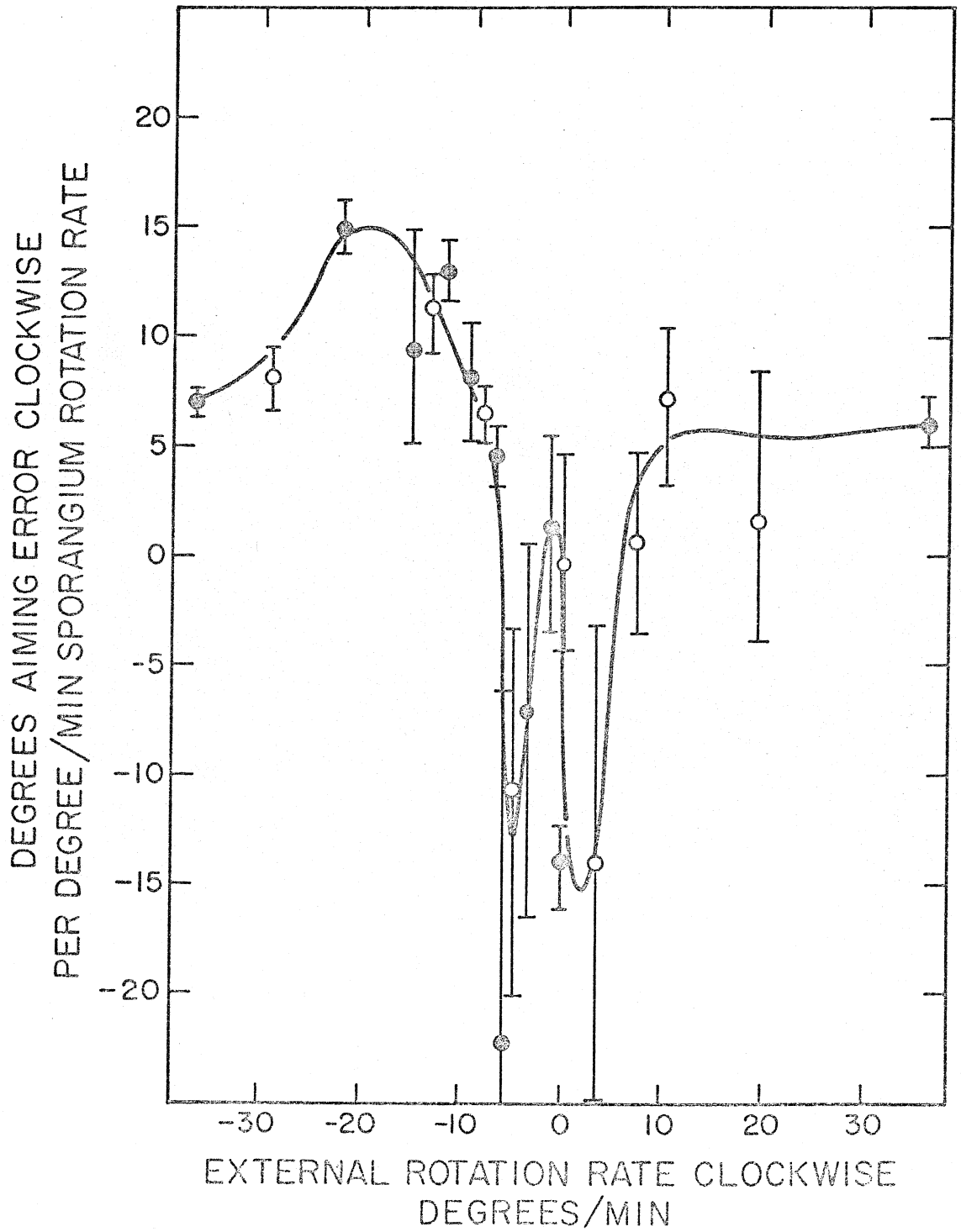
DEGREES AIMING ERROR CLOCKWISE
PER DEGREE/MIN SPORANGIUM ROTATION RATE
20
15
10
5
0
-5
-10
-15
-20
-30
-20
-10
0
10
20
30
EXTERNAL ROTATION RATE CLOCKWISE
DEGREES/MIN

regions of adaptation, one associated with the wall and the other with a postulated slower rotating portion of the cytoplasm. These experiments suggest that there is rotation of adaptation. These experiments further suggest that rotation of light relative to the locally adapted cell increases the phototropic rate and that at least part of the adaptation is rotated with the cell. This means that the major condition for phototropism is fulfilled. There is movement of the stimulating light relative to the adaptation level.

I have further suggested that the local response as a function of It/A (stimulus) should be the same as seen with the growth response. In the next sections the relationship between the two types of photoresponse are explored. The first deals with absolute intensity dependence of the photoresponses, and the second with the relative magnitude of the two responses.

5) Dependence of the photoresponses on absolute light intensity

The phototropic bending rate is a function of absolute intensity over a large part of the response range whereas the growth response, except for latency, appears relatively constant over a wide range of intensities for a particular size of stimulus.

The phototropic rate is directly proportional to the log I/I_T where I is the incident light intensity and I_T is the threshold intensity. The logarithmic dependence appears to hold at least over the range from I_T = .15 pwatts/cm^2 (blue) to 40 nwatts/cm^2 (Reichardt and Varjú, 1958). The troping rate in the "normal" range of .04 to 10 μwatts/cm^2 is constant. In the phototropic-geotropic equilibrium experiment, in particular at 2.3 g and higher (Bergman et al., 1969) the equilibrium tropic angle measured from the vertical is a decreasing function of the light intensity from threshold to 10 μwatts/cm^2, the top of the "normal" range. These data imply that the strength of phototropism is a function of the absolute intensity over the whole response range.

The growth response to a pulse is proportional to It/A where It (intensity x duration) is the stimulus and A the adapted level, from 8 pwatts/cm^2 adapted level to 10 μwatts/cm with very little absolute intensity dependence (see section IV.D-2). This means that the diminished size of the response itself will not be the cause of the

decreased phototropism at lower intensities.

Two other aspects of the growth response system, however, do change with absolute intensity. Part of the latency of the growth response is observed inversely proportional to the logarithm of the absolute intensity threshold (see section IV.D-2). The measured troping rate is probably influenced by the increased aiming error angle resulting from the longer latency at lower intensities (see section IV.D-3). The second aspect that changes with absolute intensity is the adaptation rate in the dark, i.e.,

$$\frac{d\log(A/A_D)}{dt} = -\ 1/b\ \log\ (A/A_D) \quad ,$$

A_D is the minimum adaptation level (see section IV.D-4). Although the growth response to a stimulus does not change over a wide range of A, it should be remembered that in such experiments, time is allowed for the adapted level to reach A. During phototropism however, the time schedule is fixed by the twisting rate of the cell. With lower intensities and longer adaptation times it might be expected that the troping rates would also be reduced as the effective size of the local stimuli (It/A) is reduced.

Of course near threshold the stimuli also become limited by A_D the dark "receptor noise". If in any local region the intensity is below A_D troping will be decreased also due to this cause. Some

troping will continue below an incident intensity of A_D because of the regions of focused light.

Together these mechanisms probably account adequately for the absolute intensity dependence of phototropism and suggest there is really no inconsistency between the constant size of the growth response and the absolute intensity dependence of phototropism.

6.) Relationship between growth response and tropic response

One question that remains is whether there is enough continuous local growth responses to produce a tropic response.

An estimate of the size of local growth responses can be obtained from the data of A. Jesaitis (private communication) who studied the cyclic response to a light program of 5 min of I_o followed by 5 min of I_1 where I_1 and I_o are nearly the same intensity. Following the development of Delbrück and Reichardt (1956) the amplitude of the response should be proportional to $C = (I_1-I_o)/(I_1+I_o)$. I have plotted this response for a range of C from $0 \rightarrow 0.4$ (Fig. IV-10).

Phototropism in blue light corresponds to about 5% increased growth rate on the distal side and a 5% decrease on the proximal side. For this $(I_1-I_o)/(I_1+I_o)$ equals about 0.15 or $I_1 \sim 1.35\ I_o$. This means a net step on one side of the specimen of 1.35 times would be sufficient to cause the observed phototropic rates. Since tropism results from the difference in stimuli on the two sides and the actual step change on the focused side is 5-10 times in a small region means that the growth response stimulus is probably adequate though the theory is not specific enough to check it quantitatively. Phototropism in 280 nm light corresponds to about 28% increased growth rate on the proximal side and decreased on the distal side. This is about the maximum amplitude of response observed with the cyclic response when $I_o = 0$.

Fig. IV-10.

Growth responses to small cyclic light intensity changes. Data of A. Jesaitis (private communication). The relative amplitude of the growth rate during a cyclic stimulus program consisting of 5 minutes of intensity I_o alternating with 5 minutes of I_1. I_1 and I_o are nearly the same intensity. The measure of the relative amplitude of the growth rate is taken as the total growth, G_o, in μm, during the 5 minutes of I_o, minus the growth, G_1, during the 5 minutes of I, divided by the total growth, $G_1 + G_o$. This quantity, $(G_o-G_1)/(G_o+G_1)$ expressed as a percent is plotted as a function of $(I_1-I_o)/(I_1-I_o)$.

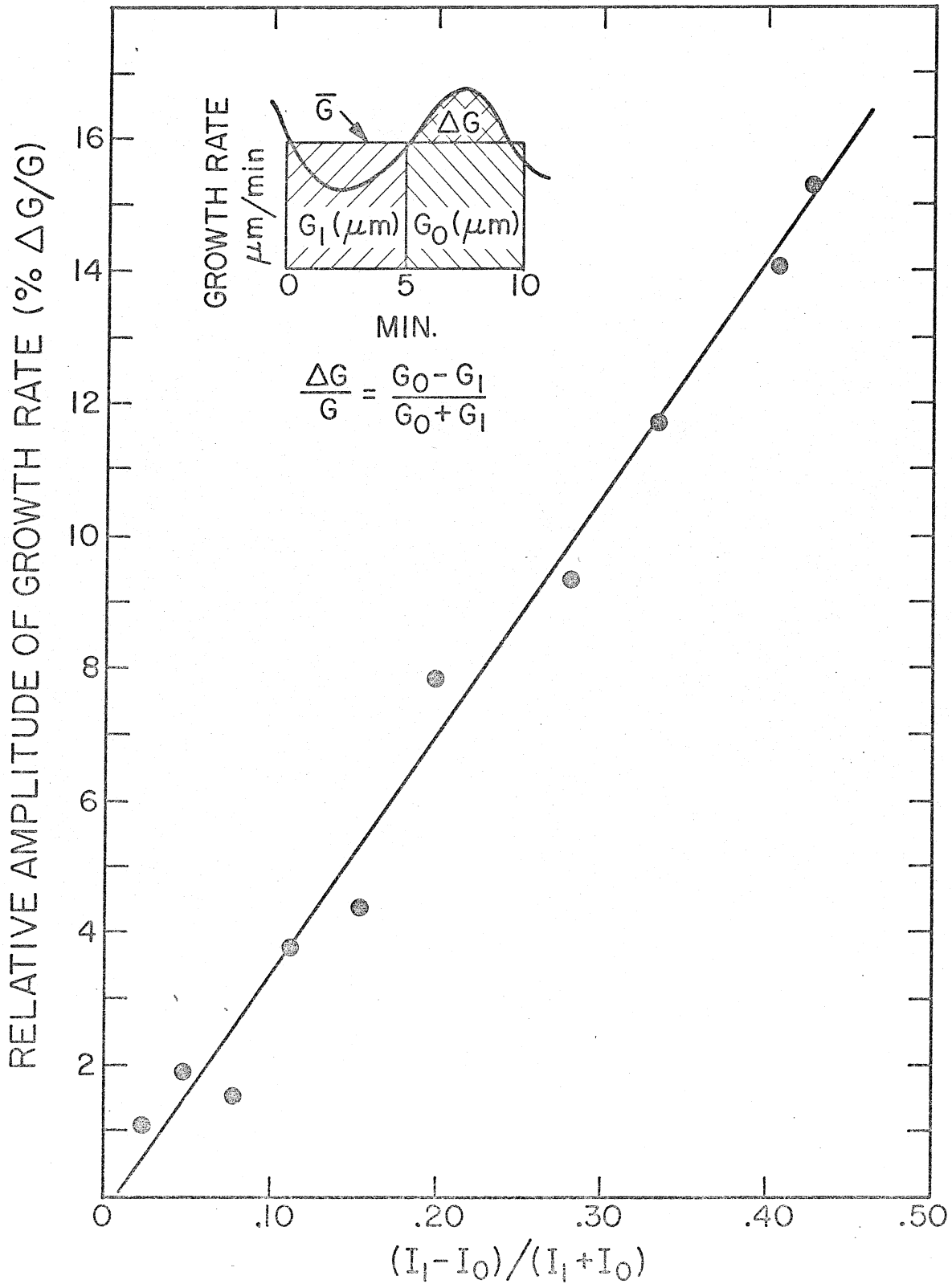
RELATIVE AMPLITUDE OF GROWTH RATE (% ΔG/G)
16
14
12
10
8
6
4
2
0
.10
.20
.30
.40
.50
(I1-I0)/(I1+I0)
GROWTH RATE
μm/min
G
ΔG
G1 (μm)
G0 (μm)
0
5
10
MIN.
ΔG/G = (G0-G1)/(G0+G1)

It is also worthwhile to look at the size of the local growth responses required to account for phototropism. A 5% increase in growth rate occurs for a 30 sec pulse of about 10 times the adapted intensity. A 28% increase in growth rate occurs for about 100 times the adapted intensity for 30 sec or a 10 times step in intensity. These values can be compared to the results with C149, Fig. IV-20. A pulse of 100 times the adapted intensity for 30 sec produces a barely noticeable response and this response is prolonged. It is no wonder that blue light phototropism is greatly reduced for C149.

At 280 nm, however, C149 tropes at $\sim 0.5°$/min (wild type 17°/min) and shows a phototropic threshold only a factor 10 above that of wild type. Probably troping is noticeable because of the enhancement of tropic rate for 280 nm discussed for wild type and because of the observed 20-25% shorter responses and latency at 280 nm. Possibly the prolonged nature of the responses particularly in blue light results in cancellation of effective troping because the later part of the response is rotated to the other side of the cell.

At this stage of our understanding these estimates suggest it is reasonable to say that steady phototropism could be produced by transient growth responses of new receptors continuously brought into play by twisting.

7.) Phototropism summary

The effectiveness of the focused light within the cell for producing phototropism in Phycomyces has been demonstrated and quantified. We have postulated that a distinct advantage accrues from the sharp gradient of the leading edge of the focused band as a result of the cell's natural twisting. We have postulated that the stimulus on each side of the specimen is a function of the ratio of the local intensity to that of lower adapted material brought into that region by twist. The stimulus is not dependent directly on the intensity on the other side of the cell with the result that the size of stimulus is insensitive to absorption and scattering of light through the cell. The stimulus is more sensitive to scattered light because this reduces the contrast of the focused boundary. Any movement of the adapted zone, arising either from rotation with the twisting cell wall, or resulting from orientation changes with respect to the light source, or from rotation of the light source will enhance the stimulus. Any such movement causes the focused light to be compared to receptor complexes adapted to a previously lower intensity.

Phototropism is a sustained effect while growth responses are transient. Under the conditions which produce phototropism, namely a non-uniform azimuthal distribution of light, troping occurs

because twist of the cell results in the continuous bringing of lower adapted material into regions of higher intensities. The same mechanism which produces a growth response due to a change in intensity relative to the adapted level produces the phototropic response. The action spectra, of these two effects, with correction due to absorption and screening, appear to be identical. Their kinetics of adaptation, their threshold for response and their latency as a function of absolute intensity are also the same. Even in the steady-state tropic response the time from stimulus to maximum response, as indicated by the aiming error data, is the same as for a growth response.

I propose the following working hypotheses on the sequence of events from stimulus to response.

Light causes some photochemical change at the photoreceptors, which may be rotating at different rates. The cell wall synthesis rate is regulated by the response of the organism to light intensity changes. This response is a function of the absolute intensity and the momentary intensity level relative to the adapted level. Once this transient growth response is initiated, it is expressed in time as the cell rotates and produces the observed aiming errors of phototropism.

At low intensities the long latency of response results in a large aiming error (Buder angle). At medium intensities in blue light at steady state some compenstation to the clockwise aiming

error occurs. The maximum of the light intensity relative to the adapted level is at the leading edge of the focused band on the distal side. This locus is counterclockwise with respect to the center of the focused light beam within the cell.

The further development of this model requires additional information. Although we know about dark adaptation (section IV.D-4), we do not know well enough how the adaptation level changes in the presence of light. Further we need to know for certain the distribution of rotation speeds of adaptation along the growing zone. Finally, we need to evaluate the role spreading of adaptation plays on phototropism.

D. CHARACTERIZATION OF GROWTH RESPONSE USING AUTOMATED MACHINE

The first major undertaking with the machine has been to provide a good physical characterization of the responses of Phycomyces.

1) The temperature dependence of response latency and shape

Fig. IV-11 shows typical light growth responses to a 30 sec stimulus of light one hundred times the adapting light, in the "normal" range as defined by Delbrück and Reichardt (1956). These are single responses taken for experiments on two specimens. The vertical scale is displaced. The adaptation light was the standard broad blue (380-500 nm) provided by a 150 watt GE1958 tungsten source passed through a Corning 5-61 filter and Schott KG-1 heat filter (Bergman et al, 1969, and Section III. C-6e). The adapted level was about 0.2 μwatts/cm^2 ($\log_2 A = -6$ in Delbrück and Reichardt (1950) units). The stimulus was 20 μwatts/cm^2 for 30 sec duration. The light source lit the spph from both sides at 60° from the vertical through a prism beam-splitter and two mirrors. Temperature was controlled by a thermoelectric element discussed in section III. C-5 and was varied from 25° to 15°C.

With a decrease in temperature by 10°C the latency lengthens from 2.5 min to 6 min without much change in the shape of the response. The total area of the response does not seem to be affected at these temperatures.

Fig. IV-11.

Responses to a 30 sec stimulus of intensity 20 μwatts/cm^2 of blue (Corning 5-61) light, 100 times the adapting intensity, as a function of temperature. Each curve is displaced relative to the growth velocity scale by 20 μm/min.

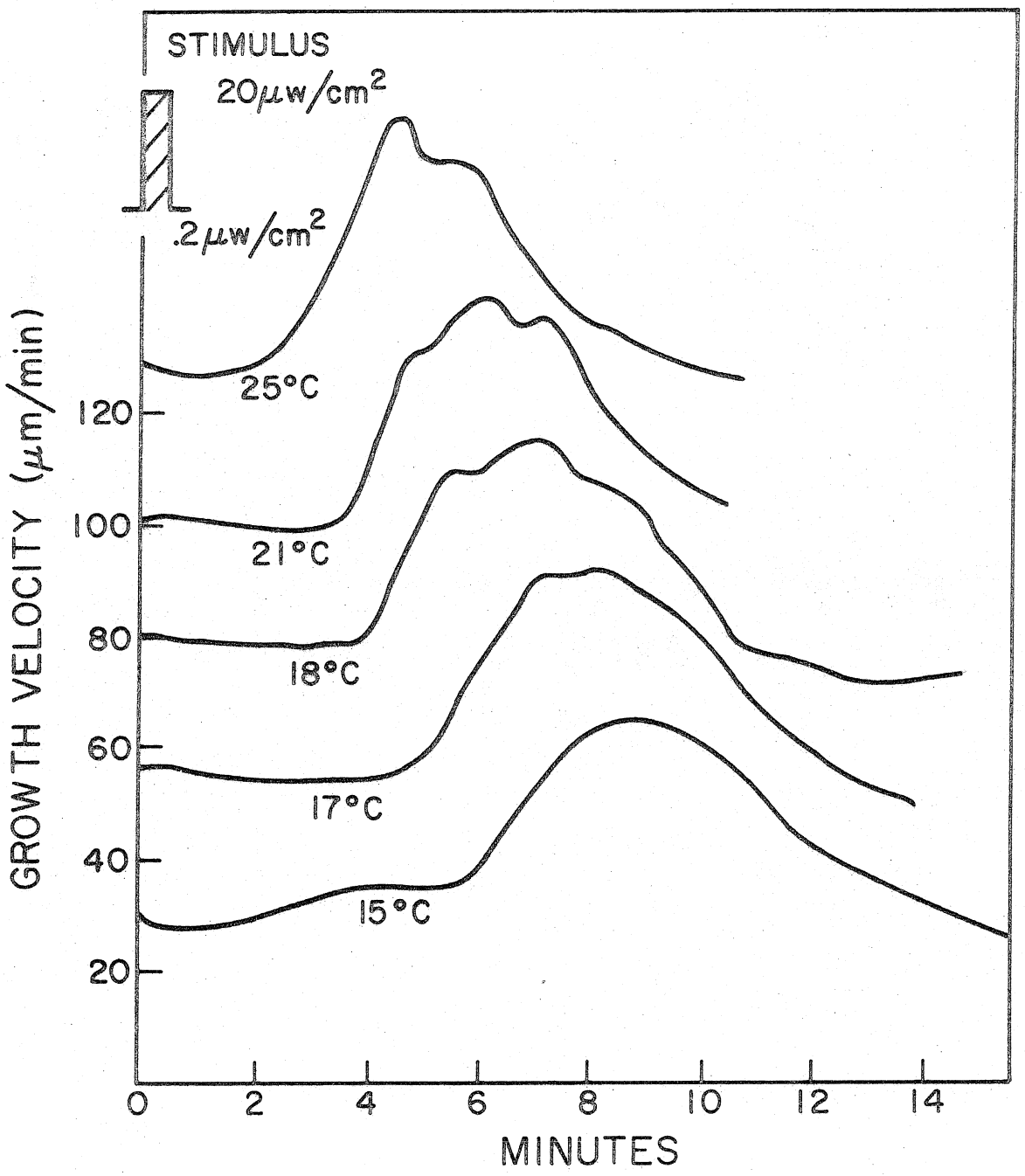
STIMULUS
20μw/cm²
.2μw/cm²
25°C
21°C
18°C
17°C
15°C
GROWTH VELOCITY (μm/min)
120
100
80
60
40
20
0
2
4
6
8
10
12
14
MINUTES

The experiment tests whether there exists a true latency between the light stimulus and the response, and if so, whether its temperature dependence is similar to the growth rate dependence on temperature. Due to the sharpness of the onset of the response, latencies can in fact be defined as the time between the start of the stimulus and this onset of response. The time of onset has been defined as the intersection of the constant baseline growth rate with a line through the 20 and 80% points of the rising slope of the initial growth rate peak.

In this range of temperatures Castle (1928) has shown that the growth rate doubles for a temperature change of 8°C with individual specimens varying from 4.5 to 11°C. The reciprocal of latency for these results doubles in about 9°C indicating a similar dependence. The magnitude of this temperature dependence indicates that both rates are probably governed by enzymatic reactions, rather than by diffusion from receptors to the cell wall.

2) Dependence of shape and latency on stimulus and level of adaptation

In the lower curve of Fig. IV-12 is shown a growth response of C2 to a large 30 sec stimulus where $\log_{10}(I/A) = 3.8$ where A is the adapting intensity and I the stimulus intensity. In the upper curve is Oort's (1932) average of 23 similar stimuli for a(+) strain of wild type. Note that the responses are similar with respect to length and shape. They both last approximately 45 min and show corresponding peaks and valleys. The advantage of the machine is clearly demonstrated here as well, since the C2 response was obtained with a single measurement.

The fine structure of the responses appears only with large stimuli. Its development, in particular the location and shape of the first peak, is shown in Fig. IV-13. Here the response is plotted for individual 30 sec pulses of 455 nm light with intensities from $\log_{10}(I/A) = 0$ to 4.5. A was 40 pwatts/cm^2 except for the dashed curve in which A was zero. Under the same conditions of A = 0 a stimulus was given with I one-tenth of the I used for the dashed response; the response observed was superimposable on $\log_{10}(I/A) = 3.5$. Therefore, for the dashed response, $\log_{10}(I/A)$ has been taken equal to 4.5. At $\log_{10}(I/A) = 2.8$, half of the responses obtained showed two distinct peaks and the other half did not. This was also true for data taken using 380 nm light. With larger stimuli the first peak dominates and the second peak is progressively reduced. We think that

Fig. IV-12.

Growth response to a strong stimulus. Lower curve: Single response of C2 to a large 30 sec duration pulse of blue light ($\log_{10}(I/A) = 3.8$ where A is the adapted intensity and I the stimulus intensity). Temperature was 20.5°C. Upper curve: From Oort (1932) average of 23 similar stimuli in lower curve under different conditions for a (+) strain of a wild type. Temperature was 17.5°C.

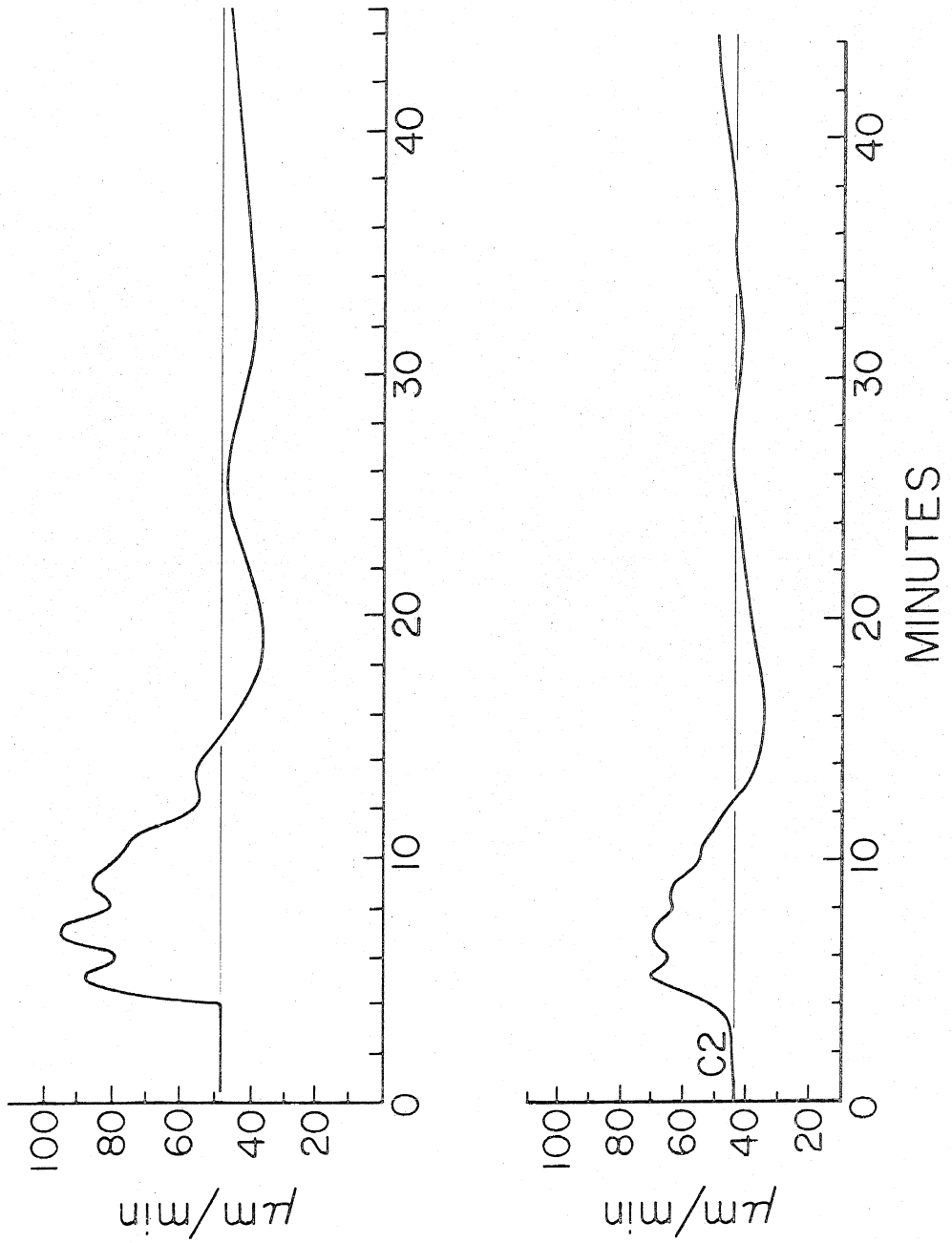
μm/min
100
80
60
40
20
0
10
20
30
40
C2
MINUTES

Fig. IV-13.

Growth responses to 30 sec pulses of 455.5 nm light of various intensities, I, given to specimens adapted to a fixed level, A. Numbers below each curve indicate $\log_{10}(I/A)$ and in brackets the number of experiments averaged. A was 40 pwatts/cm except for the dashed curve in which A was zero. In this case a stimulus was given with I one-tenth of the I used for the dashed response. The response observed was superimposable on that given here for $\log_{10}I/A = 3.5$. Therefore, for the dashed response, $\log_{10}(I/A)$ has been taken equal to 4.5. Each curve has been displaced relative to each other and only the 1.3 curve is not shifted relative to the scale. Normal growth rate of these specimens was between 35 and 70 μm/min.

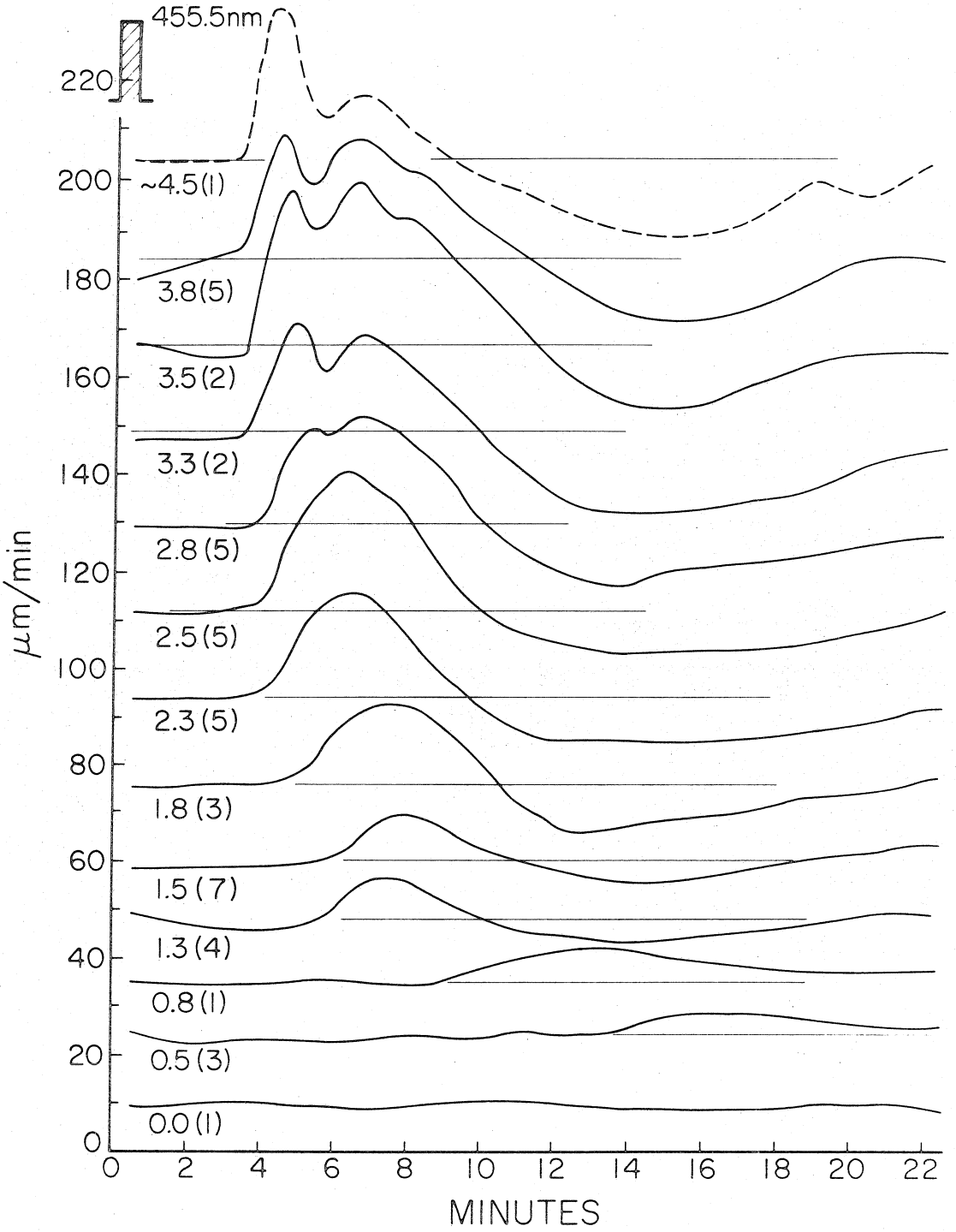
455.5nm
220
200
180
160
140
120
100
80
60
40
20
0
μm/min
~4.5(1)
3.8(5)
3.5(2)
3.3(2)
2.8(5)
2.5(5)
2.3(5)
1.8(3)
1.5(7)
1.3(4)
0.8(1)
0.5(3)
0.0(1)
0
2
4
6
8
10
12
14
16
18
20
22
MINUTES

this observed fine structure is associated with the growth regulating part of the transducer chain with the initial light sensing system, because the avoidance responses show similar fine structure. An example is shown in the upper dashed curve of Fig. IV-22 which shows a response to a "house" being lowered over the spph. This stimulus gives a step "avoidance" stimulus from four sides.

Another aspect of the light response is evident from Fig. IV-13. This is the broadening of the response for larger stimuli. The larger responses look much like those observed in response to step changes in light level.

An additional important point is how the growth response changes as a function of the level of adaptation. Fig. IV-14 shows typical individual responses of the same specimen to a 30 sec duration pulse stimuli of $\log_{10}(I/A) = 2$. Apart from the obvious longer latency at the lowest intensity level, the responses are remarkably similar; however, the higher A, the larger is the following undershoot of growth rate. There appears to be a small dependence of the response size on the level of adaptation. Similarly, Fig. IV-15 shows typical responses of the same specimen to step stimuli of $\log_{10}(I/A) = 1$. These also are remarkably similar except for latency. This point has not been investigated thoroughly but all the data indicate that there is not a major change in response to $\log_{10}(I/A)$ over a range of A between $A \cong 10$ μwatts/cm^2, where "bleaching" is believed to overtake pigment

Fig. IV-14.

Growth responses to pulse stimuli at different levels of adaptation. These are typical individual responses of the same specimen to a 30 sec pulse stimuli of $\log_{10} I/A = 2$. The adapted level is indicated for each curve. Each curve is displaced by 40 μm/min and no curve has been drawn at its absolute growth rate.

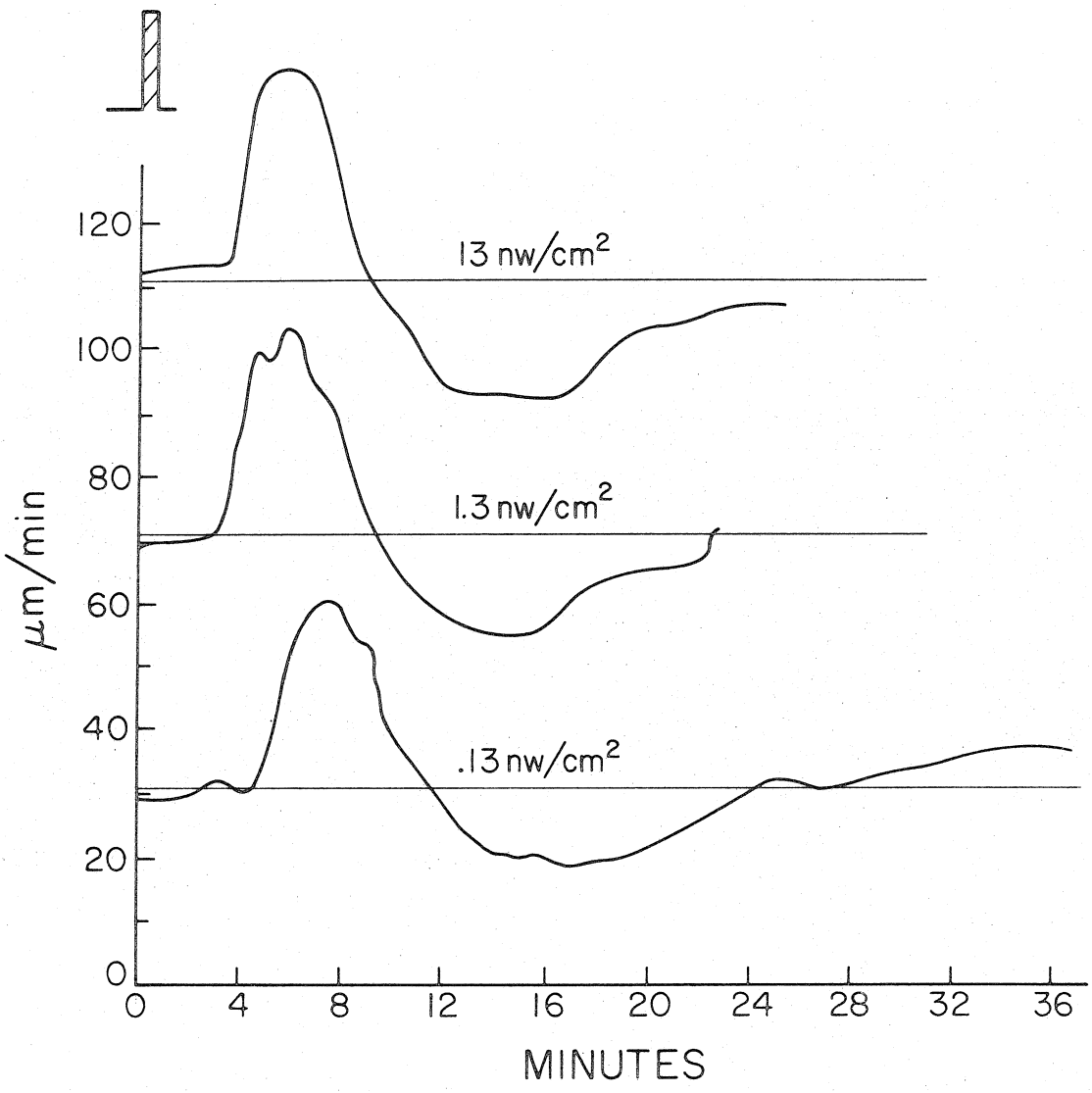
120
100
80
60
40
20
0
μm/min
13 nw/cm²
1.3 nw/cm²
.13 nw/cm²
0
4
8
12
16
20
24
28
32
36
MINUTES

Fig. IV-15.

Growth responses to step stimuli at different levels of adaptation.

Typical individual responses of the same specimen to step stimuli of $\log_{10} I/A = 1$. The adapted level is indicated for each curve. Each curve is displaced by 40 μm/min and no curve has been drawn at its absolute growth rate.

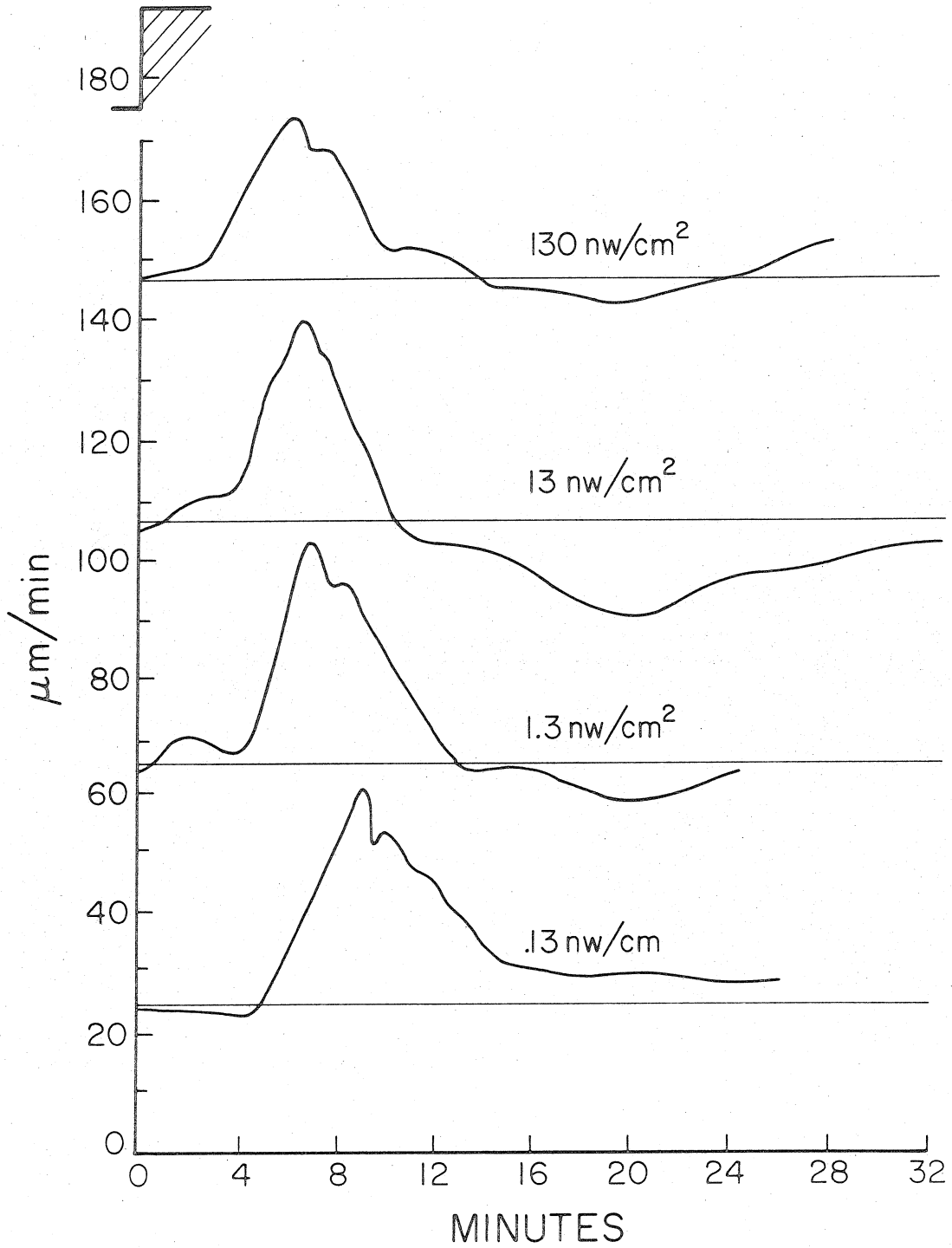
180
160
140
120
100
80
60
40
20
0
μm/min
130 nw/cm²
13 nw/cm²
1.3 nw/cm²
.13 nw/cm
0
4
8
12
16
20
24
28
32
MINUTES

regeneration and A near A_D, the threshold for a growth response. A_D is the intensity, 8 pwatts/cm^2 (455 nm) at which any further lowering of the adapting intensity produces no significant increase in the response to a stimulus of some fixed absolute intensity. The existence of this threshold for the growth response has been noted before by Delbrück, Reichardt and Harm (unpublished) and is probably similar to the "dark light" of human vision research. The phototropic threshold is 50 times lower than A_D (Bergman, 1972).

For the phototropic response measurements under unilateral light stimulation there is a strongly focused region on the distal side of the cell and as long as some of the region of focused light is above threshold there will be some response. Unlike with the growth response there is time to wait and observe any phototropic bending even after several hours. For these reasons the phototropic threshold lies significantly below A_D.

The latency of the response clearly changes as a function of the stimulus size in Fig. IV-13 from about 3.5 min for the largest pulse to about 13 min for the smallest. There is considerable uncertainty in defining latencies with small responses since fixing the latency means that one fixes the point at which the change in growth rate exceeds the error of measurements. This point can be said to occur earlier when the rate changes faster, even if the latent period is constant. Here, the latency has been taken as the time between the

Fig. IV-16.

Latencies of growth responses.

Upper curve: The solid curve is the latency as a function of $1/\log_{10}(I/A)$ where the A = 40 p watts/cm^2 (455.5 nm) and I the intensity of each 30 sec duration stimulus (data from Fig. IV-13 and tabulated in Table IV-3). The dashed curve is taken from the dark growth response latencies measured by Castle (1932).

Lower curve: Replot of data of the above solid curve as $(\text{latency}-2.4\ \text{min})^{-1}$ as a function of $\log_{10}(I/A)$. The dashed curve is taken from the dark growth response latencies measured by Castle (1932). The ordinate for the dashed curve has been changed to $(\text{latency}-4.5\ \text{min})^{-1}$.

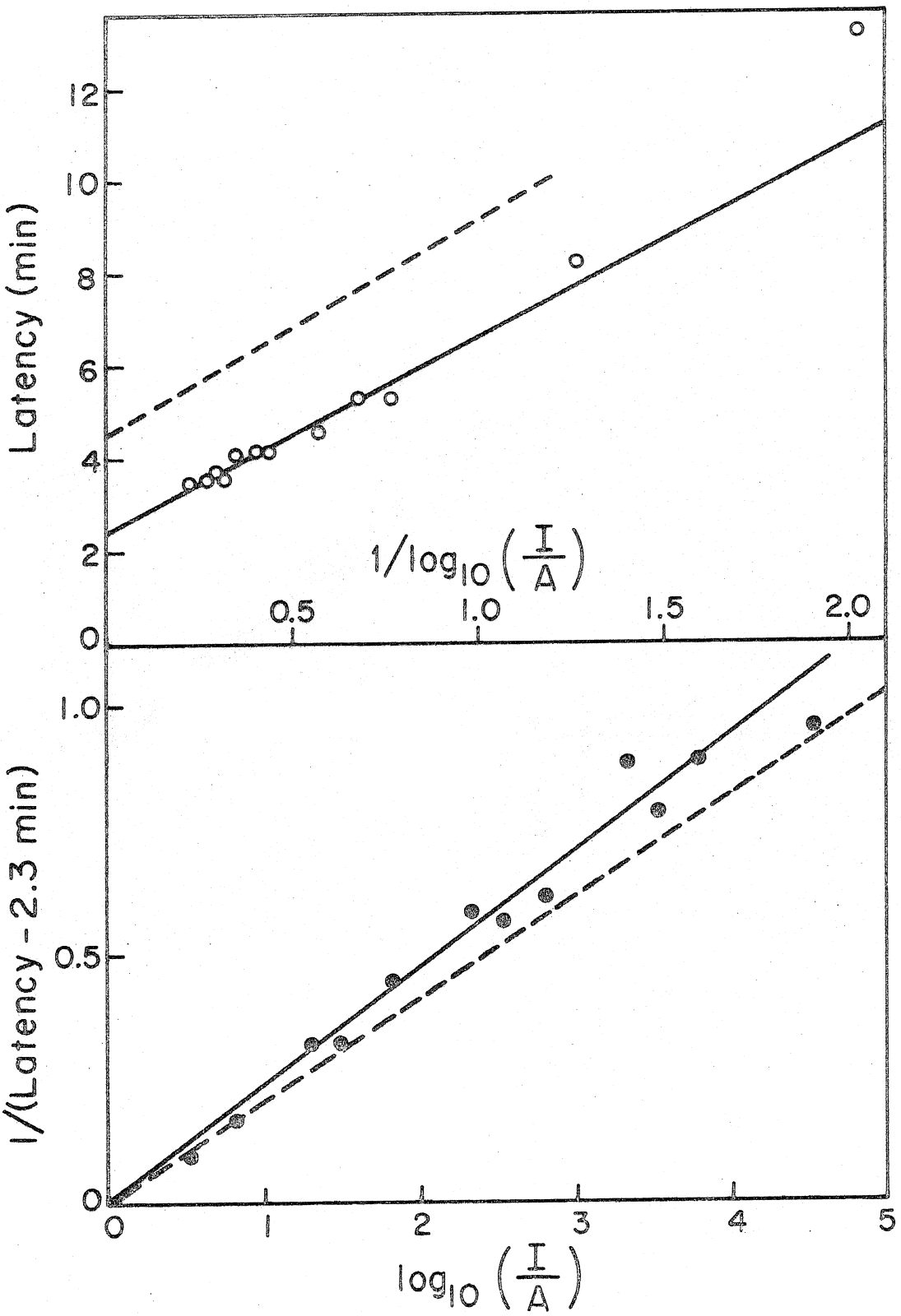
Latency (min)
12
10
8
6
4
2
0
$1/\log_{10}\left(\frac{I}{A}\right)$
0.5
1.0
1.5
2.0
1/(Latency - 2.3 min)
1.0
0.5
0
0
1
2
3
4
5
$\log_{10}\left(\frac{I}{A}\right)$

Table IV-3. 455 nm Pulse Stimulus-Response Latency

Stimulus 30 sec of I $ln_{10}(I/A)$	Absolute Intensity $x10^{-1}$ μwatts/cm^2	Latency (L) min	$1/(L-2.4)$ $(min)^{-1}$
0.0	.046	∞	
0.5	.15	13.3±1.0	.091
0.8	.29	8.5	.164
1.3	.93	5.3	.33
1.5	1.5	5.3	.33
1.8	2.9	4.5	.45
2.3	9.3	4.1	.59
2.5	15	4.2	.56
2.8	29	4.0	.62
3.3	93	3.54	.88
3.5	150	3.7	.78
3.8	290	3.54	.886
4.5*	290	3.46±.1	.945

*adapted from essentially complete darkness and estimated ~ 0.7 lower than A since reponse to a pulse of intensity of one-tenth this size gave a reponse superimposable on the other responses to a 3.5 pulse.

start of the stimulus and the intersection of a straight line fit to the 20 and 80% points of the first rising slope of the response to the horizontal baseline of the response. The spphs were adapted for at least 1 1/2 hr at 40 pwatts/cm^2 (455.5 nm).

The latency for the 455.5 nm stimuli are plotted in Fig. IV-16. The upper curve is a plot of latency as a function of $1/\log_{10}(I/A)$. This plot fits fairly well a straight line extrapolating to 2.4 min for $I \rightarrow \infty$. In the lower curve 1/(latency-2.4) is plotted versus $\log_{10}(I/A)$ giving another straight line fit going through 0 within the errors of measurement.

These results can be compared to the work of Castle (1932) who found similar dependencies for the dark growth response. Castle's results are indicated in Fig. IV-16 with a dashed line. Castle adapted the spph at various intensities, turned off all stimulating light and recorded the start of the dark growth response. The plot of latency as a function of $1/\log_{10}(I/A_D)$ where I is adapting intensity and A_D the intensity threshold for a growth response essentially parallels my curve for the light stimulus latency. The dark growth response curve extrapolates to a latency of 4.5 min for $I \rightarrow \infty$. Castle's inverse plot is also a straight line through zero at A_D = 4 pwatts/cm^2 which is in the same range as my determination of A_D.

Human subjects also show a similar dependence of latency in response to flashes of light (Bartlett and Macleod, 1954) when pre-dark-adapted.

The latency was also measured at different levels of adaptation, but keeping the same size of stimulus. This was measured for pulse stimuli (Fig. IV-14) and step stimuli (Fig. IV-15). These latencies also lie on the same positive growth response latency curve provided they are plotted as a function of $1/\log_{10}(A/A_D)$, where A is an estimate of the adaptation level as a result of the stimulus and A_D is the dark light adaptation level.

Castle (1930) also measured latency of growth responses at moderate adapted intensities (estimated ~ 7 nwatts/cm^2). He observes a rather small and different dependency of latency on stimuli. However if his latency data are plotted as a function of $\log_{10}(A/A_D)$ where A is the changed adaptation level a result of the stimulus then the same dependency and slope is observed. An estimate for A can be obtained from Delbrück and Reichardt (1956) who suggest that during a short stimulus the level of adaptation is increased from the pre-adapted level by the size of the stimulus, It (intensity x duration of pulse), divided by the time constant of adaptation.

If one considers again the latency data of Fig. IV-16 upper curve it is seen that the latencies for small stimuli are longer than expected from the other data. If the $\log_{10}(A/A_D)$ as discussed above were considered instead of $\log_{10}(I/A)$ these values would be brought down to lie on the curve. It has been shown by Castle (1929) using a constant absolute intensity of pulse that the latency is

somewhat dependent on the adapted level at the time of the stimulus. He found the larger the effective stimulus the shorter is the latency.

These results suggest that the latency can be separated into two parts, a fixed part independent of light intensity and a variable part,probably related to the receptor complex itself,dependent on the absolute adaptation level reached as a result of the stimulus and the size of the stimulus.

The fixed part seems dependent on whether the stimulus is positive or negative and on the temperature. Castle and Honeyman (1935) also showed that it is not dependent on the growth rate, but strongly dependent on the cell diameter. In their experiments,this amounted to about 0.8 min shorter for a 50 μm diameter spph then a 100 μm diameter spph. They measured this latency with a saturating pulse making this time particularly clear. The width of the response is also probably dependent on the spph diameter.

The variable part of the latency probably corresponds to the rate control of some reaction. What is most significant is its dependence on the absolute intensity or absolute level of adaptation as a result of the stimuli.

3) Dependence on wavelength

A growth response curve was obtained for C2 at both 380 nm and 455.5 nm. 10 nm bandwidth interference filters were used. The adaptation levels were 140 pwatts/cm^2 for the 380 nm experiments and 40 pwatts/cm^2 for the 455 nm experiment. The averages of several individual responses are shown in Fig. IV-13 and Fig. IV-17. These data were analyzed according to the method of Oort (1932) using the amount of extra growth above the growth in the absence of the stimulus as a good measure of the size of the response. In Fig. IV-12, upper curve the growth velocity is plotted for a response. The size of the response is the area between the response curve and the horizontal line at 48 μm/min. We found that this distance of growth (μm) was, for a spph growing between 35 μm/min and 70 μm/min, fairly independent of the growth rate. The size of each response was individually measured and these numbers averaged. Also the response curves were graphically averaged at each size of stimulus and then this average response measured as described (see Table IV-4).

In order to determine whether the response curve to a stimulus at 380 nm is different from that at 455 nm, the Oort measure of response (in μm) was fitted to the equation $R = R_o I/(I + I_{1/2})$, where $R = R_o$ when $I >> A$ and $I = I_{1/2}$ when $R = R_o/2$.

This equation does not seem to fit the stimulus-response data

Fig. IV-17.

Growth responses of C2 to 30 sec pulses of 380 nm light of intensity I above adapted level A. The numbers under each curve give $\log_{10}(I/A)$ and in brackets the number of experiments averaged. A = 140 pwatts/cm^2. Each curve has been displaced relative to each other, only the 0.8 curve is not shifted relative to the growth velocity. Normal growth rate for these specimens was between 35 and 70 μm/min.

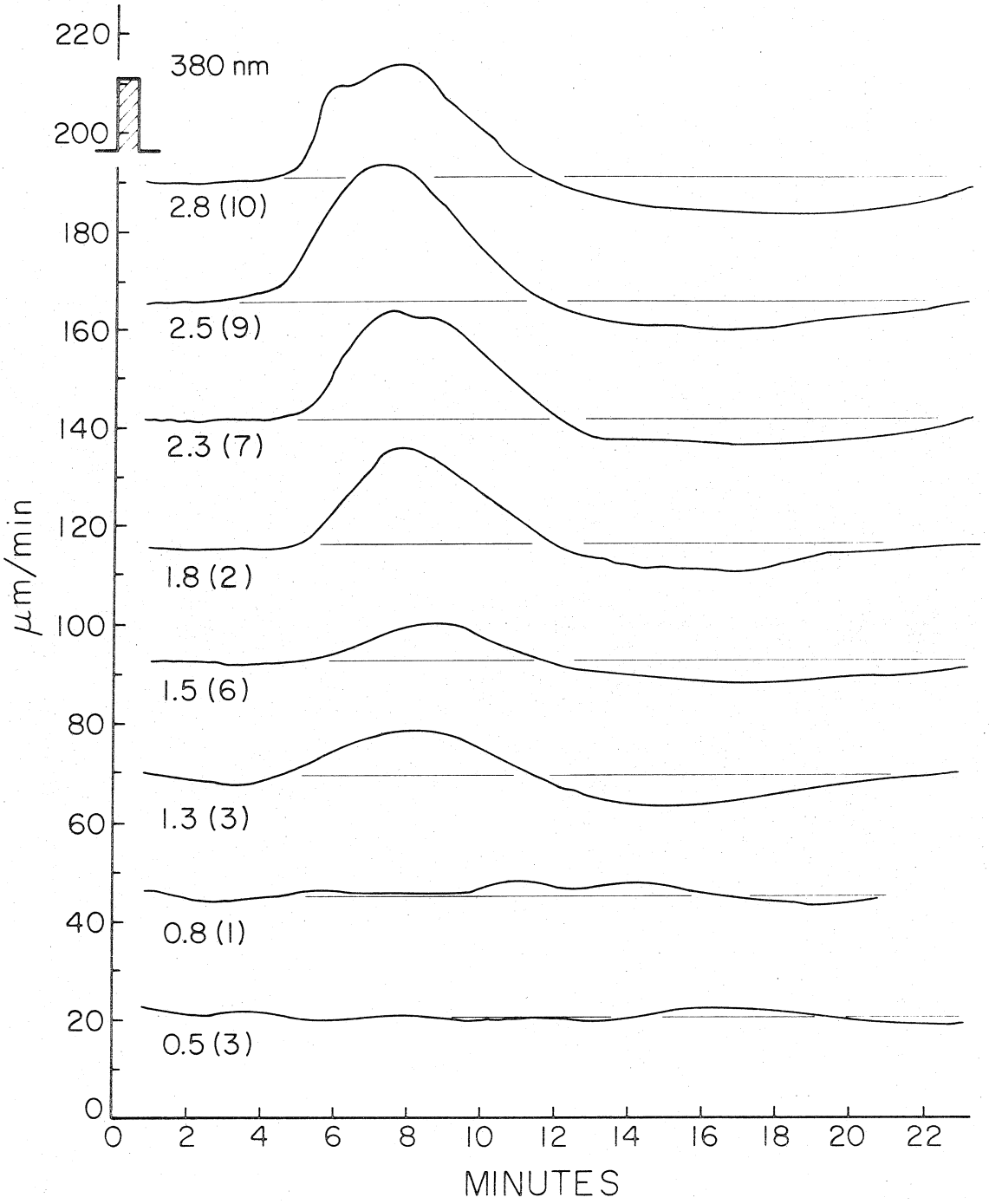
220
200
380 nm
2.8 (10)
180
160
2.5 (9)
140
2.3 (7)
120
1.8 (2)
100
1.5 (6)
80
1.3 (3)
60
40
0.8 (1)
20
0.5 (3)
0
μm/min
0
2
4
6
8
10
12
14
16
18
20
22
MINUTES

Table IV-4. Stimulus-Response Curves at 380 nm and 455 nm

	380 nm				455 nm			
$\log_{10}(I/A)$	R^1	R^2	Fit	#	R^1	R^2	Fit	#
0.5	3.4	3±3	3	5	5.7	2±3	3	3
0.8	5.7	5±7	9	1(2)	15.4	13±11	9	1(2)
1.3	33.6	45±7	26	2	22.4	30±6	26	3
1.5	25.4	31±6	34	6	27.4	29±1	36	6
1.8	73.4	61±25	54	5	61.5	75±6	57	3
2.3	87.5	92±17	85	6	70.2	86±14	88	5
2.5	103	110±13	98	8	101	83±8	101	5
2.8	94.8	93±13	111	4	99.5	106±10	113	6
3.3					94.5	115±15	123	2(1)
3.5					157	135±15	126	2(1)
3.8					116	140±15	128	2(1)

Table IV-4. (continued)

Notes:

1. R, individual responses measured separately and then response sizes averaged.
2. R, responses measured by superimposing all the responses and drawing the average and then measuring its response size.
3. Neutral density filters were used and therefore the actual intensity at two different wavelengths differ by a small amount. This has been taken into account in the calculation of the fit values and in the plot (at nominally 2 O.D., at 380 nm the actual transmission is 1.05% and at 455, .975%).

well,particularly in view of the rise of the early component of the response at high stimuli, but serves as a reasonable approximation.

The data was first fitted with a least-squares program to the linearized form of the equation

$$\left(\frac{1}{R} = \frac{I_{\frac{1}{2}}}{R_o} \cdot \left(\frac{1}{I}\right) + \frac{1}{R_o}\right)$$

and then a single curve was fitted graphically by eye to both sets of data taken together.

The 380 and 455 data with the graphically by eye fit is plotted in Fig. IV-18. Only four points lie more than one standard deviation from the curve.

The single graphical fit by eye fits both sets of data better that the individual least squares fits to the linear form of the equation according to the external error criteria (see Table IV-5).

Within the accuracy of the data there appears to be no wavelength effect. This result is contrary to some unpublished work in this area. This result does not exclude the possibility of several pigments being present, particularly if the pigment has a similar action spectra. However,it does make a two pigment hypothesis unnecessary.

Fig. IV-18.

Comparison of growth responses to 455.5 nm and 380 nm. The data of C2 of Fig. IV-13 for 455.5 nm (open circles) and Fig. IV-17 for 380 nm (closed circles) analyzed according to Oort's (1932) response measure (growth above the normal growth in the absence of the stimulus). In this figure this response in μm is plotted as a function of $\log_{10}(I/A)$ where I is the intensity of 30 sec pulse and A the intensity of adaptation. The solid line is the best graphical fit by eye of the equation $R = R_o I/(I + I_{\frac{1}{2}})$ where $R = R_o$ when $I >> A$, and $I = I_{\frac{1}{2}}$ when $R = R_o/2$ when $I = I_{\frac{1}{2}}$.

The error bars correspond to the standard deviation of the mean computed from estimates of each measurement error.

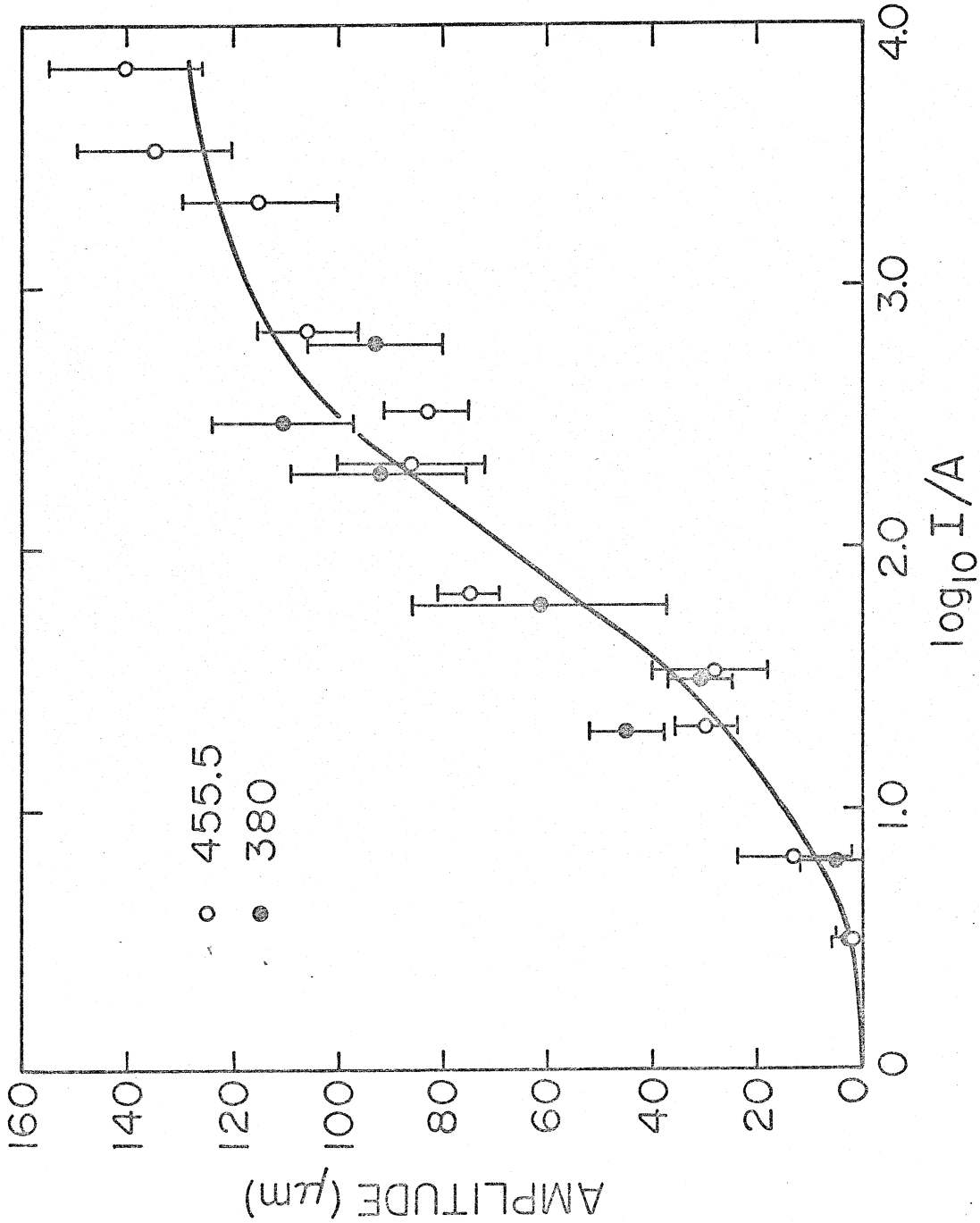
AMPLITUDE (μm)
160
140
120
100
80
60
40
20
0
0
1.0
2.0
3.0
4.0
log10 I/A
455.5
380

Table IV-5

Technique	Wavelength	R_o	$I_{1/2}$	$\log_{10} I_{1/2}$	External Error
least squares	380	106±8	31±7	1.49	1.45
least squares	455	120±7	40±8	1.66	1.52
graphical	380,455	133	95	1.98	1.38,1.38

$$\text{External Error} = \sqrt{\frac{1}{n-2} \sum_{i=1}^{n} \frac{(\chi_i - \bar{\chi})^2}{\sigma_i^2}}$$

4) Latencies and rate of dark adaptation

Castle (1932) suggested that the latency dependence on the adapted level is an expression of the slowing of the rate of adaptation at low adapted levels. Whatever the truth of his statement it suggests that the rate of change of $\log(A/A_D)$ is not constant but decreases proportional to $\log(A/A_D)$, i.e.

$$\frac{d(\log A/A_D)}{dt} = -\frac{1}{b}\log(A/A_D), \text{ or } \log\frac{A}{A_D} = K\, e^{-t/b} \quad .$$

In Fig. IV-19 the data of Delbrück and Reichardt (1956) on dark adaptation are replotted taking only the slopes of each line segment between measurements and plotting these, as a function of the log of the mean adapted level. These data suggest a straight line dependence through A_D except for a few points. This conjecture is consistent with the long time required to reach very low levels of adaptation near A_D. This dependence, of A on time, is of the same form as for human vision (Rushton, 1961). For human vision the additional information is available that the $\log(A/A_D) = a(1-p)$ where p is the unbleached fraction of the photoreceptor. In Phycomyces no information is available on pigment concentration as a function of light adaptation. That the system has some other functional similarity to the human system is indicated by the similar

dependence of latency on the strength of short stimuli. This similarity could be further tested by investigation of the rise of the level of adaptation resulting from pulse stimuli. Unfortunately, the level of adaptation is not easy to measure.

Fig. IV-19.

Rates of dark adaptation versus level of adaptation. The data was obtained from Fig. 8 of Delbrück and Reichardt (1956) on the rate of adaptation. The slope of each of their line segments between their measurements is plotted as a function of the log of the mean adapted level between these measurements. The data from the experiments adapted to a constant level before turning off the light is plotted with closed circles and the data from experiments pre-adapted with a large pulse is plotted with open circles. I have found that it takes 60 min to adapt from -10 to -17. This indicates that at low adapted intensities the curve goes down to the lower left as drawn.

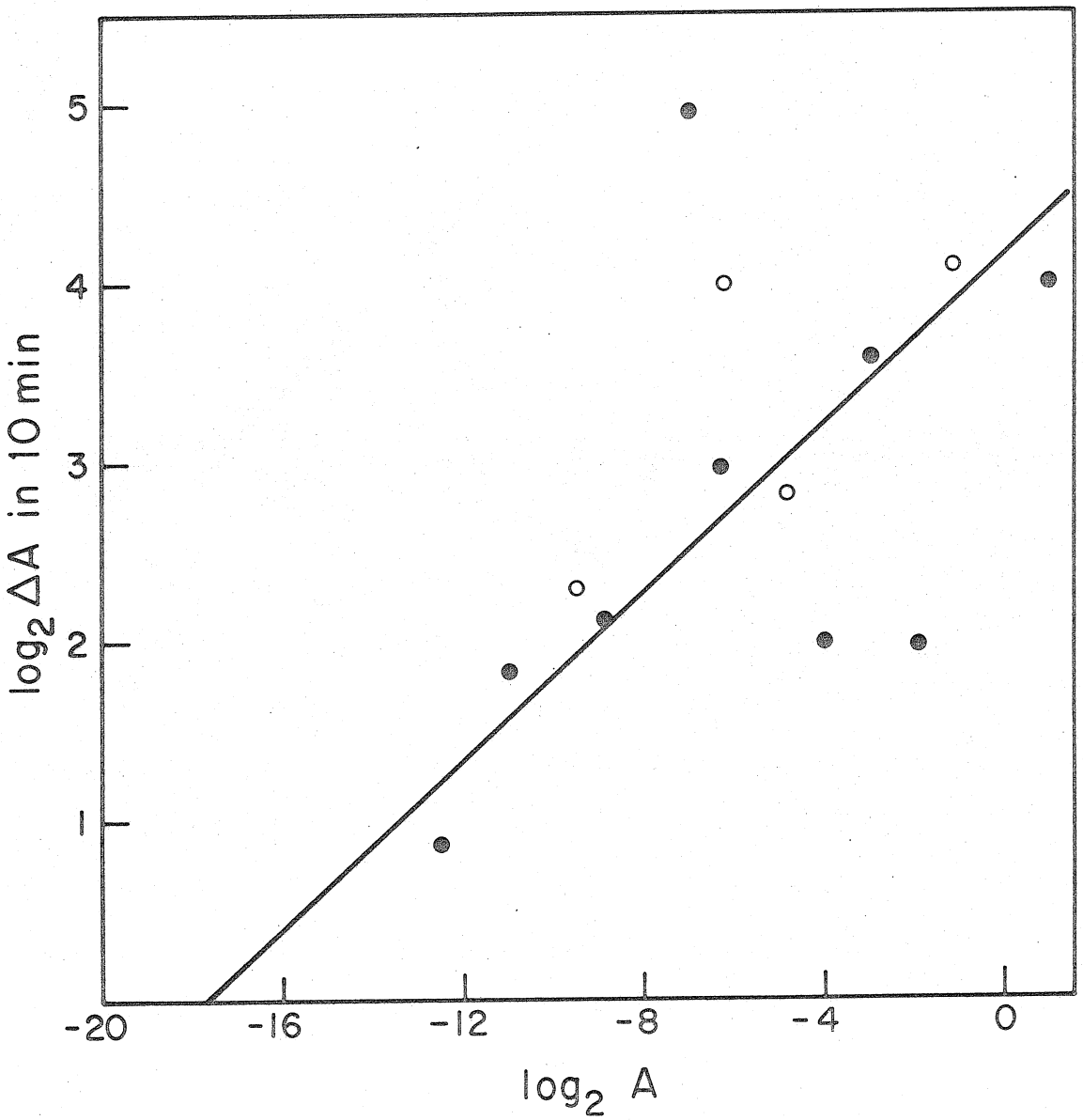
5
4
3
2
1
$\log_2 \Delta A$ in 10 min
-20
-16
-12
-8
-4
0
$\log_2 A$

5) Summary of growth response characterization data

Within the range 15° to 25°C, the response shape to a medium size pulse stimulus remains remarkably constant. The latency shows a strong dependence on temperature similar to that of the growth rate as found by Castle. Latency also strongly depends on the absolute level of adaptation resulting from the stimulus. This dependence, for the light growth response, is similar to that found by Castle for dark growth response.

A portion of the latency is proportional to $1/\log(A/A_D)$ where A is the level of adaptation before stimulation or that estimated reached during the stimulus and A_D corresponds to that intensity, adapting below which produces no additional modification of the response when stimulating above A_D. The value of A_D is 50 times higher than the phototropic threshold. Possible interpretations of this difference concern the probable effect of the focused light on phototropism and the long time of integration used in measurement of the phototropic threshold.

Change in the shape of the response has been observed as a function of the stimulus size. The fine structure observed for large pulse stimuli is believed to be associated with the growth responding system and not directly with the light responding system since other stimuli such as avoidance show similar fine structure in the response.

Experiments comparing 455 and 380 nm show the same responses complete with fine structure. There is no obvious (i.e. one with a different absorption spectrum) second photopigment system and quite likely one photopigment is responsible for sensitivity at these two peaks of the action spectrum.

The rate of dark adaptation has been reexamined with the conclusion that probably

$$\frac{d \log (A/A_D)}{dt} = -\frac{1}{b} \log(A/A_D) \text{ or } \log (A/A_D) = K\, e^{-t/b}$$

holds rather than

$$\frac{dA}{dt} = -\frac{1}{b} A \quad \text{or} \quad A = K\, e^{-t/b} \ .$$

This dependence of adaptation and the dependence of response latency on the strength of short stimuli suggest that the kinetics of Phycomyces vision are similar to the kinetics of the vertebrate visual system.

E. GENETIC DISSECTION OF RESPONSE PATHWAY

Bergman (1972) has studied a series of mutants with abnormal responses to light. He defined the classes: class (1-1), in which light does not trigger spph initiation or blue light tropism, but do "avoid"; class (1-2), those that fail only to show light tropism; and class (2), those that respond only to light with spph initiation. No mutant has been found which is completely blind.

I have characterized a number of these mutants in more detail. Class (2) mutants are presumably affected in their output apparatus. The four tested so far, C110, C63, C68 and C149, conform to this expectation. They share the common characteristic (Fig. IV-20 and Fig. IV-21) of a prolonged growth response with normal latency and weak phototropism to blue light, while having apparent phototropic thresholds for 280 nm light within a factor of 10 of that for wild type. Also the duration and latency of their growth response to a 280 nm step change of light are shorter by 20-25% compared with blue light. They also trope continuously, although very slowly (0.5°/min), even at moderate intensities of 280 nm. Although they share similarities, they are not identical as their characteristic response show.

Fig. IV-20.

Growth responses of wild type and four class (2) mutants to step changes of different size blue light (Corning 5-61). The magnitude of each step change from A to I is indicated in brackets below each curve in units of $\log_{10}(I/A)$. Each curve is displaced on the growth velocity scale; C149 (4.5) curve is drawn according to the absolute growth velocity scale.

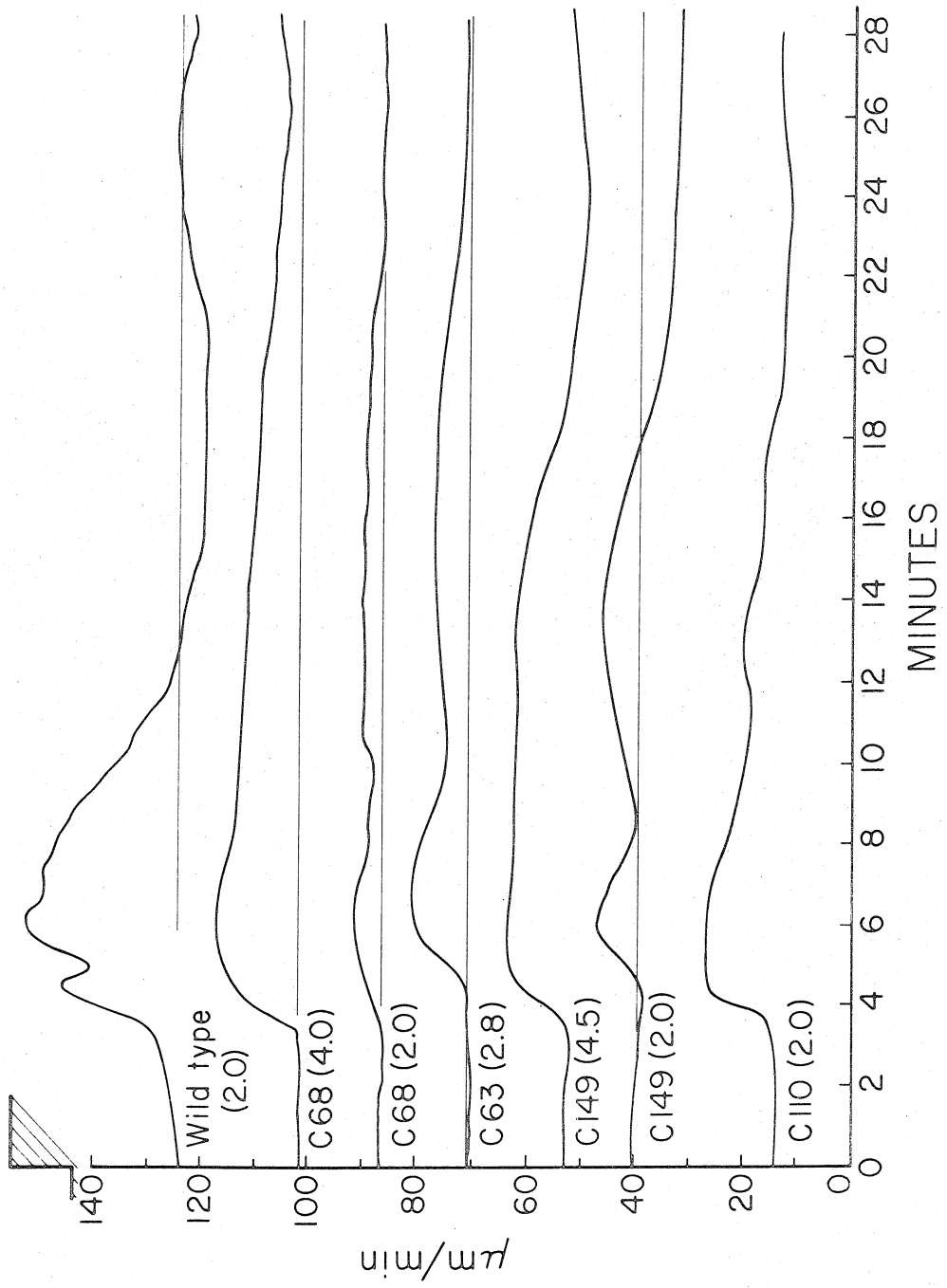
μm/min
140
120
100
80
60
40
20
0
0
2
4
6
8
10
12
14
16
18
20
22
24
26
28
MINUTES
Wild type (2.0)
C68 (4.0)
C68 (2.0)
C63 (2.8)
C149 (4.5)
C149 (2.0)
C110 (2.0)

Fig. IV-21.

Individual growth responses of three class (2) mutants (Bergman, 1972) to 30 sec pulses of different size of blue light. The magnitude of each pulse of intensity I relative to the adapted level A is indicated in brackets below each curve in units of $\log_{10}(I/A)$. Each curve is displaced on the growth velocity scale. C63 is drawn according to the absolute growth velocity scale.

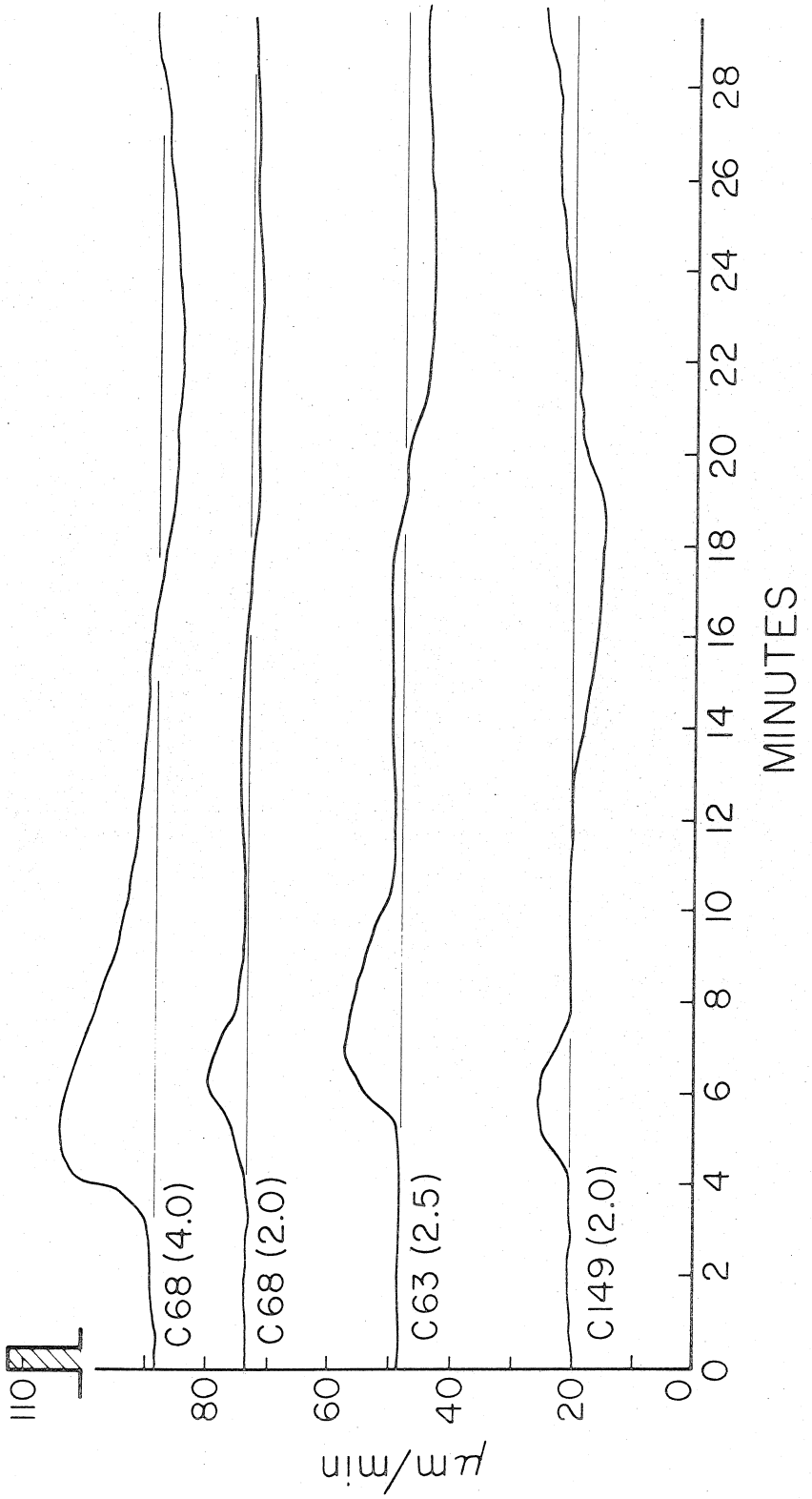
110
80
60
40
20
0
μm/min
C68 (4.0)
C68 (2.0)
C63 (2.5)
C149 (2.0)
0
2
4
6
8
10
12
14
16
18
20
22
24
26
28
MINUTES

For example, unlike the others C110 twists abnormally slowly. It may simply develop more slowly as it grows. In any case, it twists only about 4°/min after 6 cm growth and slower earlier. This mutant, as opposed to the others, shows a slight bending in the blue over a wide range of intensities (Bergman, 1972).

The best studied of these mutants is C149. It tropes at $\sim$0.5°/min at moderate intensities of 2 μwatts/cm^2 (280 nm) and only in a narrow region at the bottom of the apparent growing zone. This should be compared to bending rates of 6 to 20°/min and bending along all the entire growing zone for C2 under similar conditions. It shows normal geotropism in the dark. Near threshold intensities for response it shows the "Buder angle effect" (see section IV.C.4).

The existence of these mutants which do not respond well to light or avoidance stimuli confirms that these different stimuli feed into the same growth regulation pathway. It might be expected that if the shape of a response is primarily due to a common growth regulation apparatus then a response to a symmetric avoidance stimulus should mimic a light growth response. In fact, the response of wild type to a step up change of 100-fold intensity from .20 μwatts/cm^2 to 20 μwatts/cm^2 corresponds closely to a 1.5 cm symmetric ("house on") avoidance experiment (Fig. IV-22).

For the avoidance experiment, the shell vial containing the spph was mounted on the tracking machine stage and enclosed by a large box

Fig. IV-22.

Light growth responses and avoidance growth responses of wild type.

a) step up:

solid curve: The response to a 100-fold step up in light intensity at time zero as indicated by the arrow.

dashed curve: The response to a 1.5 cm squre glass house being lowered around the spph at time zero (positive symmetric avoidance).

b) step down

solid curve: The response to a 100-fold step down in light intensity at time zero.

dashed curve: The response to removal of a 1.5 cm square glass house (negative symmetric avoidance).

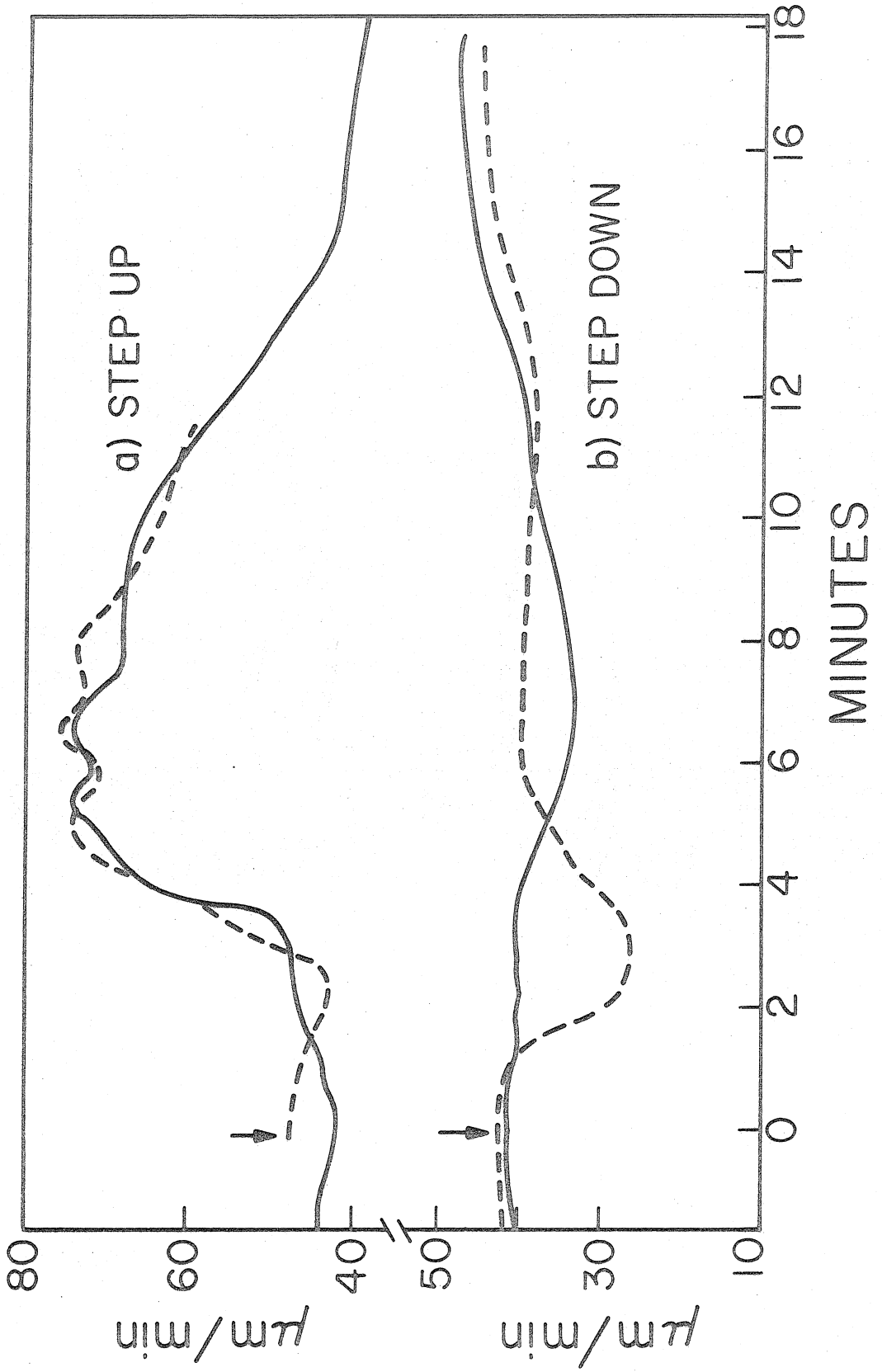
a) STEP UP
b) STEP DOWN
μm/min
μm/min
80
60
40
50
30
10
0
2
4
6
8
10
12
14
16
18
MINUTES

($\sim$.12 m^3). A small square glass house was made about 10 cm high and 1.5 cm on each side. This house was either raised or lowered around the spph. After the specimen had adapted to the relatively open air conditions of the large box for about 1 hour the small house was lowered around the spph. This constituted the positive symmetric avoidance stimulus. After 45 min the house was raised and removed from the vicinity of the specimen. This constituted the "house off" or negative symmetric avoidance stimulus.

As seen in Fig. IV-22 the step up in light and positive avoidance experiments have a similar time course. Probably the avoidance response has a shorter latency because the temperature of the avoidance experiment was $\sim$ 20°C while the light step was at about 24°C (see temperature dependency of response (IV.D-1)).

The lower curves of Fig. IV-22 show the responses to reversals of the above step changes. The response to an equivalent step down in light intensity and removal of the house ("house off") seem quite different. The latency of the negative avoidance response is about 1 min compared to the light response latency of about 4 min. The amplitude of the avoidance response is also much greater. These experiments were carried out at the same temperatures as above.

In Fig. IV-23 individual responses of C149 to a 1 cm square house "on" and "off" are shown with responses to a 100 x light pulse

Fig. IV-23.

Light growth responses and avoidance growth responses of C149. House on: 1 cm square house lowered over the cell at time zero. This response is abnormally small compared to wild type. Light pulse: 30 sec duration 100x adapted intensity pulse of blue light. House off: Response to removal of 1 cm square house. This response is similar to the response to wild type. Light step down: Response to 100x step reduction of light intensity. These responses as displaced relative to the growth velocity scale.

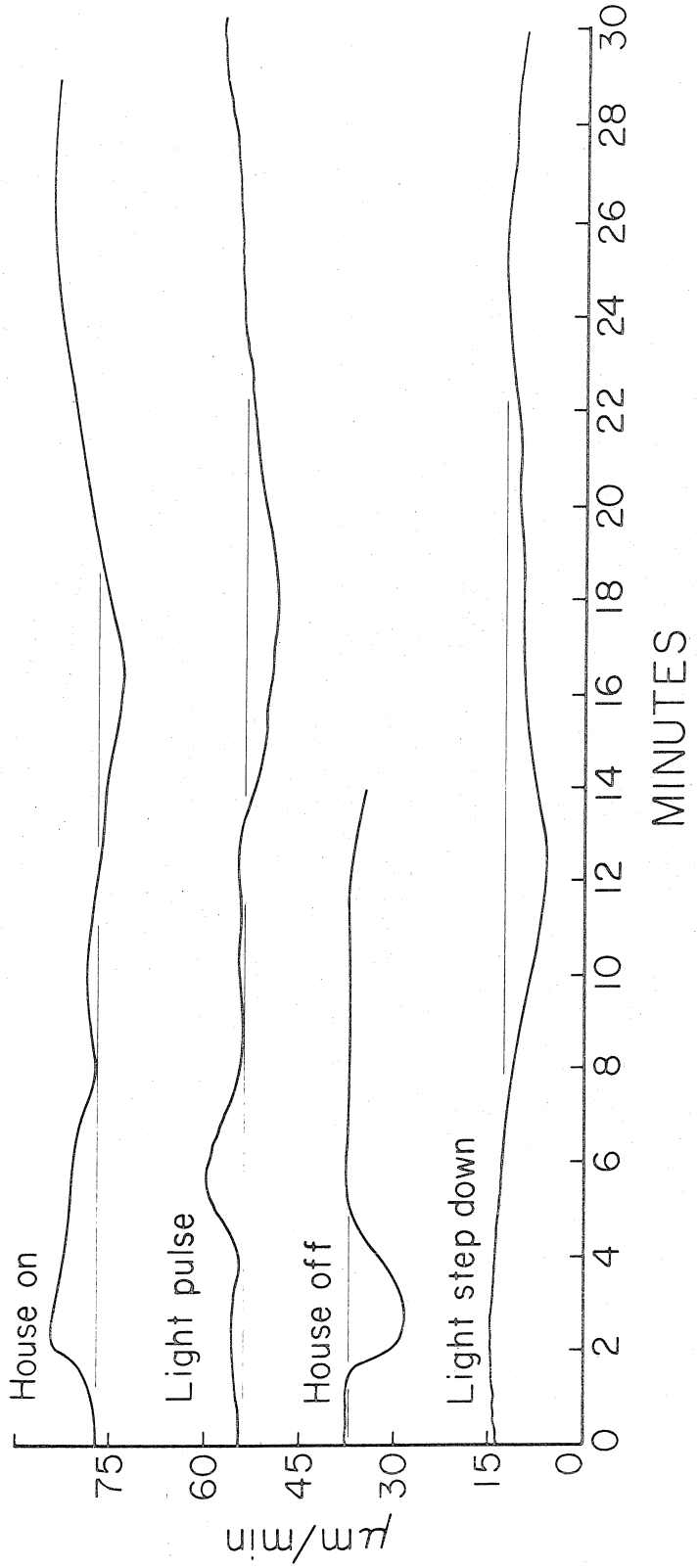
House on
Light pulse
House off
Light step down
75
60
45
30
15
0
μm/min
0
2
4
6
8
10
12
14
16
18
20
22
24
26
28
30
MINUTES

of 30 sec duration and 100x step reduction in light intensity. The "house off" symmetric avoidance response looks fairly normal but the "house on" except for latency, appears similar to the light pulse response. At least with respect to the positive responses, probably both types of stimuli are part of the same pathway, although more work is necessary.

A number of albino class (1-2) mutants (S-37, S-14, S-18, S-5) have been investigated and these show large refractory periods like those described by Oort (1932) and attributed by Delbrück and Reichardt (1956) to slowed dark adaptation. In a sequence of three large stimuli separated by 45 min, the second stimulus gave no response. Oort describes this phenomena for wild type when stimuli are separated by a much shorter time. This finding is hard to reconcile with the light adaptation explanation, but bears further work. Adaptation kinetics of these mutants have not been measured.

Only two class (1-1) mutants (Fig. IV-24) have been studied. C47 shows a normal response; except the threshold is raised by 10^4 for blue and 280 nm light. At the present time it is our best candidate for being a receptor mutant. Although it twists normally and is otherwise similar to C47, C21 is different in three respects. First it gives a somewhat prolonged growth response. Second, it shows rapid hunting with approximately 1/3 of the wild type hunting wavelength (see section IV.C-4). Third, it has about three times as large a Buder angle in 280 nm light as wild type. This is sufficient to

Fig. IV-24.

Light growth responses of C2 (normal) and two (1-1) mutants. Averaged responses to 30 sec pulses of light 100x the adapted intensity. The curve for C2 is an average of four specimens. The adaptation levels relative to the thresholds for response were the same for the different strains.

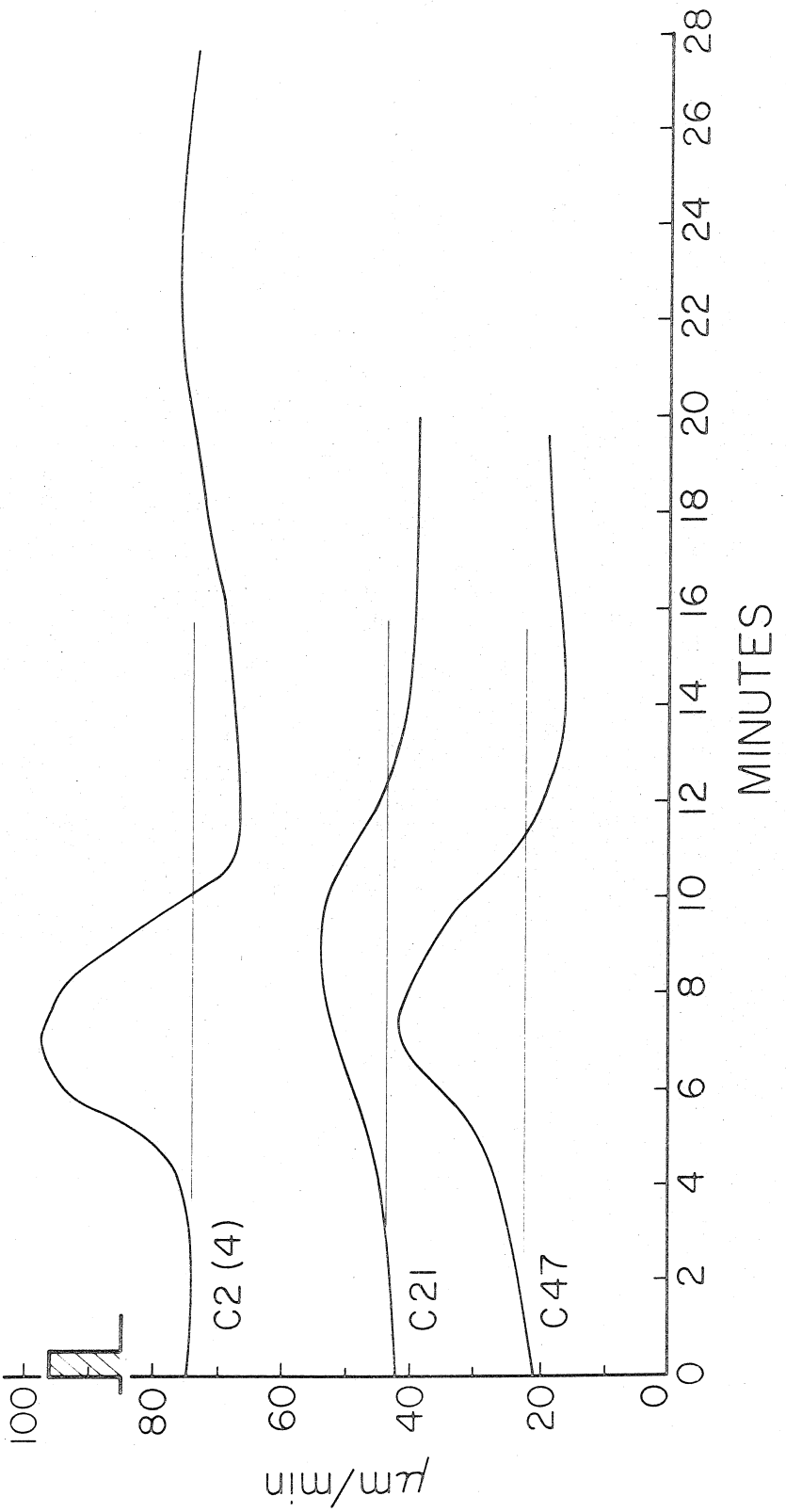
100
80
60
40
20
0
μm/min
0
2
4
6
8
10
12
14
16
18
20
22
24
26
28
MINUTES
C2 (4)
C21
C47

turn the troping direction 180° and toward the source near threshold at a geophototropic equilibrium angle of 30° from the vertical. This mutant in the phototropic-geotropic equilibrium experiment in blue light shows an abnormally fast cut off toward its apparent threshold (Bergman, 1972) which for blue light is somewhat above its 280 nm apparent threshold.

Although use of these mutants to understand the stimulus response pathway has just begun, their potential usefulness is already apparent.

REFERENCES

Bartlett, N. R., and S. Macleod 1954. Effect of flash and field luminance upon human reaction time. J. Opt. Soc. Am. 44: 306-311.

Bergman, K., Patricia V. Burke, E. Cerdá-Olmedo, C. N. David, M. Delbrück, K. W. Foster, E. W. Goodell, M. Heisenberg, G. Meissner, M. Zalokar, D. S. Dennison, and W. Shropshire, Jr. 1969. Phycomyces. Bacteriol. Rev. 33: 99-157.

Bergman, K. 1972. Sensory responses of Phycomyces: I. Blue-light control of sporangiophore initiation. II. Classification of mad mutants. Ph.D. Diss. Califor. Instit. Tech., Pasadena, Calif., pp. 101.

Blaauw, A. H., 1914. The primary-growth reaction and the cause of the positive phototropism in Phycomyces nitons. Koninkl. Ned. Akad. Wetesnschap. Proc. 16: 774-786.

Buder, J. 1920. Neue phototropische fundamentalversuche. Ber Deut. Botan. Ges. 38: 10-19.

Buder, J. 1946. Uebersicht über ergebnisse einiger noch ungedruckter arbeiten aus den botanischen anstalten der universität Breslau. Mimeographed summary of Ph.D. dissertation, University of Halle.

Castle, E. S., 1928. Temperature characteristics for the growth of the sporangiophores of phycomyces. J. Gen. Physiol. 11: 407-413.

Castle, E. S. 1929. Dark adaptation and the light-growth response of Phycomyces. J. Gen. Physiol. 12: 391-400.

Castle, E. S. 1930. Phototropism and the light-sensitive system of Phycomyces. J. Gen. Physiol. 13: 421-435.

Castle, E. S. 1932. Dark adaptation and the dark growth response of Phycomyces. J. Gen. Physiol. 16: 75-88.

Castle, E. S. 1933. The physical basis of positive phototropism of Phycomyces. J. Gen. Physiol. 17: 49-62.

Castle, E. S. and A. J. M. Honeyman. 1935. The light growth response and the growth system of Phycomyces. J. Gen. Physiol. 18: 385-397.

Castle, E. S. 1942. Spiral growth and the reversal of spiraling in Phycomyces, and their bearing on primary wall structure. Am. J. Botany 29: 664-672.

Castle, E. S. 1958. The topography of tip growth in a plant cell. J. Gen. Physiol. 41: 913-926.

Castle, E. S. 1961. Phototropism, adaptation, and the light-growth response of Phycomyces. 45: 39-46.

Castle, E. S. 1965. Differential growth and phototropic bending in Phycomyces. J. Gen. Physiol. 48: 409-423.

Castle, E. S. 1966. A kinetic model for adaptation and the light responses of Phycomyces. J. Gen. Physiol. 49: 925-935.

Cohen, R. and M. Delbrück. 1958. System analysis for the light-growth reactions of Phycomyces. II. Distribution of stretch and Twist along the growing zone, and the distribution of their responses to a periodic illumination program. J. Cellular Comp. Physiol. 52: 361-388.

Curry, G. M. and H. E. Gruen. 1959. Action spectra for the positive and negative phototropism of Phycomyces sporangiophores. Proc. Nat. Acad. Sci. 45: 797-804.

Delbrück, M., and W. Reichardt. 1956. System analysis for the light growth reaction of Phycomyces, p. 3-44. In D. Rudnick (ed.), Cellular mechanisms in differentiation and growth. Princeton Univ. Press, Princeton, N. J.

Delbrück, M. and W. Shropshire, Jr. 1960. Action and transmission spectra of Phycomyces. Plant Physiol. 35: 194-204.

Delbrück, M. and D. Varjú. 1961. Photoreactions in Phycomyces. Responses to the stimulation of narrow test areas with ultraviolet light. J. Gen. Physiol. 44: 1177-1188.

Dennison, D. S. 1958. Studies on phototropic equilibrium and phototropic geotropic equilibrium in Phycomyces. Ph.D. Diss. Calif. Instit. Tech. Pasadena, Calif., pp. 146.

Dennison, D. S. 1965. Steady-state phototropism in phycomyces. J. Gen. Physiol. 48: 393-408.

Meissner, G. and M. Delbrück. 1968. Carotenes and retinal in Phycomyces mutants. Plant. Physiol. 43: 1279-1283.

Meistrich, M. L., R. L. Fork, and J. Matricon. 1970. Phototropism in Phycomyces as investigated by focused laser radiation. Science. 169: 370-371.

Oort, A. J. P. 1932. Die Wiederherstellung der empfindlichkeit nach einem lichtreiz. Verhandel. Konikl. Ned. Akad. Wetenschap. 29: 5-47.

Reichardt, W. and D. Varjú. 1958. Eine inversionsphase der phototropischen reaktion. (Experimente an dem Pilz Phycomyces blakesleeanus.) Z. Phys. Chem. Neue Folge 15: 297-320.

Reichardt, W. and D. Varjú. 1959. Der einfluss von eigen- und fremdrotation des sporangientragers von Phycomyces auf die phototropische reaktion. Z. Naturforsch. 14b: 210-211.

Rushton, W. A. H. 1961. Dark-adaptation and the regeneration of rhodopsin. J. Physiol. 156: 166-178.

Zankel, K. L., P. V. Burke, and M. Delbrück. 1967. Absorption and screening in Phycomyces. J. Gen. Physiol. 50: 1893-1906.

Appendix A

Details of Tracking System

The purpose of this appendix and those following is to describe the machine in sufficient detail that it could be copied. It includes discussion of the problems that were considered, the problems that developed and techniques that might better be applied to help any future builder to do a better and faster job.

1. Specifications of System

The tracking system should be capable of following the most rapid acceleration that can be estimated (.1 μm/sec^2 for Phycomyces) and velocity of growth (2.5 μm/sec vertical) or horizontal velocity (8 μm/sec for UV phototropism). In competition with these requirements it should be capable of the highest possible resolution which we estimated as about ±1 μm in position on a 0.1 Hz bandwidth. The limit of resolution will ultimately be determined by the error signal which is produced optically using a HeNe laser back lit shadow image of the sporangium. For a coherent source optical resolution is commonly taken as the wavelength of light (.6 μm) divided by the numerical aperture of the lens. Practically resolution is somewhat better than that. The important parameter is the growth velocity not the absolute position, so that non-linearities in a position less than a few percent are tolerable. Noise of the same frequencies

as the signal should be kept to a minimum. A transient response to a pulse of light peaks in 5-7 min and continues 30-40 min. Even for large transient "movements" caused by a change in optics such as occurs in "avoidance house" experiments, the system should not lose the specimen.

2. Optics of Tracking System

Having decided that the best available technique for tracking involved the shadow projection of the non-growing sporangium certain criteria had to be met. Namely, the tracking system light source should interfere minimally with the natural processes of the fungus, i.e., with the light and avoidance sensitivity of the fungus.

From the tropic action spectrum measurements the relative quantum efficiency of the photopigment at 590 nm is about 4×10^{-7} of peak (450 nm) sensitivity, the highest wavelength for which a response has been observed. This measurement gives an estimated threshold at 590 nm of about 8 $\mu w/cm^2$. By extrapolation to 630 nm we obtain about 4×10^{-9} of peak sensitivity and a threshold of about 0.8 watts/cm^2 on the sporangiophore stalk. The threshold is the extrapolated point of no tropic response after 6-8 hours of adaptation to a horizontal light beam.

Photomultiplier sensitivity also drops rapidly in the red so that preferably all the light should be concentrated near the edge

of the region of Phycomyces sensitivity to provide maximum monitoring efficiency per incident energy and thus minimize heating.

A HeNe laser (632.8 nm) of 1 mw output in TEM_{00} mode was found best for these purposes. The intensity distribution of the beam has a Gaussian shape with $1/e^2$ diameter of 1.4 mm. A completely uniform beam of the same diameter would actually be better. Using a type S-11 photomultiplier (EMI 9656B) with 0.4% Quantum Efficiency (Q.E.) at 6328 nm, an intensity of 10 to 30 μw incident on the sporangium is sufficient to provide a good tracking signal.

The beam was also restricted to the region immediately around the sporangium to minimize growing zone heating.

The laser beam is filtered to eliminate all blue light entering from this point (Schott RG610, greater than 3.0 O.D. below 590 nm) reduced in intensity by a 1.0 O.D. neutral density filter (Kodak), split by a beam-splitter prism and then guided by prisms to be incident as two beams on the sporangium at 90 degrees to each other in the horizontal plane. Each beam has a total energy of about 17 μwatts. For a 500 μm diameter sporangium this amounts to about 5 μwatts incident light. The top of the growing zone is just below the $1/e^2$ point of the beam and thus should not be significantly affected.

One remaining worry is that the sporangium which is suspected of emitting the avoidance gas might be affected by local heating by the beam on two sides of the sporangium and cause bending and other

irregularities. However, as far as one can tell, avoidance experiments conducted without this beam by hand are essentially similar to machine responses. A model calculation, assuming a sphere of water of sporangium size (0.5 mm diameter) would have a convection loss of about 8 μwatt x ΔT(°C) (Sears, 1958) and an input incident intensity of 10 μwatts, respectively. If all the incident energy were absorbed then one could expect a 1.2°C rise in temperature of the sporangium. A tremendous amount of light is seen to be scattered so there should not be a significant temperature rise.

The laser light is essentially a parallel beam source providing telecentric illumination. As a result, as the spherical sporangium moves in and out of focus of the imaging lens behind the sporangium there is no change in image size. This property is important for it reduces the cross coupling between the different axes. Thus, a movement in and out of focus, for example, will not be interpreted as a vertical movement.

The lens has a working distance of 22 mm and a focal length of 23 mm (Bausch and Lomb 38-12-99 objective) with minimum distortion of 5 μm in the object plane. Such a long focus lens was chosen because it was realized at the start of the project that objects near the specimen influence the growth of Phycomyces. Stabilization of the growing zone relative to the neighboring distant surfaces is hoped to prevent any stimulus due to their presence. The experimental

condition of a moderately large house and of still air necessary to prevent vibration of the specimen, is different from most conditions of previous experimenters. Most other Phycomyces experiments have either been done in open air or in small houses. How these various conditions affect light responses is not known. For increase of working distance I would recommend Sher-Tumico Tubular Micrometer Co., 62 1/2 x projection lens or the equivalent. This lens has less than 2 μm distortion in the object plane, a field of 5 mm and about 6.2 cm working distance with 16.5 mm effective focal length. This lens system of course takes a lot more room around the fungus. Compound systems can also be used but with deterioration in distortion figures and stability.

The two images are projected with the aid of front surface mirrors and masks onto a single area 12.7 x 19.78 cm, on which they are centered 8.89 cm apart. For the horizontal axes the edge detecting light pipes are mounted on a symmetric screw arrangement (40 turns/in (15.76 turns/cm)). Turning a small 2.5 cm drive micrometer head (50 turn) precisely moves the light pipe heads symmetrically about the center point a full distance of 1.25 in (3.18 cm). The screw is threaded in opposite directions on either side of the center point. This feature allows precise centering of the light pipes on the edges of the sporangium, which can vary in size from .3 to .8 mm in diameter (1.5 to 4.0 cm in image plane). For the vertical dimension a single

detector head is mounted on a micrometer for adjustment and there is a fixed comparison head on the background light. To adjust for different sized sporangiums a variable filter (a photographic Kodak print scale) is used to balance the background light.

Due to the symmetric nature of the two horizontal pairs of light pipes there is very little cross-coupling of either channel to either vertical or horizontal error of the other axes. The vertical sensing light pipe however, is sensitive to side error since there is only one sensor on the sporangium which may become displaced from the high point of the sporangium. An approximate relation for small horizontal error is: the error in vertical = (error in horizontal)^2/(diameter of sporangium). This would not normally be a serious problem since it would typically require a 22 μm horizontal error to produce a vertical error of about 1 μm.

A more serious problem is interference between sporangiophore vibration frequency and of light detector's chopping frequency. The tracking system at present tends to oscillate over the whole amplitude of the sporangium vibration. It would help to increase the chopping frequency in order to reduce interference effects and to process the error signal differently (i.e.,in particular increase the gain of the low frequencies). This will be carried out using a system as discussed in part 3 of this Appendix.

A stiff white sheet of paper serves quite well as a screen for initial setting up the sporangium in the vicinity of the light pipes.

The flexible light pipes are 3/16 inch diameter and 30 inch long of 20 μm fiber diameter and 35% efficient (Bausch and Lomb 32-14-30) or 24 inch long 50 μm fiber Dyonics model D3a.

3. The Electronics of Tracking System

The outputs of the light pipes are chopped by a motor (Bodine type K-2 model 704 or 712), driven either at 120 or at 51.7 Hz, turning a photographically produced chopper "blade" about 25 cm in diameter. The light from both light pipes is passed through a protecting 570 nm cut-off filter (Schott OG 570) to eliminate stray light from stimulating beams, and then onto an end-on photomultiplier tube EMI 9656B type S-11 (0.4% quantum efficiency) and equivalent noise input (ENI) about 3×10^{-14} watts at 632.8 nm.

A reduction of this source of noise by about a factor of 20 could be obtained by using selected S-20 tubes at 8% Q.E. at about $1500 additional cost, for example EMI 9558B with ENI of 1.3×10^{-15} watts at 632.8 nm.

Since the energy incident onto the photomultiplier is about .02 to .05 microwatts, this is not likely to be a major noise source. The light is chopped at twice the chopper rotation frequency.

Two LS400 Texas Instrument phototransistors are used to pick up

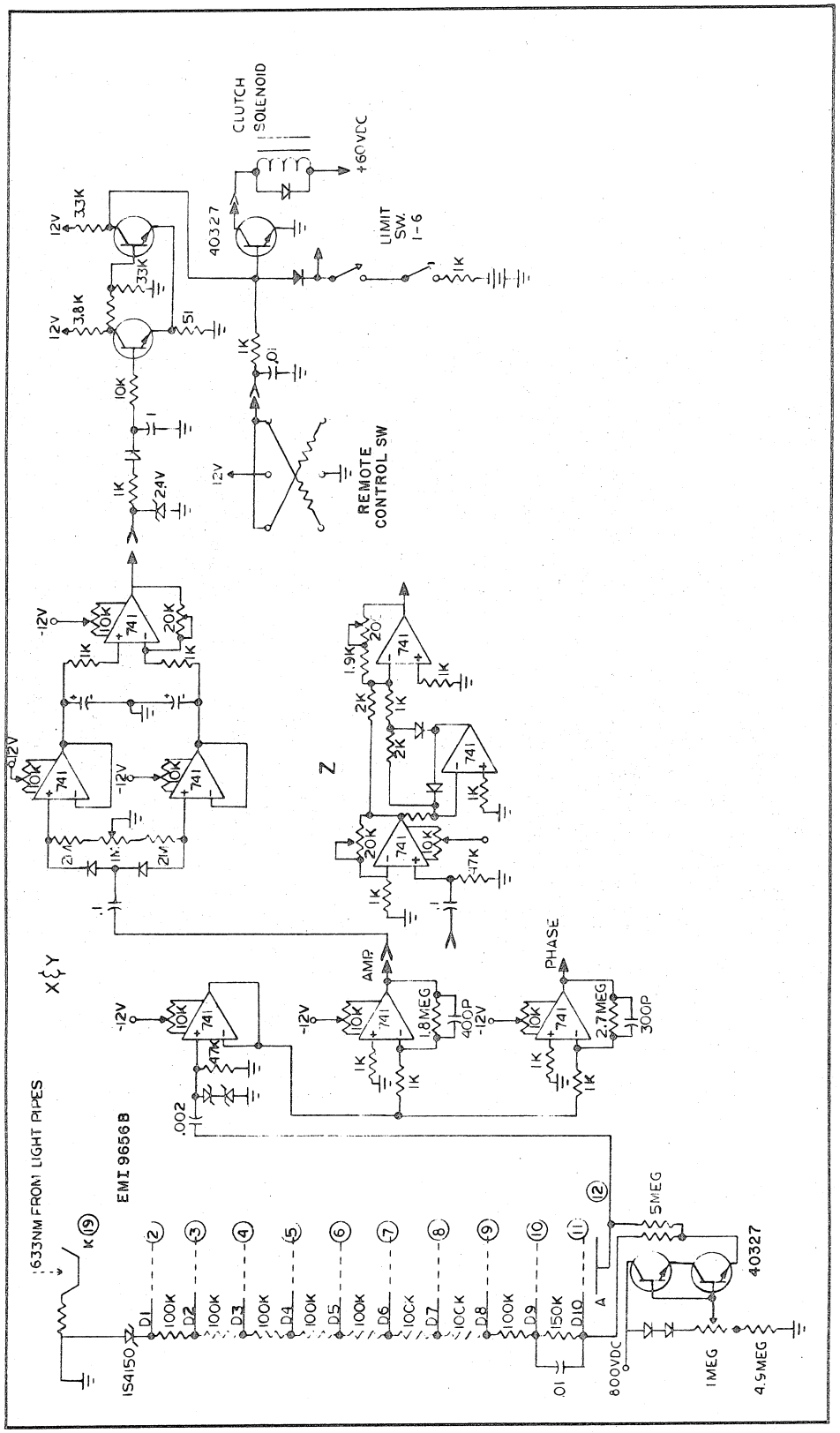

Fig. A 1. Tracking circuits: Photomultiplier detectors and amplitude control.

the phase position of the chopper. Small "grain of wheat" tungsten lights infrared pass-filtered with Schott RG715 to remove the visible light are used to excite the phototransistors. This phase reference serves all three photomultiplier circuits.

An alternative method for chopping the outputs of the light pipes is to use a tuning-fork mirror system as advertised by Bulova, but this seems to be no better than the chopper wheel in frequency response or other errors. A moving-coil galvanometer scanner such as those of General Scanning, Inc. (Brosens, 1971) have definite advantages, although at much higher cost. The advantages are that each light pipe could be shone on the same small area of the photomultiplier tube rather than at a considerable distance, as presently done, to prevent surface irregularities from influencing the comparison of the two light pipes. Also a higher frequency of chopping may be used while still allowing a high ratio of the duration of one beam passed relative to the transition between light pipe beams. The technique involves moving a mirror in almost step fashion from one angle to another and back.

The synchronization pulse from the phototransistor triggers phase reference flip-flop (see circuit Fig. A-2) for each axis. These flip-flops gate the signal from the photomultipliers. One difficulty with the light chopping is that the transfer from one light pipe to the other is not smooth. A partial summing of the two signals or a small gap in signal produces a large transient.

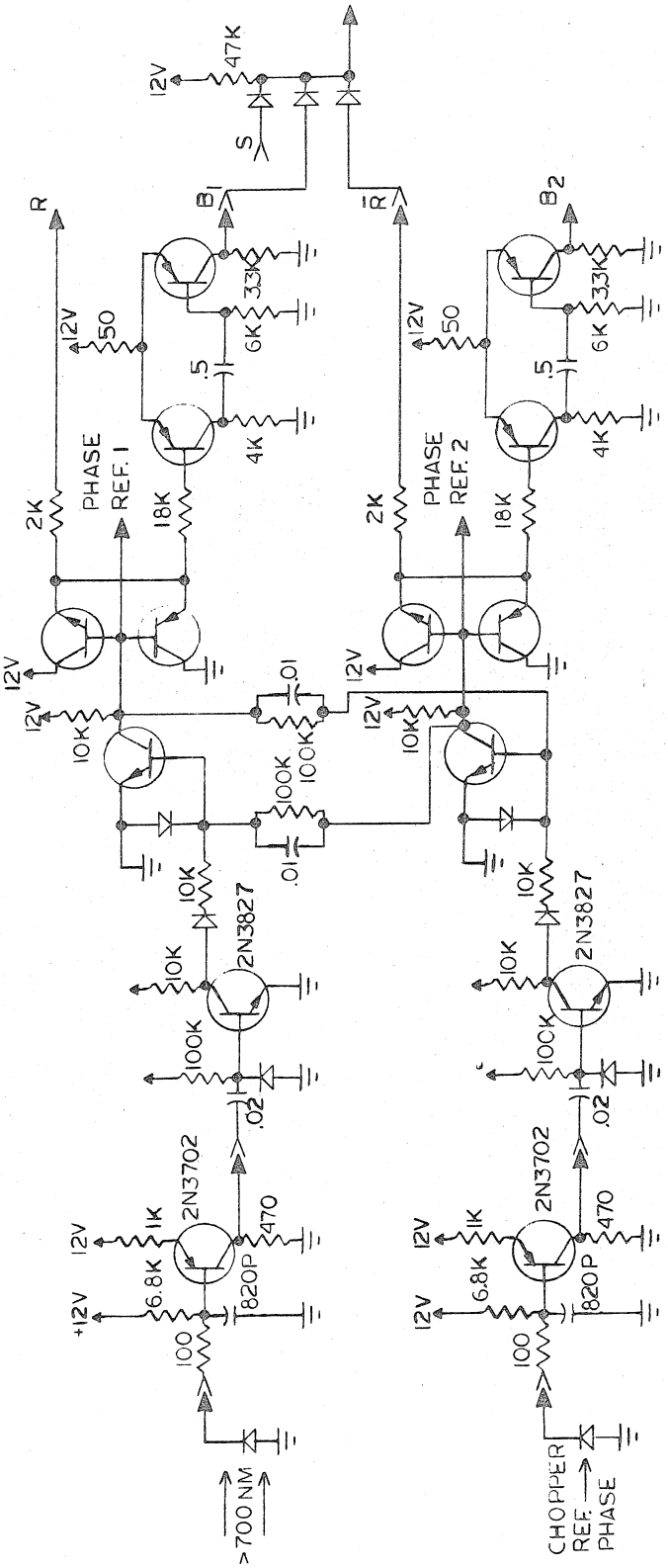

Fig. A-2. Tracking circuit: Phase detection and spike blanking.

To cure this problem a gating-off pulse triggered by the phase reference signal blanks this transient at the phase signal gate. This phase signal is amplified about 10^4 and held to zero base line. This signal is analog AND ed to both the right and left phase reference gates provided by the flip flop reference. The "true" signal sets a filtered flip flop or comparator which drives a triac circuit which in turn controls the direction of the two-phase split capacitor motor (Hurst DC-DA 1 rpm) driving the stage. A triac circuit is used because triac has the property of "latching" or staying on once turned on until the current across it goes to a small value. This means a control triac can be used to trigger the driving triac at low or zero current eliminating the transient problem associated with sudden current changes in induction circuits such as that of a motor.

The amplitude signal is formed by putting the phase signal through an absolute value circuit with 10 x gain and filter. This signal then operates an electromagnetic clutch which controls power transfer from the motor to the micrometer screw which in turn drives the stage.

A remote control switch allows manual operation of the stage drive while one sets up the sporangiophore into tracking position. Gain setting is provided by voltage control to the photomultipliers.

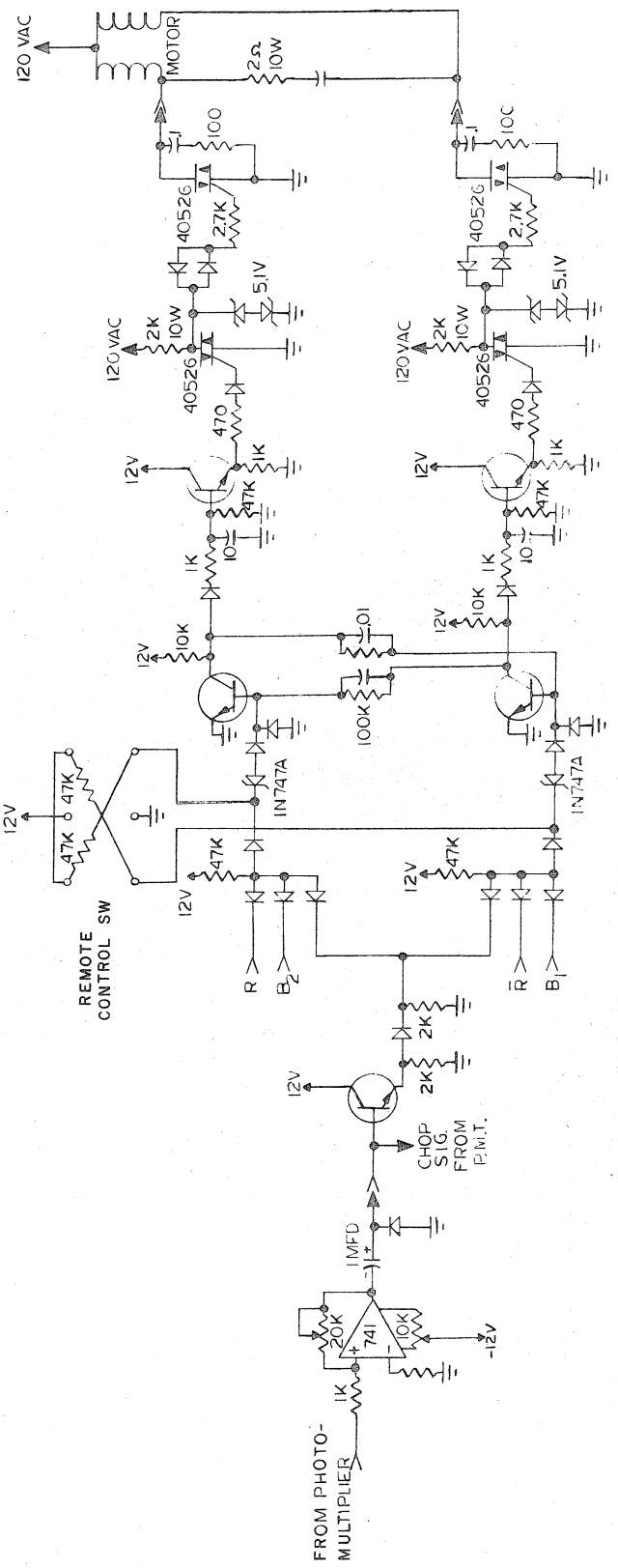

Fig. A-3. Tracking circuit: control of motor direction.

To provide equal gain on all axes, each photomultiplier tube is balanced with a voltage-drop and isolation circuit from the high-voltage regulated DC power supply (Power Designs Model 2K-10) to each tube.

The motors provide a Go-No-Go system either forward or backward with a reversing from full speed forward to full backward in about 1 sec, and to full speed from stop to 20 msec. The full speed is 8.3 micron/sec at the stage. The clutch provides stopping in 0.3 μm at the stage.

Several advantages and disadvantages of such a system should be pointed out. If a system has a backlash larger than the error you desire, then a correcting system optimally should go through this dead band at maximum velocity (H. James et al., 1947). This is provided with an on-off system of the type used here. Unfortunately, with this particular motor there is no way of getting a signal which says which way the motor is actually moving. Since the time constant of the motor is about 1 sec it is possible to overshoot each time and therefore oscillate back and forth over much further than desired if the gain to the system is slightly above optimal. A small amplitude high frequency oscillation is of no consequence if the frequency is much greater than the high frequency cut-off of the measuring filter. The present system oscillates at .3 Hz which

really is too close to the .1 Hz desired and used measuring bandwidth. Thus unfortunately these motors and clutches have to be reversed and operated at a much higher frequency than they were designed. An electromagnetic clutch is limited to about 12 closures/min of constant duty. The constant reversing of the motor results in high current continually going through the motor causing heating and wear. In spite of these fears I have had only one failure and no failures in the last 500 hours of operation. The gears also soon have about 4 μm of backlash and wear quickly. In its favor it can be said to have high cost effectiveness since it does a good job inexpensively. The main difficulties are accommodating vibration of the sporangium and providing high reliability.

Several alternative systems can be suggested. If a high frequency proportional and low frequency integral control system is used in conjunction with a DC torque system one goes at minimum speed through the dead band reducing the ability of the system to respond. The characteristics at null then determine the accuracy of the system. However, this system could be very successfully used particularly at the limited accelerations found for the fungus provided (1) backlash is minimized, (2) the high frequency gain is held high and (3) the position output is filtered to minimize the high frequency oscillations. As previously discussed there is

sufficient signal-to-noise ratio of the error signal to servo the stage to high tolerances. This is particularly true because all the backlash, etc., is within the feedback loop. The reduction of backlash involves using high quality and therefore expensive gears (less than .3 micron backlash) and careful servicing of the stage such as replacing springs on a regular basis and oiling the ball-bearing slides.

Other advantages of a DC torque motor control system should be mentioned. Such a motor has a very large dynamic range essentially over 2000-fold unlike the present on-off system. If properly driven it should provide a very smooth following of the growth. Added advantages of such a system are the ability to servo the stage to a starting position automatically and capability of using the feedback tachometer output, as a crude velocity indicator which can be filtered and displayed on a meter or chart recorder. This tracking system has been almost completely built and will be installed while I am completing this thesis. To accommodate a DC torquer the electronic circuits would have to be modified. The procedure in the modified system will be taking the signal from the photomultiplier pre-amp circuit and then using what is effectively a lock-in amplifier such as a dual FET analog gate on the two halves of an absolute value circuit. The phase of the lock-in would be controlled from the present phase reference circuit and with spike blanking. The output

would then be plus or minus depending on the direction of error except for zero at the blanking pulses. This signal could then be conditioned to provide a suitable signal for a DC torquer. A convenient commercial unit would be Servo-Tek Bi-Mode Servo DC Torquer with 10 x gear reduction, followed by Harmonic Drive precision gear 160 x reducer to micrometer head to provide sufficient precision and gear reduction.

4. Control of Vibration

Floor vibrations transmitted to the Phycomyces are a problem when the spph is long and when equipment vibrates the floor. Isolation above 50 Hz can be achieved with commercial layered pads at cost of $10. The table is designed so that its center of gravity is below the supporting columns and therefore will be stable when supported by springs at each corner. Springs with 10 cm of deflection cost about $250, and isolate above 1 Hz. Even with shock absorbers the table will have considerable bounce and any additional load will permanently change the tilt of the table affecting the alignment of apparatus not on the table. To achieve low frequency vibration isolation and permanent alignment with the room active 2-chamber air systems are available which use active leveling to ±25 microns relative to the floor. Such air pressure systems cost from $1500 to $3000 and should be used if there is a serious problem.

These considerations were taken into account during the machine's development but never instituted.

5. The Stage

The motors drive micrometer screws two turns per millimeter of stage travel. Each of these micrometers in turn drives a hydraulic piston forcing water along teflon tubes to hydraulic slave pistons which drive the stage (David Kopf Model 1207B modified hydraulic drive on special three-dimensional stage). The purpose of this complication is high effective vibration isolation of the stage from the driving motors.

While the Kopf stage is very stiff and has a minimum backlash of 1-2 microns it represents the quality available at its cost. The backlash is large relative to the precision required in measurement. As mentioned in the introduction much superior performance is possible with a machine of this type. However, it should be pointed out that to obtain significantly higher performance a complete integrated servo system stage and measurement system would have to be designed as a single unit. This will be discussed briefly in the measurement section.

REFERENCES

Brosens, P. J. 1971. Fast retrace optical scanning. Electro-Optical Systems Design. 3(4): 21-24.

James, H. M., N. B. Nichols, and R. S. Phillips (eds.). 1947. Theory of servosystems. New York. McGraw-Hill, 1965 Dover Publications.

Sears, F. W., 1958. Mechanics, wave motion and heat. London. Addison-Wesley.

Appendix B

Details of Data Collection

1. Stage Position Measurements

The stage position is measured by the clasic LVDT (Linear variable differential transformer Schaevitz -500-HR) which provides an electrical output proportional to the displacement of a separate moveable core. Three coils are spaced on a cylindrical coil form and a rod-shaped magnetic core is positioned axially inside this coil assembly providing for magnetic flux linking the secondary coils. The core is rigidly fixed to the moving element of the stage. The transformer coil assembly is rigidly fixed to the non-moving stage support for that axis. The primary center coil is excited by a 10 KHz voltage stabilized oscillator. The outer secondary coils are connected in series opposition so that the two voltages in the secondary are opposite in phase.

This provides a net output equal to the difference of these voltages. The voltage in each secondary is proportional to the amount of induced voltage due to the position of the core. Comparison to the phase of the excitor determines at which end the core is, so that using an appropriate bridge circuit a DC level proportional to the position of the core can be achieved.

This signal has "infinite resolution", practically about 10 ppm or .25 μm and linearity of .25% full scale. The core exerts

negligible friction on the casing so that the position transducer does not interfere with the stage performance. This AC signal (see stage position circuit, Fig. B-1) goes through an isolator stage, a transformer and then a range control (half and full scale) which is an attenuator and then is reamplified. The full scale attenuated signal is only ±3.5 mv or about .26 μV/μm of stage position and thus is a suspect source of noise. However, the dominant source of noise is due to the tracking. There are three such identical circuits, one for each axis. When the stage is not driven the noise and drift stay within ±.5μm on the best channel with no significant long term drift after 45 min of warming up. Circuit cards of the Lufkin Model 940 electronic gauging unit are used for oscillator amplifier and detector. Each axis signal, now a DC level, is compared to a DC level and amplified 20, 40 or 80 x. This amplified signal is then passed through a third order low pass filter with about 3 sec time constant.

Finally each signal is fed to a four channel A/D converter and the z-axis channel to an analog differentiator. There is considerable difficulty in accurately differentiating using either digital or analog methods particularly in the presence of a wide band of frequencies; hence the heavy third-order filter. The differentiator (see analog-differentiator circuit) has been used with a typical input signal of .3 mv/sec for a sporangiophore growth velocity of

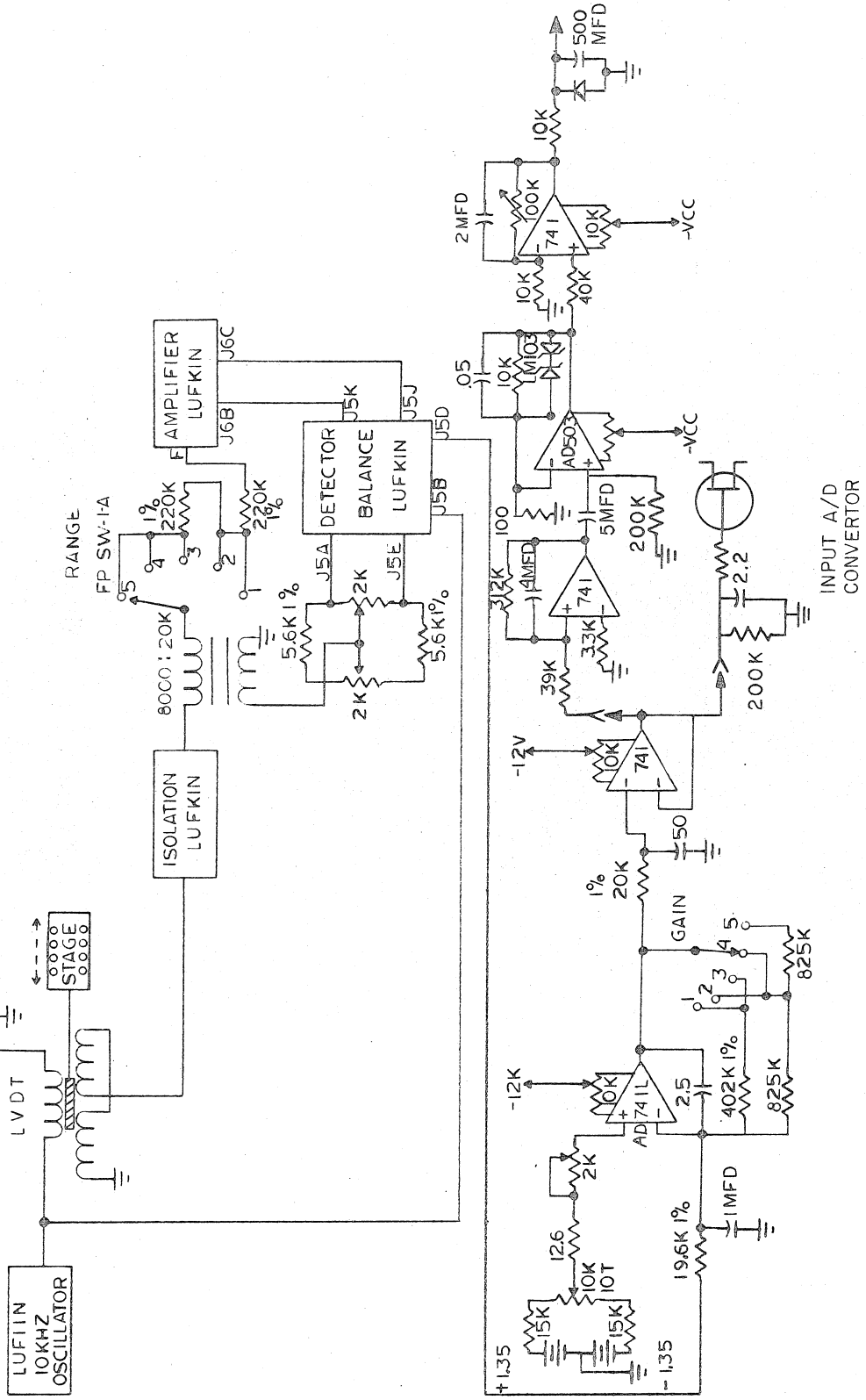

Fig. 3-1. LVDT detected stage position and analog differentiator circuit.

30 μm/min. The output is 1 volt per 100 μm/min growth rate. However, the range has only been ±1 volt on the input and therefore only one-eighth of the total range. This has necessitated resetting the DC balance at 45 min intervals. Because of the desire to prevent "hanging-up" or saturation of the operational amplifiers the differentiating op amp is limited in its voltage swing by two LM103 zener diodes back to back. Since it is desired to differentiate only the lowest frequencies a high RC must be used and this is incompatible with the use of diodes parallel to the resistor; therefore a simple RC circuit exterior to the op amp is used and signal is fed into the high impedance non-inverting input.

Normally, this analog differentiated signal is fed to a strip chart recorder (Hewlett-Packard 7100BM with 17500A pre amp-electric writing) for monitoring the experiment. In fact for many exploratory experiments the on-line vertical velocity is all that is needed. Eventually it would be valuable to include at the same time the direction of bend and the angle of bend (see Appendix H).

On the A/D converter approximate differentiation is carried out by adding the new point value and then subtracting the new point value from the next memory location (see differentiation modification circuit Fig.B-2). This gives the difference between successive data points as a simple differentiation. More sophisticated techniques will be discussed in Appendix C.

The three axes of position information are fed to separate analog digital (A/D) converter of the SD (signal digitizer) 1/4 Fabri-Tek (now Nicole Instruments) ± 1 volt full range A/D converter. This particular converter has a linearity of .05%, a 130 μsec conversion time and uses the Wilkinson run-down technique. The fourth A/D converter monitors the Fabri-Tek DC balance noise present and is used to subtract this from the true signal.

The range provided by the 12 bit A/D converter with 1 bit resolution of .763 μm is about 3 mm or above one hour of experiment. The DC balance control however allows one to record anywhere over the 25 mm stage range. To increase the range available without decreasing the resolution I designed a circuit modification (Fig. B-2) to do 64 A/D conversions at each data point so that instead of about 240 μsec per point including conversion time and storage there is about 16 m sec per point. Each of the 64 digitizations is added into memory and differentiation mode is preserved. The memory holds 18 bits without overflow so that it is just large enough to accommodate these additions. The signal to converter noise ratio is improved by a factor of 8.

What follows is a description of the circuit modification to do 64 A/D conversions per data point both in normal and differentiate mode. The circuit consists of TTL integrated circuits mounted in the

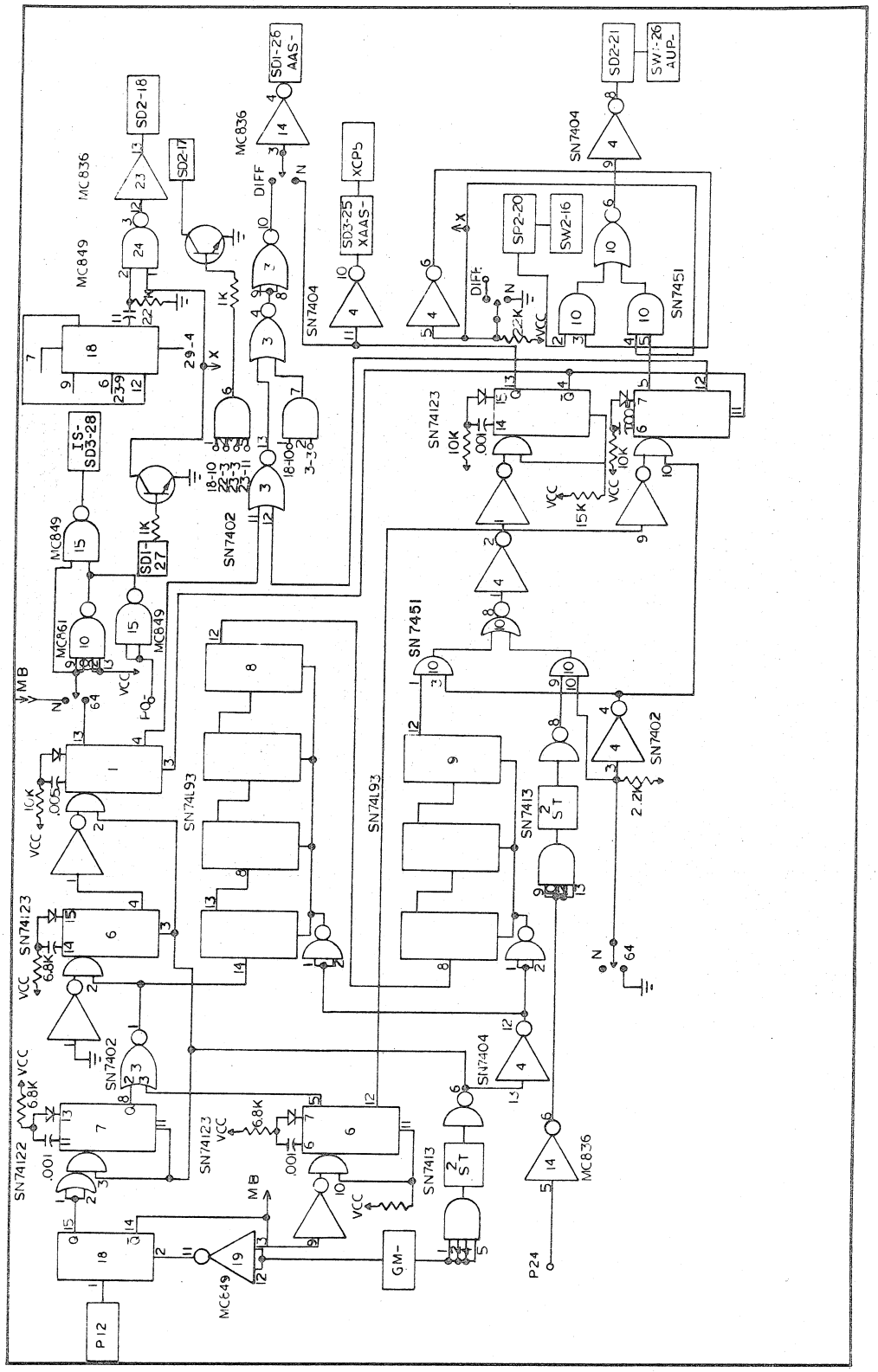

Fig. B-2. Instrument computer 64x and differentiation mode modification.

Fabri-Tek SD 1/4 A/D convertor which is a mixture of RTL and DRTL logic. Although the manufacturer reached a compromise 4.2 volts supply which is outside of the recommended values for TTL, the circuits work well enough.

The purpose of the modification is to change the hard wired program within the normal functioning framework without destroying the normal capability. Also a signal is sent out to the experiment control programmer which signifies for all options that another new data point has been reached (XAAS). There are four modes of operation. In the completely normal mode on program pulse #12 to IC D18 of plug-in causes this flip-flop to change state and connected through switch SW2-2 causes IS pulse which restarts program pulser to give commands #13-24 thus completing digitization and storage of the four A/D convertors. The normal, AAS, memory address advance signal controlled by switch SW2-1 passes through IC's D14,2,4,5, and D14 again to rest of computer. The other control signal, AUP, which sets the address advance direction is controlled by SW1-1 and in normal mode just feeds through to the main computer AUP without change.

In normal differentiation a small card modification causes the A channel digitized value to be added to the present address and then subtracted from the next address, i.e. the address is advanced and then subtracted in.

In 64x normal undifferentiated mode the $\overline{IS}$ signal is given twice each cycle at program pulses 12 and 24 until 64 complete cycles

have been carried out. $\overline{IS}$ is first triggered by the clock and then is inhibited at end of 64 complete cycles. A delay in $\overline{IS}$ pulse allows the last count to occur without the $\overline{IS}$ pulse.

In 64x differentiate mode each value must be added to the present address and subtracted from the next address after AAS and then must return 63 times ($\overline{AAS}$ and $\overline{AUP}$) back to the present address. Finally, on the 64th time $\overline{AUP}$ is inhibited. This is in addition to $\overline{IS}$ inhibited on 64th end of cycle from IC 5.

The main disadvantage of the 64x modification is that the memory does fill and therefore cyclic averaging is not possible without overflowing. The problem is somewhat reduced in the differentiate mode since only small differences occur between measurements so that Δz may be cyclicly added. However, the other axes whether position x or y and/or angles will appear garbled. For near vertical growth these may be adjusted to near zero and an average deviation from vertical measured.

For complete information on actual growth rate during bending it is necessary to know not only x,y and z positions from second to second but two projections of the angle of the growing zone to the vertical, preferably at right angles. This need arises because the center of curvature of the bending is not at a constant distance from the sporangium but 1 to 3 mm below it (see Appendix C and H). Therefore it is necessary when needed to multiplex the angle measurements

with x and y since there are only 4 channels available for recording.

The four A/D converter results are held in registers which are fed to their respective 256-word memory locations where they may be averaged on successive cycles or just held in their groups for output onto digital magnetic tape (Cipher 70H without read) or onto a recorder (Hewlett-Packard 7034) or onto oscilloscope display (Tektronix 561A). The data collection is controlled by a central clock in the Fabri-Tek (Nicole Instruments) SW2C sweep plug-in. This central controlling clock also provides the time base for the experiment programmer (see Appendix G).

The original clock was not convenient and has been changed to a basic constant 100 kHz crystal oscillator (Fig. B-3). This is divided down by factors of 10, seven times giving a basic time from 100 kHz (10 μsec) to .01 Hz (100 sec) between pulses of the clock selectable with the front panel eight-position single pole decimal switch (Digitran series 800 mini switch). Three digit accuracy may then be provided by further counting to any present number set on the three ten-position binary coded decimal (BCD) switches (Digitran).

The total range is limited by conversion rate requiring at least 250 μsec normally or 20 msec at 64x setting at a minimum to an extravagant 10^5 sec (3 days) per interval between points. This allows maximum flexibility for any purpose.

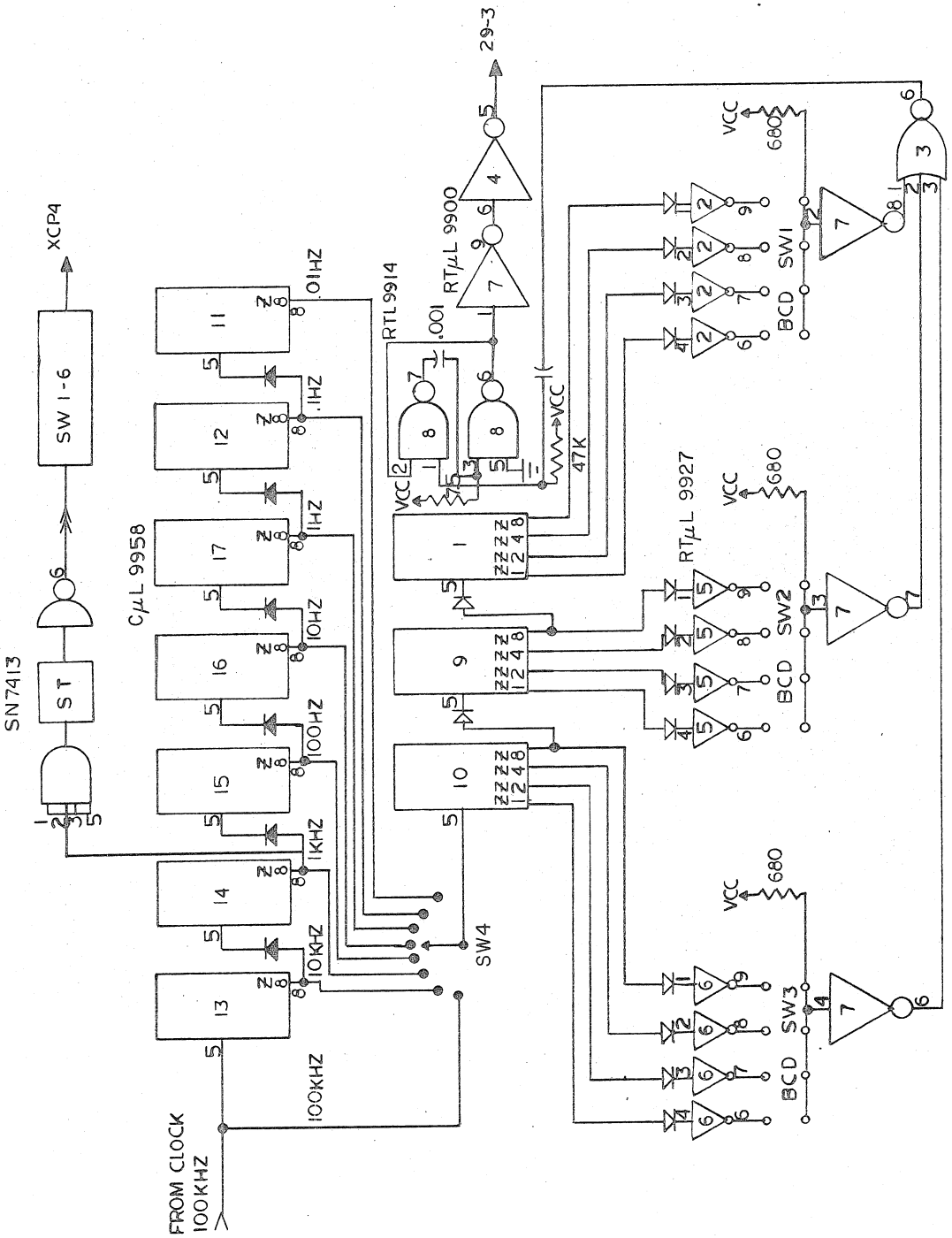

Fig. B-3. Instrument computer clock modification.

2. Limitations of stage and measurement system and data collection

Apart from the servo tracking system which is presently being modified to provide more optimal performance the main remaining limiting factors are (1) the stage performance, (2) the measurement of its position, and (3) measurement of the tilt of the spph.

The stage has a large backlash relative to the precision required.

Further, the piggyback system of supporting each stage axis of travel on top of another is disadvantageous in several respects. First, the bottom stage supporting the upper two has high inertial and load problems. Second, the system is subject to thermal and non-alignment error due to changes of supporting axis affecting the movement of another. Third, stages so piggybacked are quite susceptible to vibration. Finally, they are not convenient for accurate measurement of the actual stage position. Such stages however can be adequately made if sufficient care is taken.

The LVDT's have a linearity of 0.25% and at best a 0.25 μm resolution with a bandwidth of 0.2 Hz. Also they necessitate analog circuits plus an A/D converter, both of which are subject to DC and other noise. The signal level out of the analog circuit corresponds to 32 μvolts/μm displacement.

Such sources of error such as temperature causing shifts of mirrors, lenses and other components, imperfect alignment of axes and LVDT nonlinearity are slowly varying functions of time and

therefore not dangerous; the main errors that are the same bandwidth as our signal are the electronic and LVDT noise and drift.

Of course the A/D converter digitizing noise, nonlinearity and drift are also a serious problem, particularly since the velocity must be calculated from small differences. All drift and noise will appear directly. The situation has been improved by 64x modification of the A/D converter. All these problems can be greatly reduced by the design of a completely integrated tracking servo and measurement system taking advantage of recent technology in microcircuits and stage design.

Two alternative systems will be described below. One particular system also provides precise position information.

There are commercially available two-dimensional stages (Mechanical Technology, Inc. and others) which are numerically controlled integrated circuit timers using a stiff guide system in which the driving motors are exterior to the moving elements and are fixed and vibration isolated.

These motors drive gas bearing guides which move the stage like the x-axis of an xy recorder. Gas bearings allow the use of hard surfaced metals enabling precise machining of adjacent surfaces making for high precision. They also make possible fast response with no hysteresis effects and they minimize thermal gradients.

A three dimensional stage using the same principle is commercially feasible. Placing an interferometer corner cube prism on each guide would allow a single fixed laser and three interferometers to monitor

the stage movement in x, y and z. This technique would not be limited in range as is the present instrument. If the stage can be made with sufficiently small backlash, i.e., less than 0.2 μm then it is also possible that incremental optical encoders could be used to provide digital output at one-fifth the cost and potential trouble of the interferometers. A proved laser interferometer is Hewlett-Packard HP5525A which would provide digital on-line readout directly and presumably fairly reliably. This has a resolution of 0.16 μm or with digital smoothing 0.02 μm. If a micrometer screw is used with a typical pitch of 500 μm/revolution, then incremental shaft encoders (e.g. Disc Instruments, Inc.) are available with 0.25 μm resolution without any special couplings. An optical encoder output can also be digitally smoothed. The micrometer screws do not provide the precise position information of the laser interferometer, however their linearity and lead error can be less than 0.1% and therefore quite adequate. Such a system could be calibrated with a laser interferometer measuring system to determine its specifications.

Both of these systems eliminate DC drift, digitization problems and with the availability of integrated circuits digital filtering and processing can be done immediately on-line (see Appendix C) (Gold and Radar, 1969).

Using the angle measurements (see Appendix H-2) digitized directly with an encoder to whatever desired resolution a small micrologic computer can calculate during the experiment, such

parameters as growth rate corrected for tilt and bending of spph, a measure of bending point distance from the sporangium, orientation of the spph, and bending rate and direction. Using accurate D/A converters which are relatively inexpensive, any calculated function can be immediately displayed on the oscilloscope, strip chart, or whatever.

The servo drive signal is available to the precision of these systems so such a project is feasible. The optical encoder system is also simple and should be highly reliable.

With the advent of large scale integrated micrologic circuits the need for expensive analog handling of the signal and expensive computer analysis can be reduced. Considerable on-line information can be provided. A growth velocity known to 1% at .1 Hz is not an unreasonable goal even in the presence of spph bending and non-vertical orientation.

REFERENCE

Gold, B. and C. M. Radar. 1969. Digital Processing of Signals. New York, McGraw-Hill.

Appendix C

Details of Data Analysis

The problem of analysis essentially involves the identification of the noise and the real signal. In our case the main problem is to obtain as "uniform", "smooth" and as accurate a growth velocity as possible from the digital displacement measurements. Several sources of noise and distortion exist. The servo system oscillates about a "dead band" region producing an oscillation of .03 Hz or slower. Further, both the analog signal provided by the LVDT's, the amplifier and the DC balance circuit has circuit and power supply noise. In order to eliminate errors in the A/D conversion and sampling circuit a low pass filter is used but, of course, this also provides a distorting phase delay. The analog filtering however does mean that the random nature of the A/D conversion noise can be easily treated.

Essentially with the analog filter it can be assumed that there is no true significant third derivative in the signal over a period of each measurement, i.e. over ten to fifteen seconds. It is practical to measure at one second intervals, therefore a number of measurements are made on essentially the same signal and therefore one gains $\sqrt{N}$ in signal-to-noise ratio. This may be applied as a least deviation approximation. These depend on using the property that a real signal is of analytic nature in the neighborhood of the point of

interest while the noise is of non-analytic nature.

In the least-squares technique in a second order polynomial approximation one is effectively assuming that the second derivative of $f(x)$ is practically constant over the neighborhood used and this method of smoothing will smooth out any second derivative discontinuity. This technique is simple because it can be reduced to summation of neighboring weighted points. I have used the least-squares technique to obtain the first derivative, in this case the growth velocity.

Another approach is to consider an entire set of data as one unified whole then determine its characteristics to find clues with which to separate noise from the true function. An example of this approach is to fit the data to a Fourier series of n terms. If the function is everywhere continuous but the derivative discontinuous the terms decrease with n^{-2} if the function is discontinuous n^{-1}. Noise however will not converge. Precautions with respect to the boundary condition are of course necessary. The optimum approach appears to be to reflect a functioning $g(x) = f(x) - (\alpha + \beta x)$ choosing α and β so that $g(0) = 0$, $g(\ell) = 0$ to obtain an odd function which eliminates a discontinuity in function or derivative for then the asymptotic order of magnitude of the Fourier goes as n^{-3}. The procedure would be to plot only the inverse Fourier transform (Fourier synthesis) of a limited frequency above which is only noise. An improvement over this procedure as I have used it could be to

somewhat smooth the frequency domain values to reduce unreal oscillations in the plotted time domain.

Several other properties are worth mentioning. The Fourier transform has put the function f(x) into the frequency domain. Therefore any filtering possibilities are immediately and easily available as most filters can be easily expressed in the frequency domain. This technique can also, if desired, simply correct for the phase delay produced by the analog filtering. This Fourier analysis is also ideally suited for correlation studies, search for periodicities, etc. If each term is squared one has the power spectrum as a function of frequency. If only the noise terms are used one obtains the standard deviation of the noise.

The technique suffers from the difficulty of not responding to the difference of each neighborhood.

If the eye makes an approximation to a curve it makes several assumptions about the data. It throws out wild points unless a discontinuity is expected and applies a least-deviation approximation. During periods of little change it smooths more than in periods of rapid changes, i.e. it sets a second derivative criteria as in cubic spline approximation or least-squares second derivative approximation. These last methods have been much neglected until recently and their use and application occupy much of the last decade's numerical analysis literature.

Considerable new work is being carried out in this field due to the technological developments and the efforts to talk to computers (Van Veen, 1969, 1970).

A better future alternative to the procedures I used are continuously variable filters in the form of spline smoothing. This procedure measures the standard deviation of the velocity in the absence of stimuli and then minimizes $\Sigma f''(x)^2$ of the fitting function within the limit set by this standard deviation (Reinart, 1967, 1971). The procedure like least-squares technique reduces to a summation of weighted neighboring values with the addition of another factor which is the positive real root of a biquadratic equation at each point.

REFERENCES

Reinart, C. H. 1967. Smoothing by spline functions. Numerische Mathematik. 10: 177-183.

Reinart, C. H. 1971. Smoothing by spline functions. II. Numerische Mathematik. 16: 451-454.

Van Veen, F. (ed.). 1969. Special issue on fast Fourier transform. IEEE Audio and Electroacoustics. AU-17: 65-172.

Van Veen, F. (ed.). 1970. Special issue on digital filtering. IEEE Audio and Electroacoustics. AU-18: 81-212.

Appendix D

Details of Visual Observation

Visual observation is via a closed circuit television system. The type of vidicon tube, RCA 7335B, was selected for red response, ($\sim$ 80% of peak at 600 nm). Light from a 60 watt GE1958 quartz iodide lamp filtered with Schott RG610 (3.0 O.D. at 590 nm) and KG 3 heat absorbing glass back lights the spph. Any small lamp would be adequate since 95% of the light is thrown away, i.e., only 0.1 $\mu w/cm^2$ used. The camera is a Sylvania 800 specially modified to drive the Sony Surveillance Videocorder (a modified PV-120V) for time lapse at 1 frame per second.

When the camera and recorder are required for other lab work a Shiba Electric Co. camera and Packard Bell TV monitor are used.

Appendix E

Details of Light Source Selector

Light Source and Side Selector Circuits

The light source and side selectors are nearly identical. The light source selector circuit (Fig. E-1) consists of control to a motor (Stepcon Motor size 17, 90°/step, Automation Development, Co.) and their controller boards which position a mirror so that light A or B will shine on the specimen or neither light. The motor is a permanent-magnet motor with four coils and each is connected to a power line and individual brown, orange, blue and yellow wires. Grounding brown results in an opposite poled electromagnet to grounding orange and similarly for blue and yellow. One and only one of each pair is always on. In rotating the PM 90° only one changes per pulse for rotation. Knowing which are on determines which light source is on. By logically "anding" these motor inputs the four possible positions are determined and drive front panel lights bulbs on the experiment programmer that tell whether the motor is causing light source A or B or none to be shone on the specimen.

Provision is included to program the timing of any change in source, i.e. either to off or to other source.

The side selector is the same as the source selector except the mirrors are rotated to shine light on either the left or right

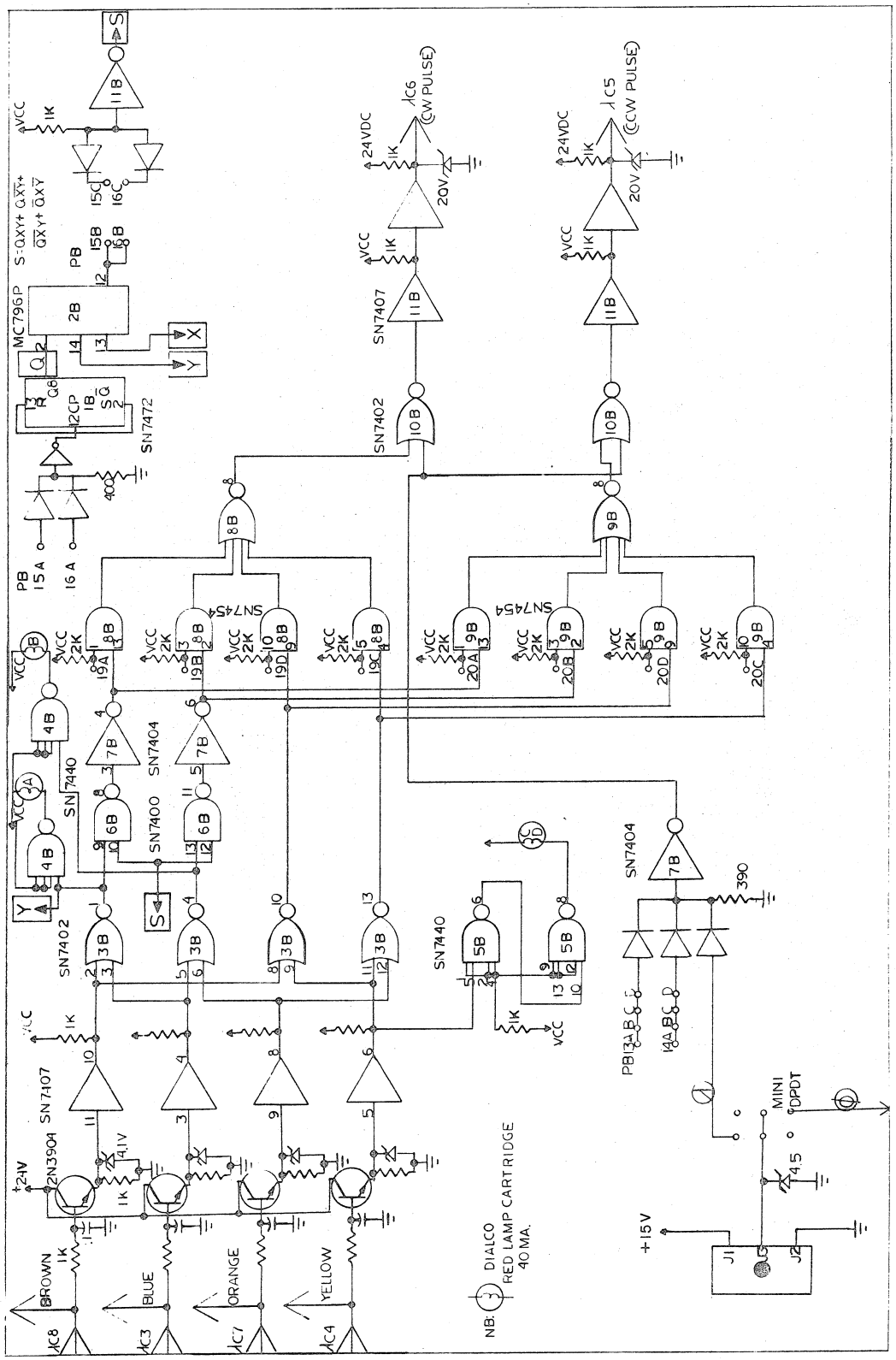

Fig. E-1. Light source selector control circuit.

side of the specimen or neither.

Provision is also included to allow longer time on one side than the other (Fig. E-2). This is controlled by using a delay from a fixed rate driving pulse, i.e. a command is delayed each time in going from left to right while not delaying from right to left.

One further feature is that cooperation with the light source selector allows alternation between light A on the left side and light B on the right side, to light A on right and B on left.

These provisions were especially designed for action spectra studies. For growth action spectra one rapidly alternates side and changes source every 5 min. For ultraviolet versus visible phototropic studies one keeps the side constant for long periods, but alternates the source. For visible only phototropic studies one keeps light A on left and B on right and after long periods reverses them as discussed above.

Optics of the Light Source and Side Selection

After the double monochromator light passes through the neutral density wedge it is converged by two spherical lenses providing a parallel beam with respect to the slit into horizontal direction although diverging in the vertical direction. A 1" diameter 50 mm f1 and 1.5" diameter 50 mm f1 quartz lenses are used. This light is

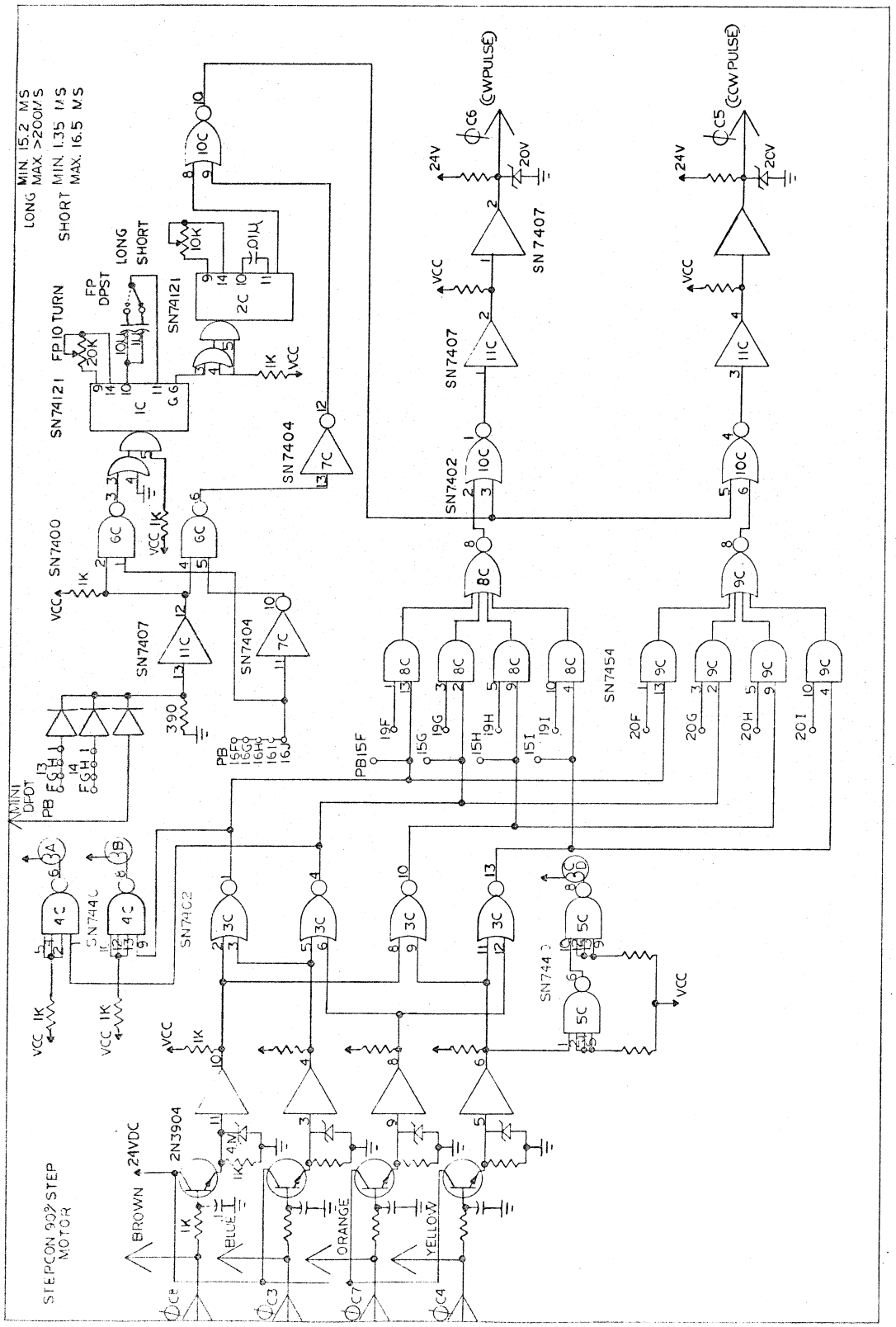

Fig. E-2. Lit side alternator control circuit.

then focussed with the Bausch and Lomb 5 element crystal quartz-fluorite lens or by cylindrical lenses (1.5", 50 mm f.1 and .75" 25 nm f.1. lens) which make the diverging beam parallel in both directions. Mirrors are Balzar Alflex "A" High UV type from Rolyn.

Appendix F

Details of Light Source Intensity Control

The 6" diameter, 1/8" thick O.D. wedge is driven by a Superior-Electric Slo-Syn motor, SS50-1008, and Superior-Electric STM1800V translator module with a 4x precision gear reducer from PIC Design Corp.

Three up-down decade counters (Fig. F-1) keep track of the position of the O.D. wedge (Kodak 6" A6040). Initially the wedge is zeroed to the discontinuity between 4.0 and 0.15 O.D. and then counters set to zero. After this then each step with directions is recorded and displayed by red front panel digital lights on the experiment programmer.

There are three intensity levels (Fig. F-2 to 4) selectable on the front panel. The programmer could be modified so that any position corresponding to any intensity desired could be read in.

Pushing of the intensity initiate button drives the O.D. wedge to position corresponding to the number set in the first 3 digit BCD Digitran mini-switch. The rate driver is determined by the pulse source, 200 Hz, 10 Hz manual push button, or ramp clock which is selectable on the front panel patch board (Fig. G-4). A positive pulse to the I_2 initiate will result in the I_2 flip-flop being set, which will result in the turning off of I_1 or I_3 and then the

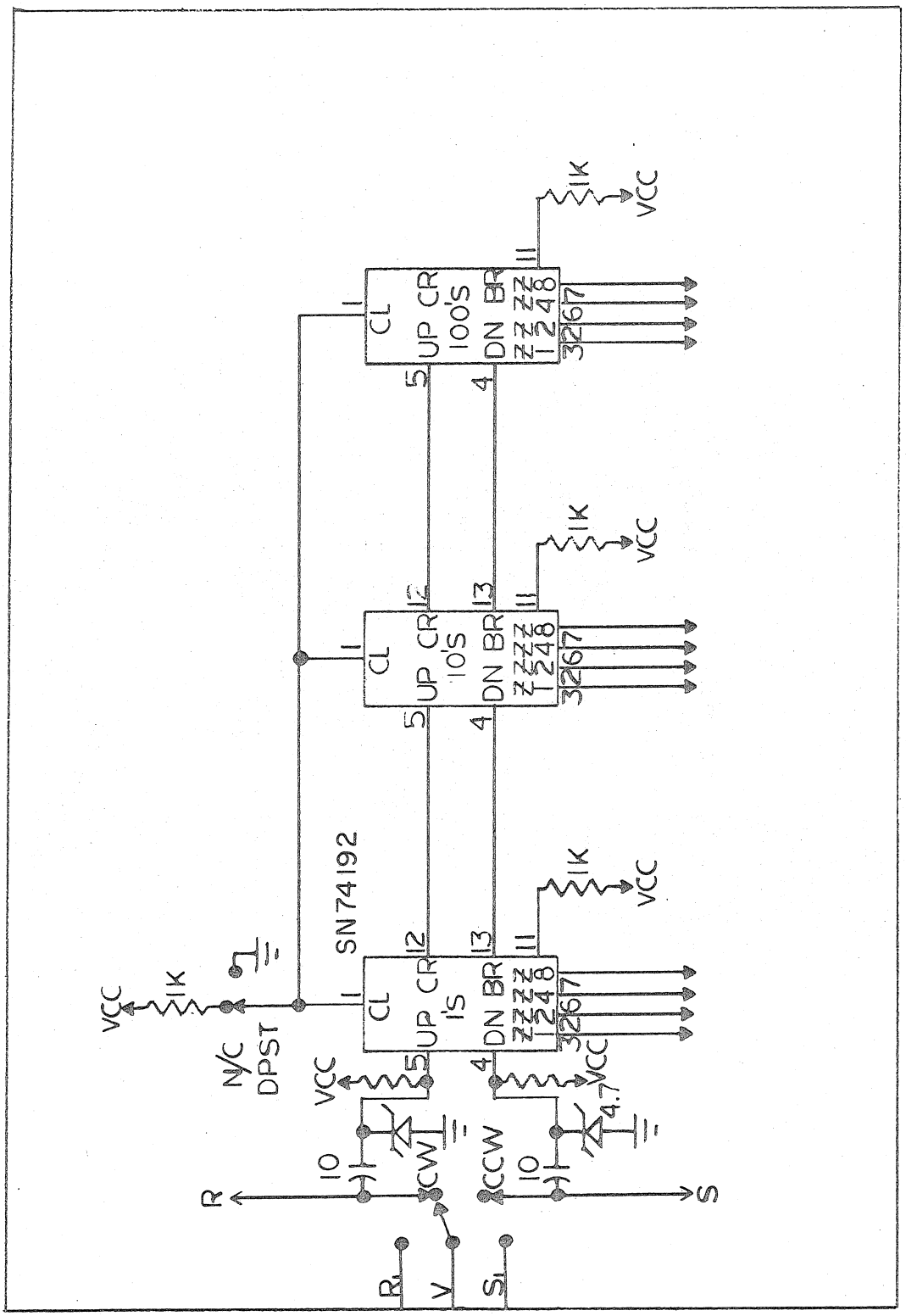

Fig. F-1. Intensity control with O.D. wedge: O.D. wedge position counter.

comparison of the preset I_2 level number to the actual position number. If level $I_2 > I_1$ and the actual level A was initialized to I_1, then A = I_1 and the O.D. wedge is then turned through the intermediate intensities to I_2. I_2 being greater than A determines the motor direction. The rate driver is determined by the pulse source. Each level may have different sources so that a ramp to level 2 from level 1 may be followed by a step back to level 1. If A equals any preset I the appropriate light will turn on indicating the change has been completed. A manual control is provided to set the wedge anywhere you want. The actual position will always be displayed in the digital display lights. Attaining A equal to a preset I level will also turn off the ramp generator as for an exponentially increasing light program, the so-called "Sunrise" experiment.

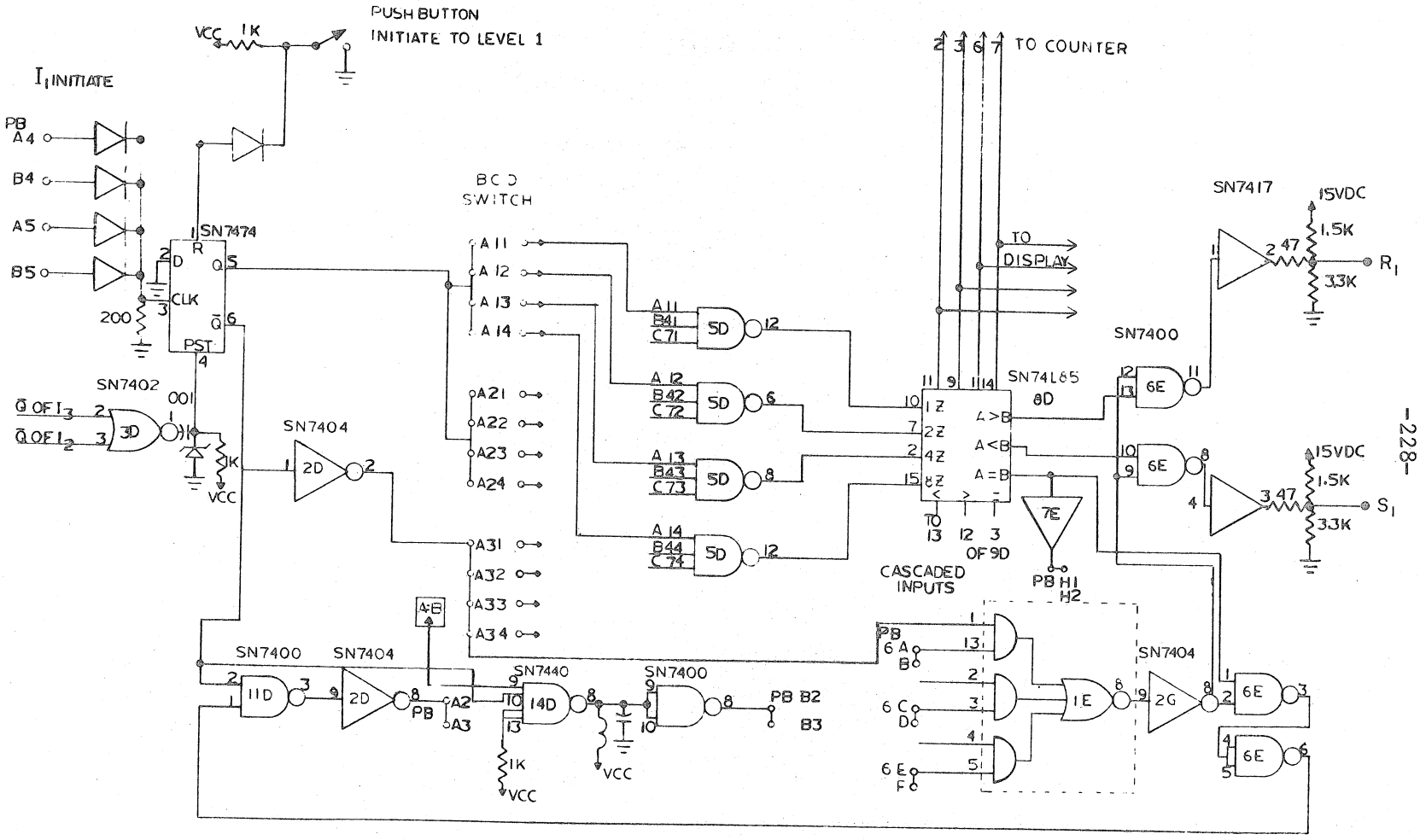

Fig. E-2. Intensity control with O.D. wedge: I_1 level and 100's digit comparator.

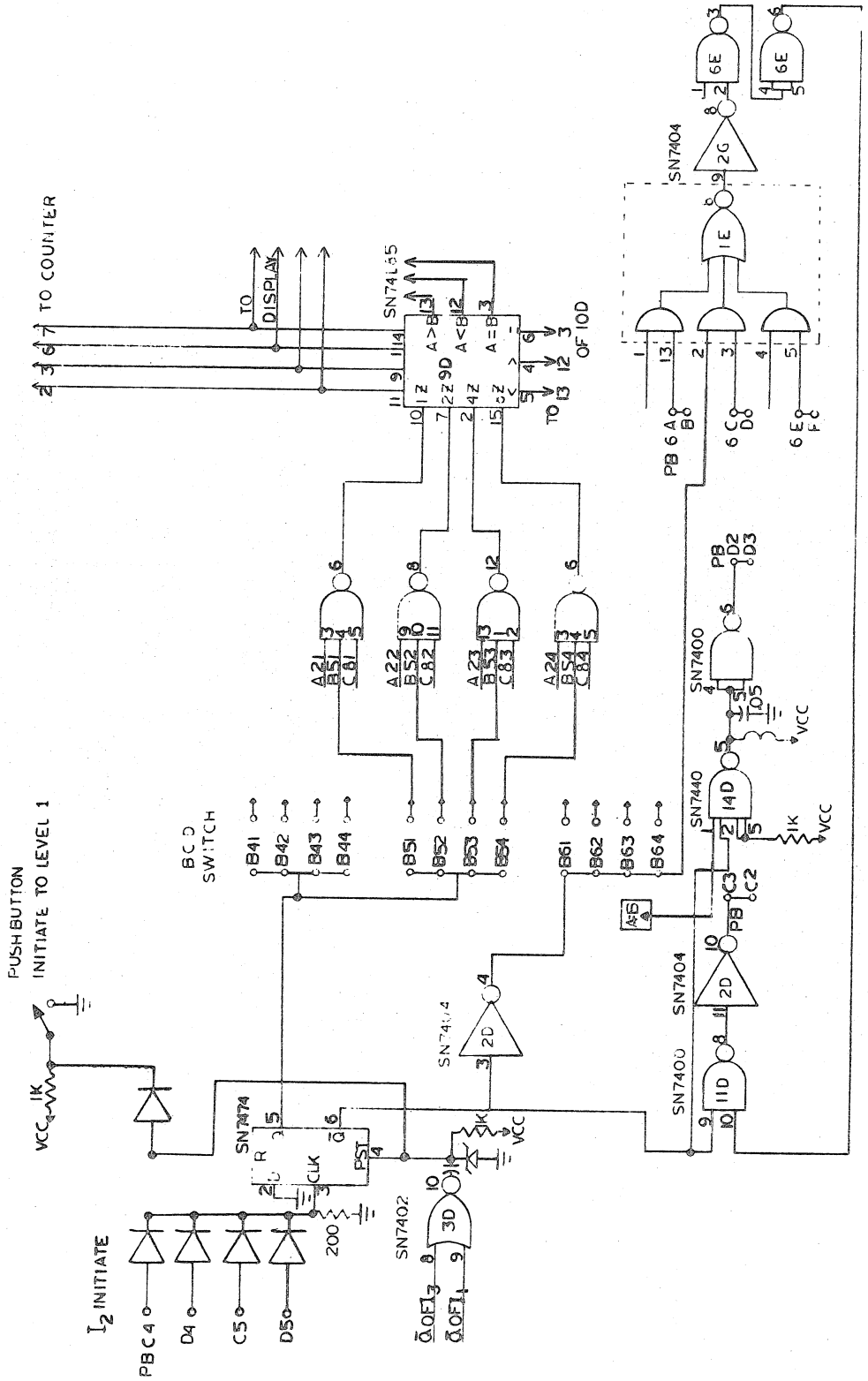

Fig. F-3. Intensity control with O.D. wedge: I_2 level and 10's digit comparator.

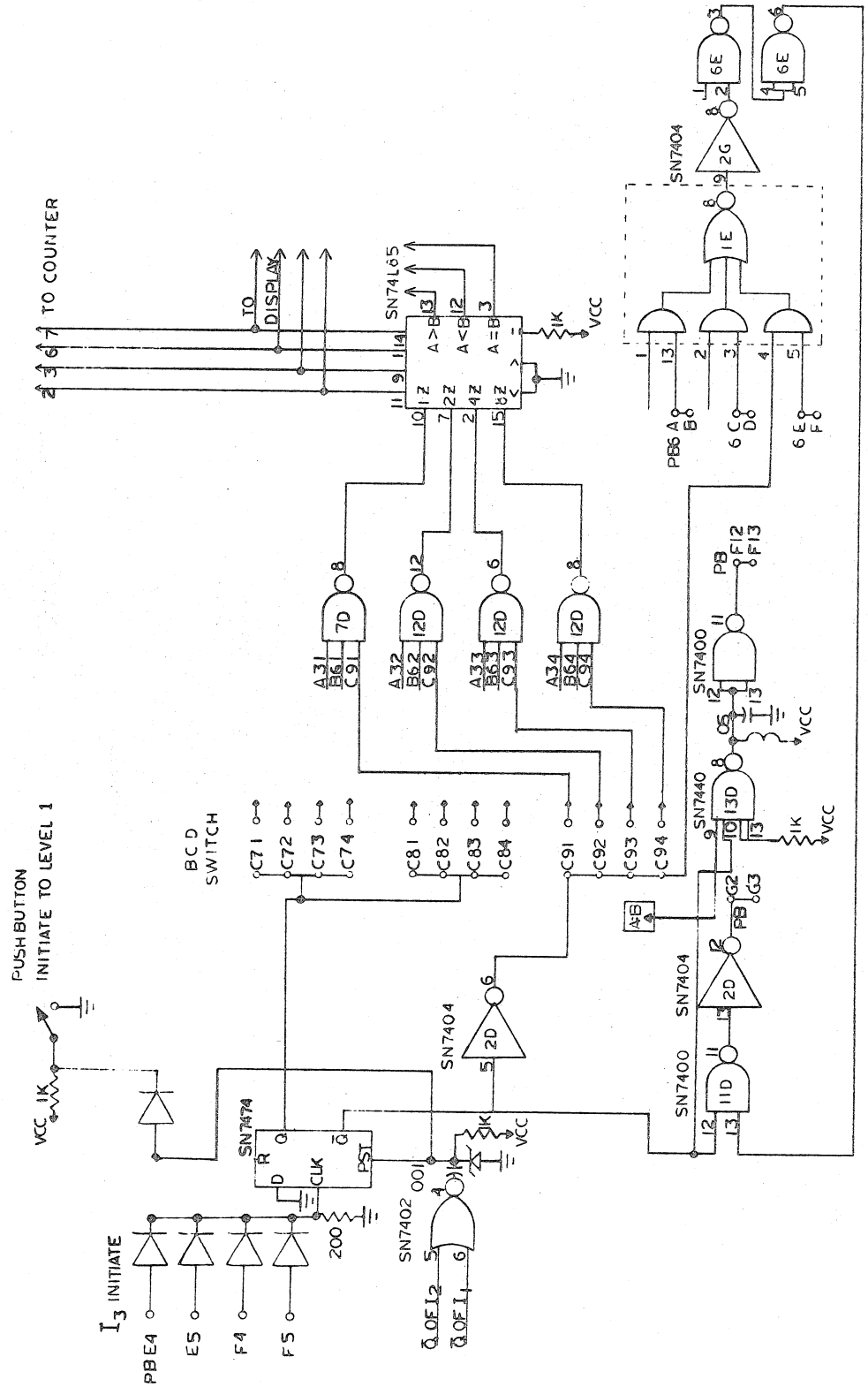

Fig. F-4. Intensity control with O.D. wedge: I_3 level and 1's digit comparator.

Appendix G

Details of Data Handling Programmer

1. Ramp and light pulse clock

This circuit (Fig. G-1) makes use of the control clock of the main computer as described in Appendix B-1, p.199. The clock feeds 1 KHz continuously when SW2c modified clock internal reset $\overline{SW}$ is set to non-reset.

The purpose of this circuit is to provide a means of timing pulses of light within the capabilities of the optical density wedge system and control rates of "sunrise" stimuli using optical density wedge changes. A step change in intensity is provided by a 200 Hz output. This is maximum safe rate of change for the wedge and corresponds to approximately 1 sec per O.D. change. The length of the pulse is controlled from the dividing down of the 1 KHz clock and should be in the range 0.5 sec to 1000 sec. Actual step changes can be controlled by the memory address unit. Control is by divide by ten counters. The last two most significant digits allow setting to the exact digit with Digitran BCD mini-switches. An external clock may also be used to drive the 1 to 1000 counter and the O.D. wedge. Random sequences may be run for obtaining random functions. The clock is initiated by a positive pulse. For the case of a ramp, after initiation the time set is the time between steps of

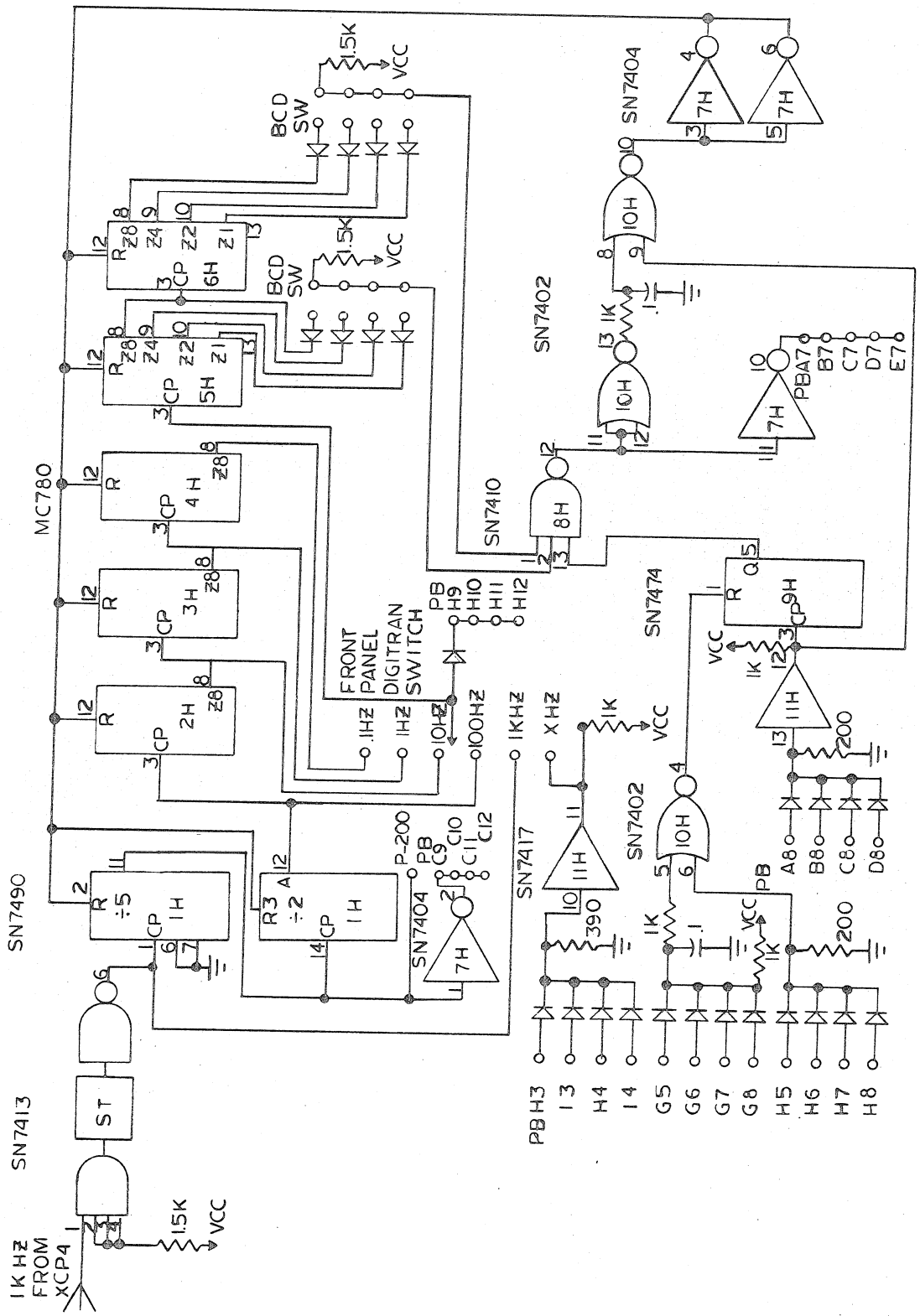

Fig. 31. Experiment Programmer: Ramp and pulse clock.

the O.D. wedge ~ .005 O.D. per step. For normal rates this time is about 1 sec to 4 sec. Only when a preset level A has been reached, i.e. A equals B of O.D. wedge control, are the pulses which drive the motor control no longer connected.

In the case of programming pulse stimuli the P200+ output is connected to the pulse drive input and when A = B is reached no further driving occurs.

2. Address Control

The $XAAS^{-}$ signal from the signal digitizer 64x and differentiation modification (Fig. B2) provides a single negative pulse per memory address.

The purpose of the address control (Fig. G-2) is to provide the means to synchronize experiment changes with data collection, and in particular, to provide convenient means to do useful signal averaging of repetitive experiments. The modified control clock controls the interval between addresses or data points. The address control sets the number of data points in any desired repetitive cycle.

As an example, one can set a 10 min cycle, 5 min of condition A followed by 5 min of condition B. One wished to see with a resolution of 10 sec the shape of the response. Setting the data interval to 10 sec and the last address preset digit switch to 60 satisfies this

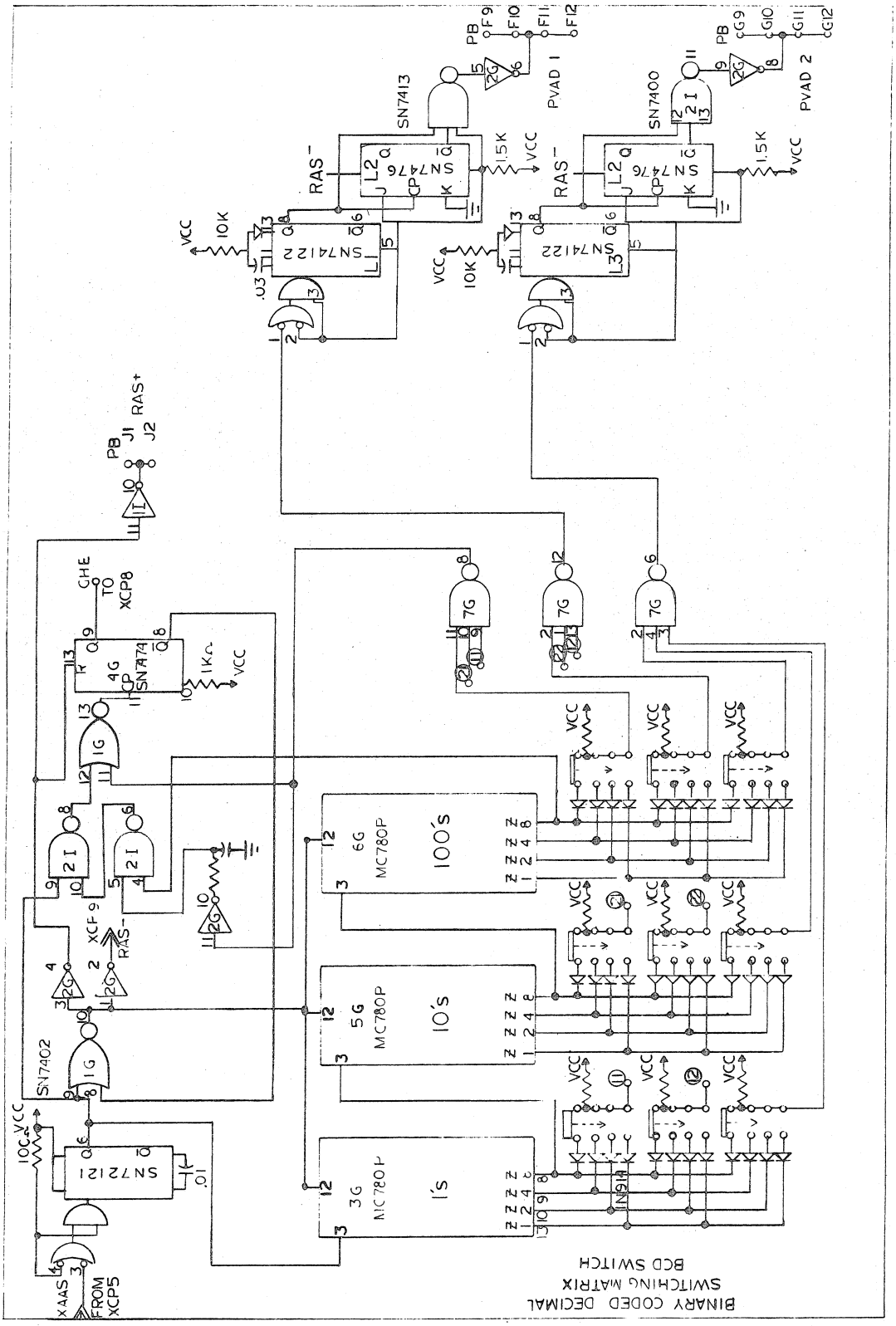

Fig. G-2. Experiment Programmer: Computer address counter and variable address output.

desire. This program is extremely useful for growth action spectra studies.

When 60 is reached RAS+ signal is triggered on the next XAAS$^-$ and the main computer address counter is reset to zero and then data can be put onto magnetic tape at the same time. At two other preset variable addresses pulses may be elicited and used at the patch board. As in the above example, it might be desired to have the maximum amount of positive growth in the left half of memory and the negative in the right half for easier comparison. Therefore the first preset address could be set at 10 and the second at address 40.

During the experiment the actual address is immediately available in the front panel digital display.

3. Digital Display

The digital display multiplexes the main computer address or data point of the cycle and the position of the optical density wedge. The number viewed is selected by a front panel switch. The display consists of three alpha-numeric seven segment diffused planar GaAs P emitting diodes (MAN 1 Monsanto) and are easily visible being 1/4" high red digits.

The circuits consists of conventional and/or invert gates for multiplexing and a seven segment driver for each digit IC.

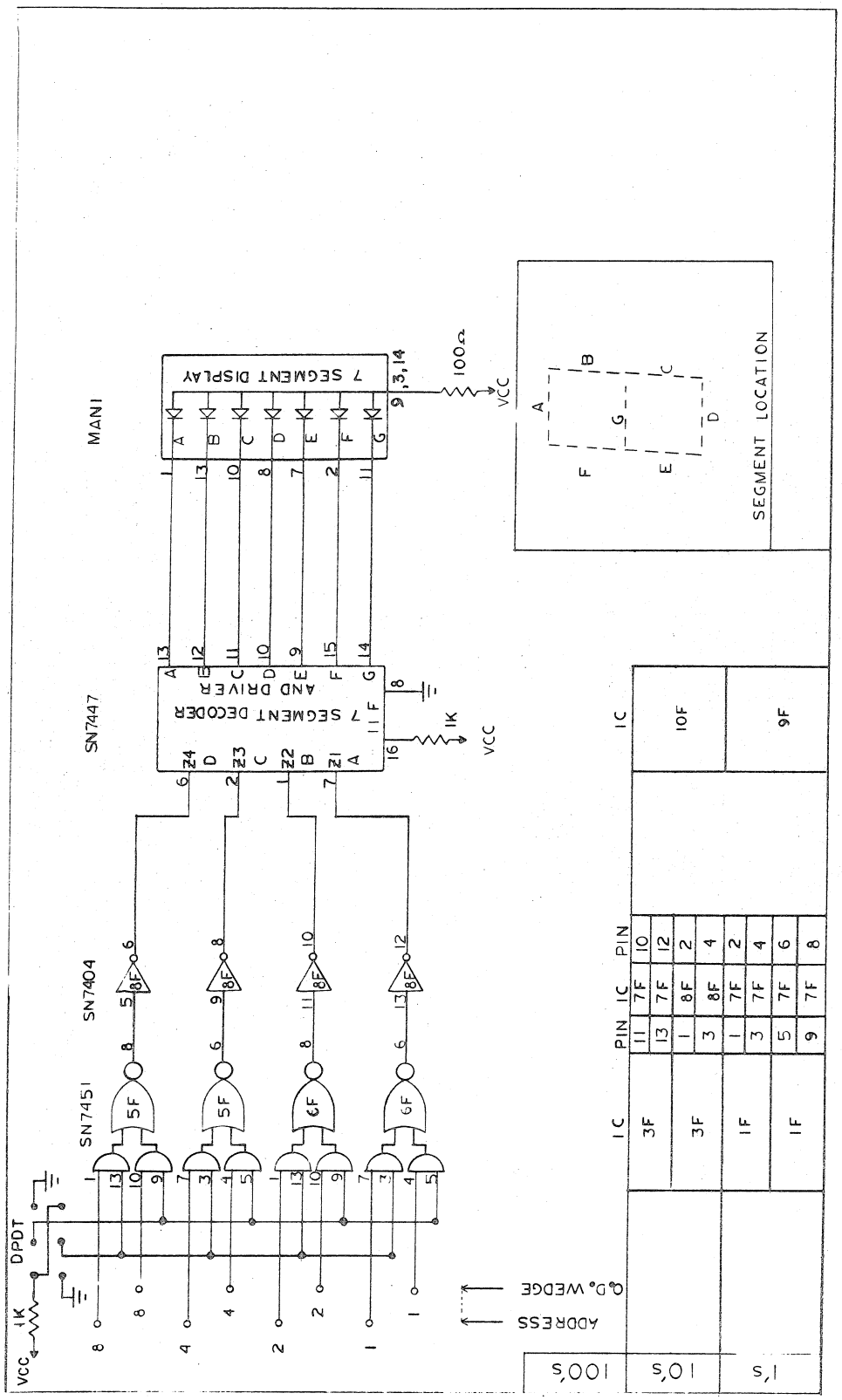

Fig. G-3. Experiment Programmer: Digital display for address and O.D. wedge position.

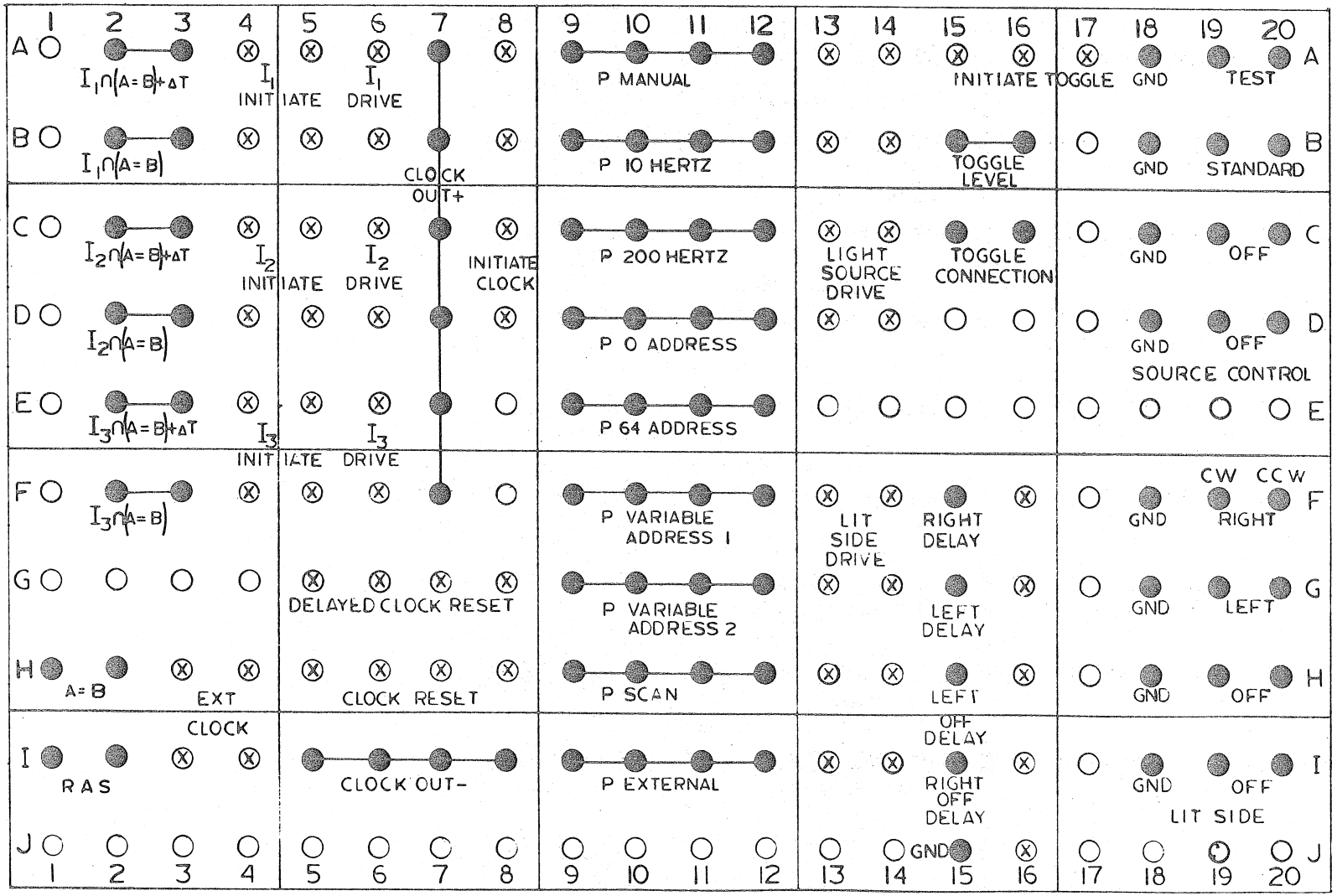

Fig. G-4. Experiment Programmer: Patch board. x inputs, ● outputs, 0 not connected.

Appendix H

Suggestions for Reasonable and Worthwhile Expansion of Present System

1.) High Intensity

Present laser gives a maximum of 10 mw/cm^2 488 nm intensity deliverable on the spph. This is sufficient that Phycomyces does not respond, i.e. the photopigment appears to "bleach". However this intensity may be insufficient to study the reciprocity failure of wild type due to the need to provide a lot of energy in a short time.

I would suggest use of a 2 or 4 watt Spectra Physics or Coherent Radiation Laboratory argon ion laser. A number of spectra lines are available from 351.1 to 514.5 nm. The strongest with respect to stimulating Phycomyces is at 488 nm and is equivalent to about 2000 mw of broad blue light with the 4 watt laser. Spectra Physics also have a "cavity dumper" which allows the laser to be pulsed at high energies up to 75x the average energy provided the average energy is not exceeded. Pulses may be as short as nanoseconds. This system could greatly facilitate study of reciprocity failure. Studies of kinetics of "bleaching"and hypothesized recovery of photosensitive pigment is almost a virgin field and undoubtedly warrants attention.

2.) Spph Angle Measuring Device

In order to provide accurate growth rates and a sensitive measure of assymetric growth changes, the angle of the specimen should be measured.

Photodiodes (ex United Detector Technology PIN-40) are highly sensitive to red light such as the HeNe 6328 laser and could be used as sensors. Of course the already tried light pipe and photomultipliers used for the sporangium tracking could also be used. However, the same accuracy is not needed. Applying the tracking resolution criteria to the angle measuring device invisaged would give ±.015° error in the angle; ±.05° would certainly be acceptable.

It has been found that the shadow of the edge of the spph stalk serves quite well as the target just as does the sporangium shadow. Placing of two sensors one on each side of the stalk shadow image and allowing them to be servoed in a circle about the center of the sporangium image, i.e. where the tracking system keeps the sporangium centered, would provide measurement of the stalk angle. The sensors on each edge would be moved to keep the same amount of light on each sensor. The servoed angle would be the spph stalk angle and may be measured with a potentiometer on the same shaft as the servo-motor and reducer or with an incremental shaft encoder and associated counter. A cheap 80:1 gear reducer such as Harmonic Drive HDUP-20-80-2 would allow, with rapid hunting across the dead band, a resolution

of ±.05° at 0.1 Hz bandwidth. Our present A/D converter would be sufficient to record this. Since it would be desirable to record the projection of both angles and other possible information and x,y,z coordinates, time multiplexing would be necessary to record all the information on our 4 channel A/D converter and instrument computer.

As a suggestion for a future system a modest hardwired computer program could continuously calculate the true growth rate and display it during the experiment. (See section 4 of this Appendix.)

3.) Uniform Illumination

a) Rotating Light Source. One of the major difficulties with bilateral illumination is the hunting of spphs both slow (20 min to 60 min periods) and fast (5-7.5 min periods)(Dennison, 1958). The rates and amplitudes depend on the mutant. This is observed at least for wild type and C5 (car-10) to be relatively absent if the spph is rotated rapidly (2 rpm) relative to its response characteristic. This means hunting is due to the unsymmetrical light distribution around the spph. As already discussed,interference of this bending on the measurement of the growth rate is considerable,particularly in the absence of compensation from angle measurements. Thus it would be desirable to provide a means to either rotate the specimen or the light beam or otherwise provide uniform illumination.

The machines accuracy would suffer a great deal if the spph had to be rotated, however rotating the light source is a good alternative and one system is practical for all wavelengths from 200-800 nm. Basically, it could be similar to the present bilateral system in which several sources of light are channeled down from above. For parallel light, such as from a laser, this presents no problem. A quartz rotating rhomboid prism or mirror equivalent could transfer the exciting beam from the axis center perhaps 2 cm away and then rotating a 45° cone whose center is aligned with the axis center would diverge the light in a horizontal plane to another fixed convergent 15° cone which would reflect the light down on the specimen at 60° from the vertical. If an arc lamp were used a collimator would be necessary to get a reasonably parallel and uniform beam at the specimen.

Speed of the rotating prism or mirrors and mirror cone could be regulated to any speed or direction and could therefore allow flexible light programs of the type in which the light sources rotates at the speed of the cell wall for the study of rotation of adaptation.

b) Light pipe source. An alternative scheme for providing a uniform light distribution is a number of light pipes arranged in such a way that they come radially from all around the spph at some angle to the vertical. This scheme is not practical, however, in the ultraviolet.

4.) Calculation of the Growth Rate

In the present system most frequently $\Delta z/\Delta t$ is used as the growth velocity. This is processed in the manner already described (Appendix C) or is the result of analog differentiation (Appendix B). When the spph is bending or is orientated away from the vertical the true growth rate is not $\Delta z/\Delta t$. In fact, with a rapidly, although small amplitude "hunting" is seen with C21, values of $\Delta z/\Delta t$ vary from -60 μm/min to +85 μm/min with, I suspect, a constant growth rate. During negative phototropism to ultraviolet (280 nm) light bending of 17°/min will result in -300 μm/min and possibly 360 μm/min vertical velocities whereas the true growth rate is 30 μm/min. This is the extreme case but errors of smaller magnitude are dangerous. It would be preferable to measure the angle of orientation directly as well as the velocities of the sporangium trajectory, however this feature is not included in the present system. The true growth has been calculated using the formula:

$$\Delta g = \Delta x\bar{\ell} + \Delta y\bar{m} + \Delta z\bar{n} + (\Delta x^2 + \Delta y^2 + \Delta z^2)/2S$$

where S is the assumed distance to the bend and Δ represents differences in variable during Δt, and ℓ,m,n are the directed cosines of the orientation.

The direction cosines are calculated from the equation

$$n(0) = n(-\Delta t) + [\Delta z - n(-\Delta t)] \cdot \Delta g/S$$

This procedure is not totally reliable because of its numerical instability.

To improve the situation the angles of orientation can be directly measured (see Section 2, Appendix H). A good approximation for the growth velocity is then

$$\frac{\Delta S}{\Delta t} = \frac{(\Delta x\bar{l} + \Delta y\bar{m} + \Delta z\bar{n})/\Delta t}{1 - \frac{1}{4}(\Delta l^2 + \Delta m^2 + \Delta n^2)} \quad \text{or } \dot{S} = \dot{x}l + \dot{y}m + \dot{z}n$$

where $\dot{x},\dot{y},\dot{z}$ are the sporangium trajectory axes velocities, $\bar{l},\bar{m},\bar{n}$ are the average direction cosines during Δt, and Δl, Δm, Δn are the changes in the direction cosines during Δt. This equation is derived from consideration of two successive lines at $t = 0$, $t^1 = \Delta t$ of known orientations and angle $\delta = \cos^{-1}(ll^1 + mm^1 + nn^1)$ apart. These lines correspond to the axes of the spph stalk. The bending point is taken as the point of their minimum separation. The distance from the center of the sporangium to bending point is

$$S_d \cong \frac{\Delta x\Delta l + \Delta y\Delta m + \Delta z\Delta n}{\Delta l^2 + \Delta m^2 + \Delta n^2}$$

If the distance between the lines is not small the calculation breaks down, i.e., if

$$d = \frac{\Delta x(mn^1 - m^1n) + \Delta y(n\ell^1 - n^1\ell) + \Delta z(\ell m^1 - \ell^1 m)}{\sin \delta}$$

is not small. The beauty of $\dot{S}$ is its simplicity, which means it could be calculated on-line and immediately displayed.

Other indications of growth velocity are:

1. $\dot{z}$ true if no bending and specimen vertical; and

2. $\dot{g} = \dot{z}/n$ which is true if no bending occurs.

Parameters for display with a suggested bandwidth of 0.03 to 0.10 Hz:

1. $\dot{z}$; 2. $\dot{S}$; 3. δ bending rate;

4. bending direction relative to source of stimuli, if there is a defined direction of source; 5. spherical coordinates of orientation θ,ϕ; and 6. distance to bending point.